


2017-03-31

Exploring New Therapeutic Strategies for Osteoarthritis: From Genetic Manipulation of Skeletal Tissues to Chemically-modified Synthetic Hydrogels

Henry Huang
University of Massachusetts Medical School

Let us know how access to this document benefits you.

Follow this and additional works at: https://escholarship.umassmed.edu/gsbs_diss

 Part of the [Cell Biology Commons](#), [Molecular, Cellular, and Tissue Engineering Commons](#), [Musculoskeletal Diseases Commons](#), and the [Orthopedics Commons](#)

Repository Citation

Huang H. (2017). Exploring New Therapeutic Strategies for Osteoarthritis: From Genetic Manipulation of Skeletal Tissues to Chemically-modified Synthetic Hydrogels. GSBS Dissertations and Theses. <https://doi.org/10.13028/M20M4V>. Retrieved from https://escholarship.umassmed.edu/gsbs_diss/919

Creative Commons License



This work is licensed under a [Creative Commons Attribution-NonCommercial 4.0 License](#)
This material is brought to you by eScholarship@UMassChan. It has been accepted for inclusion in GSBS Dissertations and Theses by an authorized administrator of eScholarship@UMassChan. For more information, please contact Lisa.Palmer@umassmed.edu.

Exploring New Therapeutic Strategies for Osteoarthritis: From Genetic Manipulation of Skeletal Tissues to Chemically-modified Synthetic Hydrogels

A Dissertation Presented

By

Henry Huang

Submitted to the Faculty of the
University of Massachusetts Graduate School of Biomedical Sciences, Worcester
in partial fulfillment of the requirements for the degree of

DOCTOR OF PHILOSOPHY

March 31st, 2017

M.D. / Ph.D. Program

Exploring New Therapeutic Strategies for Osteoarthritis: From Genetic Manipulation of Skeletal Tissues to Chemically-modified Synthetic Hydrogels

A Dissertation Presented
By
Henry Huang

This work was undertaken in the Graduate School of Biomedical Sciences
M.D./Ph.D. Program

The signature of the Thesis Advisor signifies validation of Dissertation content

Jie Song, Ph.D., Thesis Advisor

The signatures of the Dissertation Defense Committee signify completion and approval as to style and content of the Dissertation

David C. Ayers, M.D., Member of Committee

William R. Kobertz, Ph.D., Member of Committee

Jae-Hyuck Shim, Ph.D., Member of Committee

Karen L. Troy, Ph.D., Member of Committee

Hong Zhang, Ph.D., Member of Committee

The signature of the Chair of the Committee signifies that the written dissertation meets the requirements of the Dissertation Committee

Paul R. Odgren, Ph.D., Chair of Committee

The signature of the Dean of the Graduate School of Biomedical Sciences signifies that the student has met all graduation requirements of the school.

Anthony Carruthers, Ph.D.,
Dean of the Graduate School of Biomedical Sciences

March 31st, 2017

Acknowledgments

First of all, I would like to thank my thesis advisor, Dr. Jie Song, for the opportunity to be part of her lab. Jie's passion for a multidisciplinary approach to develop new translational therapies was evident to me the first day we met seven years ago. Despite my limited research experience, she saw in me the potential to become a great scientist. None of the work presented here would be possible without her thoughtful and selfless guidance. As a mentor, Jie was always available to discuss experimental results; but she also permitted me to freely tackle scientific problems of my own accord. She reminded me to be patient and optimistic, even when I faced perpetual disheartening results early in my thesis work. I am grateful for all her efforts to make me a better thinker and for pushing me to overcome my many limitations. Thank you, Jie! You exemplify the dedicated, hardworking, and enthusiastic scientist whom I will strive to emulate for the rest of my research career.

I would like to thank a number of current and former members of the Song lab who have shaped me scientifically and personally during my time in the lab: Dr. Jeffrey Lange, who was a clinical and scientific role model, guided me in lab while I was still a first year medical student. Dr. Tera Fillion Potts and Dr. Artem Kutikov, who were both exceptional graduate students, were invaluable resources to have in lab and they paved the way for me to succeed. Dr. Jianwen Xu, who shared with me the importance of mentorship, maintained a high level of scientific rigor in his ideas and experiments. Dr. Jing Zhang, who endured many late evenings in lab with me, prompted me with appropriate questions that drove my research project forward. Dr. Pingsheng Liu and Dr. Ben Zhang were patient and taught me many fundamental concepts relating to polymer and material science. Dr. Yu Tan, whom I collaborated with on a clickable hydrogel project, reminded how much more enjoyable and fulfilling research is when you are not working alone. Jordan Skelly, who never fails to make the work environment entertaining, provided technical expertise and creative ideas to every research project she was involved in. She was also the backbone that defined our lab dynamics and culture.

In addition, I would also like to thank various individuals who have directly and indirectly contributed to the body of work described here. April Mason-Savas assisted me with all things histology related and in troubleshooting the processing and staining of different hydrogel specimens. Dr. Sally Trabucco and Dr. Yahui Kong from the Zhang lab taught me a lot about Smurf2 biology, animal work and the majority of the molecular biology techniques I know. Stacey Russell performed microCT scans of my skeletal tissue samples and assisted me in the imaging processing. I would also thank Chris Raskett, for teaching me the principles of the DMM

surgical procedure and for our methods discussion of RNA isolation and processing from skeletal tissues. I would also like to acknowledge Dr. Jeffrey Nickerson and Jean Underwood from the Cell Biology Confocal Core for their assistance in obtaining immunofluorescence imaging of my hydrogel specimens. I would also like to recognize the summer students whom I mentored, especially Michael Moverman and Gregory Molica, and their help in collecting preliminary data for the hydrogel project.

Furthermore, I would like to thank the members of my thesis research advisory committee Dr. David Ayers, Dr. William Kobertz, Dr. Paul Odgren and Dr. Hong Zhang for their scientific guidance and unwavering moral support throughout my research years. The biannual gathering of this incredible group of scientists from multiple disciplines into a single conference room has always been a humbling experience for me. I only hope that there will be more opportunities in my future to work with another similar group of diverse scientists.

Finally, I would like to thank my family and MD/PhD friends whose support outside the lab has kept me going over the years. A special thanks to my wife, Michelle, who stood by me in my decision to enter this program and who gave me the confidence I needed whenever I was in despair. I am also blessed with my daughters, Audrey, Haley, and Zoey, who bring tremendous joy to my life and I cannot wait to see them take on new challenges in this ever-changing world.

Abstract

Osteoarthritis (OA), a degenerative disease of articular joints, is the leading cause of chronic disability in the US and affects more than a third of adults over 65 years old. Due to the obesity epidemic and an aging population, the prevalence of OA is expected to rise in both young and old adults. There are no disease modifying OA drugs. Therefore, providing any treatment options that delay the onset or progression of OA is highly desirable. The scope of this dissertation examines two different strategies to promote translational therapies for OA. The first approach investigated whether Smad ubiquitin regulatory factor 2 (Smurf2), an E3 ubiquitin ligase, could be a potential therapeutic target for OA. The second approach examined the incorporation of small chemical residues to enhance the physical and bioactivity of a bioinert scaffold for cartilage tissue repair.

Overexpression of Smurf2 in chondrocytes was shown to accelerate spontaneous OA development in mice. We hypothesized that reduced Smurf2 expression could slow the progression of OA and enhance the performance of cells for cartilage repair. By performing surgical destabilization of the medial meniscus (DMM) on Smurf2-deficient mice, loss of Smurf2 was shown to mitigate OA changes in young mice but this protection diminished in older mice. Assessment of Smurf2-deficient chondrocytes *in vitro* revealed an upregulation of chondrogenic genes compared to wild-type; however, these differences were not seen at the protein level, deterring its potential use for cell-based therapies. During the course of this study, new insights about how age and sex affects different joint compartments in response to DMM surgery were also uncovered. These results broadened existing understanding of DMM-induced OA in mice but also questioned the validity of such a model to identify disease modifying targets that are translatable to OA in humans with advanced age.

Due to a lack of innate repair mechanisms in cartilage, damage to cartilage increases the risk of developing OA early. Tissue engineering provides a unique strategy for repairing damaged cartilage by delivering cells in a well-controlled environment that can promote the formation of neotissue. We hypothesized that synthetic chemical residues could enhance the mechanical properties of a bioinert scaffold and promote matrix production of encapsulated chondrocytes. Covalent incorporation of small anionic or zwitterionic chemical residues in a polyethylene glycol-based hydrogel improved its stiffness and resistance to fluid flow, however, the resulting physical environment can also exert a dominant negative effect on matrix production of encapsulated chondrocytes. These results suggest that modulating the

biosynthesis of chondrocytes with biochemical signals requires a concurrent reduction in any conflicting mechanotransduction signaling, emphasizing the importance of a degradable system to promote new cartilage formation.

In summary, this dissertation establishes Smurf2 as a modulator of OA progression but implies that other factors such as age or protein(s) with redundant Smurf2 functions may play a role in limiting its effect as a therapeutic target. This work also reveals fundamental biology about how chondrocytes behave in response to physical and chemical cues in their microenvironment, which will aid in the design of better scaffolds for cartilage tissue engineering.

Table of Contents

Signature Page	ii
Acknowledgements.....	iii
Abstract.....	v
Table of Contents.....	vii
List of Tables	ix
List of Figures	x
List of Abbreviations.....	xi
Copyrighted Materials Produced by the Author	xii
Chapter I: Introduction.....	1
1. Osteoarthritis (OA)	1
2. Challenges in Developing Disease Modifying OA Drugs.....	1
3. Pathogenesis of OA.....	3
Articular Cartilage, Chondrocytes, and Cartilage Matrix Degradation	3
Subchondral Bone and Osteophytes	7
Synovial Inflammation and Proinflammatory Cytokines	9
4. Clinical Trials of Potential OA Drugs.....	10
5. Spontaneous and Induced Mouse Models of OA	12
Mouse strains with spontaneous OA	13
Genetically-modified mice with OA-like Phenotype	13
Non-surgical Induction of OA.....	13
Surgical Models.....	14
6. Tissue Engineering Strategies to Repair Articular Cartilage Defects	16
Post-traumatic OA and Articular Cartilage Damage	16
Cartilage Tissue Engineering.....	17
Natural versus Synthetic Hydrogels.....	18
Cell Types	19
Biochemical, Mechanical and Other Cues that direct Chondrocyte Behavior	20
7. Overview of Dissertation.....	21
Chapter II: Skeletal Characterization of Smurf2-Deficient Mice and In Vitro	
Analysis of Smurf2-Deficient Chondrocytes	24
1. Introduction.....	24
2. Materials and Methods	26
3. Results	31
4. Discussion	41
5. Acknowledgments	44

Chapter III: Age-dependent Changes in the Articular Cartilage and Subchondral Bone of C57BL/6 Mice after Surgical Destabilization of Medial Meniscus.....	<u>45</u>
1. Introduction.....	<u>45</u>
2. Materials and Methods	<u>46</u>
3. Results	<u>48</u>
4. Discussion	<u>56</u>
5. Acknowledgments	<u>59</u>
Chapter IV: Anionic and zwitterionic residues modulate the stiffness of photo-crosslinked hydrogel and the cellular behavior of encapsulated chondrocytes ..	<u>60</u>
1. Introduction.....	<u>60</u>
2. Materials and Methods	<u>62</u>
3. Results	<u>65</u>
4. Discussion	<u>74</u>
5. Acknowledgments	<u>76</u>
Chapter V: Discussion and Future Perspectives	<u>77</u>
1. Summary of Key Findings and Significance of Dissertation Work	<u>77</u>
2. Future Directions	<u>80</u>
3. Concluding Remarks	<u>82</u>
References.....	<u>83</u>

List of Tables

Chapter II:

[Table 2.1](#) Sequences of primers used for quantitative RT-PCR

List of Figures

Chapter I:

[Figure 1.1](#) Depiction of chondrocyte and collagen fiber organization and the different zones in articular cartilage.

[Figure 1.2](#) Overview of signaling pathways involved in chondrocyte hypertrophy.

[Figure 1.3](#) Overview of signaling pathways and structural changes in the development of OA

[Figure 1.4](#) Diagram of mouse knee and the combination of ligament transections and meniscectomy needed to induce different severity of OA.

Chapter II:

[Figure 2.1](#) Summary of experimental design for skeletal characterization

[Figure 2.2](#) Smurf2 protein and gene expressions in WT (+/+) and Smurf2-deficient MT (T/T) skeletal tissues and primary cells.

[Figure 2.3](#) Age- and sex-specific cortical bone and trabecular bone analyses of WT and Smurf2-deficient MT mice.

[Figure 2.4](#) Age-specific knee joint phenotypes of male WT (+/+) and Smurf2-deficient MT (T/T) mice.

[Figure 2.5](#) Differential severity of knee joint articular cartilage erosions in young (4 month) and old (21 ± 1.3 month) male WT and Smurf2-deficient MT mice after DMM surgery.

[Figure 2.6](#) Knee joint subchondral bone analyses in 4 months old male WT and Smurf2-deficient MT mice upon surgical induction of OA by DMM.

[Figure 2.7](#) Quantitative gene expression analyses of key anabolic and catabolic markers in WT and MT iMACs.

[Figure 2.8](#) Smurf protein expression changes upon 24-h treatment of TGF- β 3 and IL-1 β .

[Figure 2.9](#) Western blot quantification of Smurf2 and Smurf1 proteins in WT and MT iMACs.

Chapter III:

[Figure 3.1](#) Age-dependent changes in articular cartilage degradation of male mice 2 months post-DMM

[Figure 3.2](#) Age-dependent changes in subchondral bone plate thickness of male mice 2 months post-DMM

[Figure 3.3](#) Age-dependent changes in osteophyte size and quality of male mice 2 months post-DMM

[Figure 3.4](#) Comparison of different tissue compartments of the joint between 12M male and 12M female mice 2 months post-DMM

[Figure 3.5](#) Age-dependent changes in different joint structures of female mice 2M post-DMM

Chapter IV:

[Figure 4.1](#) Formulations, swelling and compressive behaviors of modified vs. unmodified PEGDMA hydrogels

[Figure 4.2](#) ECM production by iMAC in modified vs. unmodified PEGDMA hydrogels

[Figure 4.3](#) Metabolic activity and cell viability of iMACs in modified vs. unmodified PEGDMA Hydrogels.

[Figure 4.4](#) ECM production by hAC in modified vs. unmodified PEGDMA hydrogels

List of Abbreviations

- 2D --- 2 dimensional
 3D --- 3 dimensional
 α MEM --- alpha-minimum essential media
 ACI --- autologous chondrocyte implant
 ADAMTS --- a disintegrin and metalloproteinase with thrombospondin motifs
 AGE --- advanced glycation end product
 ALK --- activin-like kinase
 BM --- bone marrow
 BMP --- bone morphogenic protein
 BMSC --- bone marrow stromal cells
 CCK-8 --- cell counting kit-8
 COMP --- cartilage oligomeric matrix protein
 DMA --- dynamic mechanical analysis
 DMEM --- Dulbecco's Modified Eagle's Medium
 DMM --- destabilization of the medial meniscus
 DMOAD --- disease modifying osteoarthritis drug
 ECM --- extracellular matrix
 FITC --- fluorescein isothiocyanate
 GAG --- glycosaminoglycan
 HA --- hyaluronic acid
 hAC --- human articular chondrocyte
 HIF-1 α --- hypoxia-inducible factor-1 alpha
 IGF-1 --- insulin-like growth factor-1
 IL-1 β --- interleukin-1beta
 iMAC --- immature murine articular chondrocyte
 MIA --- monosodium iodoacetate
 microCT (μ CT) --- micro-computed tomography
 MMP --- matrix metalloproteinase
 MRI --- magnetic resonance imaging
 MSC --- mesenchymal stem cells
 MT --- mutant
 NMR --- nuclear magnetic resonance
 NSAID --- nonsteroidal anti-inflammatory drug
 OA --- osteoarthritis
 PEG --- poly(ethylene glycol)
 PEGDMA --- poly(ethylene glycol) dimethacrylate
 Saf-O --- Safranin-O
 SBMA --- sulfobetaine methacrylate
 Smad --- highly conserved proteins that transduce extracellular signal in the TGF- β family.
 The abbreviation is a portmanteau of the homologs found in *caenorhabditis elegans* (SMA, proteins along the small pathway) and *drosophila* (MAD, mothers against decapentaplegic).
 Smurf2 --- Smad ubiquitin regulatory factor 2
 SPMA --- 3-sulfopropyl methacrylate
 TCPS --- tissue culture polystyrene
 TGF- β --- transforming growth factor-beta
 TNF- α --- tumor necrosis factor-alpha
 Wnt --- portmanteau of Wg (wingless-type MMTV integration site) and int-1
 WT --- wildtype

Copyrighted Materials Produced by the Author

This dissertation is a compilation of projects that have been published or submitted for publication. The citation associated with each chapter is listed below. The majority of work presented is originally obtained and analyzed by the author. Contributions from co-authors and other individuals are described in the acknowledgment section at the end of each chapter.

Chapter II:

Huang H, Veien ES, Zhang H, Ayers DC, Song J. Skeletal Characterization of Smurf2-Deficient Mice and In Vitro Analysis of Smurf2-Deficient Chondrocytes. *PLoS One*. 2016 Jan 27;11(1):e0148088.

Chapter III:

Huang H, Skelly JD, Ayers DC, Song J. Age-dependent Changes in the Articular Cartilage and Subchondral Bone of C57BL/6 Mice after Surgical Destabilization of Medial Meniscus. *Scientific Reports*. 2017 Feb 9; 7:42294

Chapter IV:

Huang H, Ayers DC, Song J. Anionic and zwitterionic residues modulate the stiffness of photo-crosslinked hydrogel and the cellular behavior of encapsulated chondrocytes. *Manuscript in preparation for submission*

Chapter I: Introduction

1. Osteoarthritis (OA)

Osteoarthritis (OA) is a degenerative disease of articular joints that leads to chronic pain and ultimately loss of function. It is characterized by articular cartilage degradation, subchondral bone sclerosis, osteophyte formation and varying levels of synovial inflammation. OA is the most common form of arthritis and is a major cause of chronic disability¹. At the individual level, it affects functions of daily living and reduces quality of life; while on a population level, it remains a significant socioeconomic burden due to lost wages and increased healthcare expenditure^{2,3}. Because age is the primary risk factor for OA development, the prevalence of OA is expected to rise as the human population continues to age. However, even among younger adults who are less than 65, hip and knee OA are on the rise as a result of the obesity epidemic and an increase in traumatic joint injuries^{4,5}.

In contrast to rheumatoid arthritis, which is ten times less prevalent than OA⁶ but has seen clinical success with numerous anti-inflammatory agents^{7,8}, there are currently no regulatory approved disease-modifying OA drugs (DMOADs). Clinical management of OA focuses on physical therapy and exercise in order to build strength and increase tolerance for joint function. In the context of obesity, weight loss along with exercise has shown the most significant reduction in joint pain and enhancement of function⁹. Joint pain is also pharmacologically managed with acetaminophen and non-steroidal anti-inflammatory drugs (NSAID), followed by intraarticular injections of hyaluronic acid (HA) or corticosteroids. After these non-surgical options have been exhausted, total joint arthroplasty is recommended for patients with severe pain and joint deformity. While the positive outcomes of joint replacement on pain relief, quality of life and physical function among the elderly is well-established^{10,11}, the need for DMOADs remains for the younger adults who are at higher risk for revision surgeries^{12,13} and can outlive the lifetime of their implants.

2. Challenges in Developing Disease Modifying OA Drugs

For years, the lack of research into DMOAD has been steered by the misperception that OA is a wear and tear disease caused by the natural aging process. Only in the past few decades have researchers acknowledged OA as a degenerative disease of the entire joint affecting multiple tissue compartments and involving numerous proinflammatory cytokines. While basic science research has uncovered many molecular signals involved in articular

cartilage degradation, subchondral bone sclerosis and synovial inflammation, the initiating factors and key regulators that drive disease progression remain poorly understood¹⁴. In addition, other challenges exist for the development of DMOADs, such as correlating imaging studies to disease progression and outcome measures, tackling the discrepancy between clinical symptoms and joint structure, and stratifying OA patients according to their disease presentation and clinical symptoms.

Even though the diagnosis of OA is based on clinical symptoms (chronic pain, stiffness, instability), imaging techniques remain the most objective assessment of joint structure to confirm the diagnosis and to monitor disease progression. Plain radiographs are the most convenient and cost-effective modality to indirectly monitor articular cartilage destruction through progressive joint space narrowing¹⁵. However, it is increasingly evident that plain radiographs are less sensitive to detect early OA changes compared to magnetic resonance imaging (MRI) regardless of pain¹⁶. MRI has become a dominant imaging modality among the research community to test DMOADs, allowing unparalleled assessment of multiple joint structures, including cartilage loss, synovial inflammation, meniscal tears, osteophytes, and bone marrow lesions¹⁷. In addition, various scoring systems such as the Whole Organ Magnetic Resonance Imaging Score (WORMS)¹⁸, Boston Leed Osteoarthritis Knee Score (BLOKS)¹⁹ and the MRI Osteoarthritis Knee Score (MOAKS)²⁰, have been developed over the years to provide semi-quantitative scores of OA-related changes detected on MRI. Although the responsiveness and reliability of MRI-based measurements of knee OA is being validated²¹, additional work is necessary to identify the key findings most predictive of OA severity and need for joint surgery²².

Another fundamental issue with developing OA drugs is the discrepancy between joint structure and clinical symptoms. Since cartilage is not innervated, pain associated with OA is thought to be a result of synovial inflammation and effusion²³. Meanwhile, joint space narrowing as measured by plain radiographs, remains the gold standard for assessing efficacy of DMOAD²⁴, and it is unclear whether countering these structural changes confers clinical benefit of reduced pain or increased function. Bedson and Croft have proposed that better standardized protocols of taking x-rays of the joint and standardized definition of knee pain could improve the correlation between radiographic knee and pain but evidence of a strong correlation is lacking²⁵. Therefore, it is more likely that clinical trials for OA therapy will be divided by drugs that relieve pain from those that modify joint structure. As the role of cytokines in OA pathogenesis becomes clearer and molecular crosstalks between structures are revealed, biological agents²⁶ targeting cytokines or growth factor receptors may eventually be effective at treating both pain and structural changes simultaneously.

Due to the multifaceted nature of OA and the presence of comorbidities, the disease impact and progression varies significantly among patients, and therapy should also be tailored accordingly. Numerous studies have utilized radiographic knee OA to stage disease progression^{27,28} and enhance its predictive value^{29,30}, but there is an increasing need for biochemical markers to assess dynamic changes within the joint and to detect early signs of joint abnormalities. The utility of biomarkers for diagnosing OA and directing therapeutic strategies is profound³¹. Ideally, they could facilitate early diagnosis of OA, stratify patients according to different OA symptoms, act as a surrogate for clinical endpoints and assess patient responsiveness to particular therapies. Many proposed candidates for OA biomarkers are related to the metabolism and degradation of bone or cartilage, including telopeptides of type I and II collagen and cartilage oligomeric matrix proteins (COMP). While some of these have shown promise in early clinical trials^{32,33}, none have shown sufficient discrimination to aid in the diagnosis or prognosis of individuals with OA³⁴. With continuous advances in molecular biology, imaging techniques, and next generation sequencing, the phenotyping of OA patients can improve and clinical endpoint for pharmacotherapy can be better defined.

3. Pathogenesis of OA

Articular Cartilage, Chondrocytes, and Cartilage Matrix Degradation

Although the pathogenesis of OA is multifactorial and its etiology remains largely unclear, the progressive destruction of articular cartilage remains a hallmark of the disease. Articular cartilage is a specialized tissue that lines the end of long bones. It provides a frictionless surface for movement and the mechanical forces to withstand compressive loads and shear forces. Articular or hyaline cartilage is a multiphasic tissue made up of 60-85% water, 15-20% of type II collagen, 4-7% of proteoglycan and only one cell type, the chondrocyte³⁵. The distribution and orientation of these extracellular matrix (ECM) proteins and chondrocytes are highly dependent on their location within cartilage as defined by 4 different zones (superficial/tangential, transitional/middle, deep and calcified) (Figure 1.1). The superficial zone, which provides the most resistance to shear forces, is made up of collagen fibers and chondrocytes oriented parallel to the surface. In contrast, the transitional or middle zone layers contain a mixture of randomly oriented collagen fibers and proteoglycans, which provide optimum resistance to compressive and tensile forces. The relatively inactive metabolism of chondrocytes in the superficial zone, however, increases its susceptibility to fibrillations and allows shear forces to penetrate into deeper layers³⁶. The deep and calcified zone contain collagen fibers oriented

perpendicular the surface and acts as an anchor for cartilage to the underlying subchondral bone and is thought to be an intermediary for force transmission between the two structures³⁷. During OA, the presence of multiple tidemarks also suggests that calcified cartilage can advance towards the deep zone and contribute to the thinning of the hyaline cartilage above³⁸.

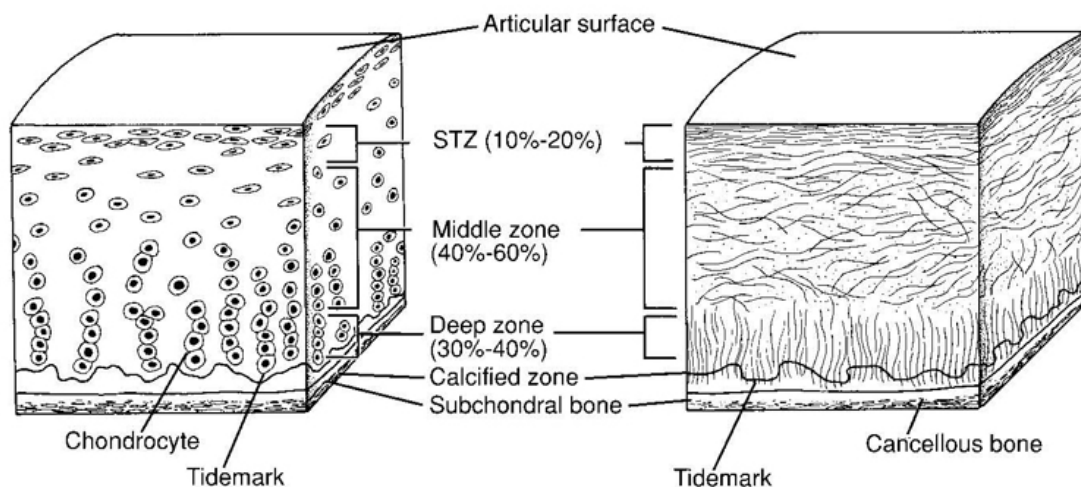


Figure 1.1 Depiction of chondrocyte and collagen fiber organization and the different zones in articular cartilage.

(STZ = superficial tangential zone) Figure is reproduced with permission from Buckwalter JA, Mow VC, Ratcliffe A. Restoration of Injured or Degenerated Articular Cartilage. *J Am Acad Orthop Surg.* 1994 Jul;2(4):192-201. http://journals.lww.com/jaaos/Abstract/1994/07000/Restoration_of_Injured_or_Degenerated_Articular.2.aspx

Resident chondrocytes, which are solely responsible for remodeling cartilage ECM, rarely undergo division after skeletal maturity and appear stable throughout adulthood. They maintain a low metabolic activity and low turnover rate of cartilage matrix proteins, with the half-life of cartilage collagen calculated to be over 100 years³⁹. As a consequence of aging⁴⁰ or other stressors like mechanical injury or inflammation⁴¹, the health of chondrocytes can be jeopardized and the balance between ECM production and degradation becomes dysregulated.

One evidence of this dysregulation is the phenotypic shift of resident chondrocytes towards hypertrophy, resulting in increased expression of type X collagen⁴² and proteolytic enzymes such as matrix metalloproteinases^{43,44,45} (MMP) and aggrecanases (ADAMTS)^{46,47}. During embryonic and postnatal skeletal development, chondrocytes undergo hypertrophy and apoptosis as part of endochondral ossification, where cartilage ECM is calcified and remodeled into bone⁴⁸. In the absence of disease, articular chondrocytes maintain their phenotype by inhibiting maturation, allowing them to produce the specific ECM proteins found in hyaline cartilage. Under aberrant conditions or stimuli, the adult resident chondrocytes are propelled towards terminal differentiation and apoptosis, initiating a seemingly irreversible signaling

cascade of cartilage degradation and mimicking the endochondral ossification process seen in development⁴⁹.

Signaling molecules driving chondrocyte hypertrophy have been identified from the creation of genetically-modified mice. While these factors do not demonstrate a causative effect, they provide insight and potential targets to reverse the hypertrophic chondrocyte phenotype. Many transcription factors have been shown to regulate chondrocyte hypertrophy (Figure 1.2A) such as runt-related transcription factor-2 (Runx2)⁵⁰, hypoxia-inducible factor-2alpha (HIF-2 α)⁵¹, Indian hedgehog (Ihh)⁵², beta-catenin (β -catenin)⁵³ and nuclear factor of activated T cells (NFAT)⁵⁴. Among these, Runx2 is a master regulator of chondrocyte hypertrophy and is a downstream target of multiple signaling pathways, including transforming growth factor-beta (TGF- β)⁵⁵, bone morphogenic protein (BMP) and Wnt/ β -catenin⁵⁶ (Figure 1.2B). A shift in signaling activation from the TGF- β to the BMP pathway is thought promote chondrocyte differentiation and hypertrophy. E3 ubiquitin ligases, such as Smad ubiquitin regulatory factors (Smurf) have also been linked to modulating intracellular Smads downstream of TGF- β /BMP signaling and can modulate Runx2 expression (Figure 1.2B). Whether Smurfs are involved in driving OA pathogenesis through chondrocyte differentiation and hypertrophy is not as clear.

Despite the involvement of these signaling molecules to drive chondrocyte hypertrophy, the exact cause of these aberrant signals remains unclear. Various stimuli, such as cartilage fragments caused by microtrauma or mechanical and oxidative stress^{57,58} from joint injury, are potential triggers for the release of proinflammatory cytokines from synoviocytes and/or chondrocytes to initiate the OA process. Indeed, proinflammatory cytokines (such as interleukin-8⁵⁹, S100 proteins⁶⁰, and NF κ B signaling^{61,62,63}) have been shown to accelerate the hypertrophic phenotype of chondrocytes. An interesting hypothesis proposed by Blaney Davidson et al. is that age can cause a change in cell surface receptor expression on chondrocytes leading to abnormal downstream signaling⁶⁴. They showed that an age-induced shift in activin-like kinase (ALK) receptors from ALK5 to ALK1 on mammalian chondrocytes resulted in TGF- β signaling activation via Smad1/5/8 to promote hypertrophy and MMP-13 expression⁶⁵.

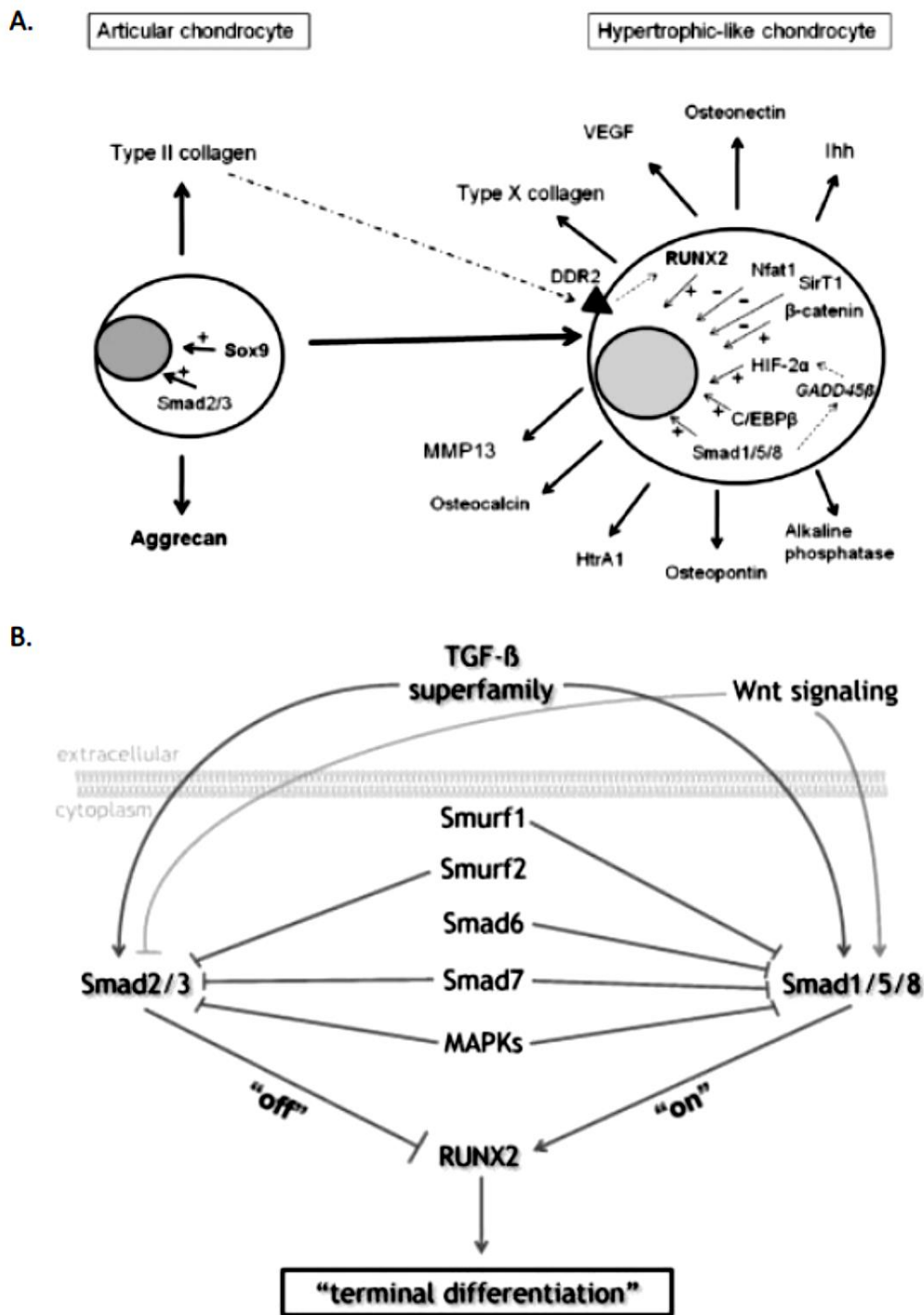


Figure 1.2 Overview of signaling pathways involved in chondrocyte hypertrophy.

(A) Transcriptional factors that modulate chondrocyte phenotype and the associated proteins that are secreted. Figure is reproduced with permission from van der Kraan PM, van den Berg WB. Chondrocyte hypertrophy and osteoarthritis: role in initiation and progression of cartilage degeneration? *Osteoarthritis Cartilage*. 2012 Mar;20(3):223-32. [http://www.oarsijournal.com/article/S1063-4584\(11\)00332-3/abstract](http://www.oarsijournal.com/article/S1063-4584(11)00332-3/abstract). (B) Regulation of downstream targets of the TGF- β superfamily affects chondrocyte hypertrophy. Figure is reproduced with permission from van der Kraan PM, Blaney Davidson EN, van den Berg WB. A role for age-related changes in TGFbeta signaling in aberrant chondrocyte differentiation and osteoarthritis. *Arthritis Res Ther*. 2010;12(1):201. <https://arthritis-research.biomedcentral.com/articles/10.1186/ar2896>

<https://arthritis-research.biomedcentral.com/articles/10.1186/ar2896>

Other than the phenotypic shift towards hypertrophy, aging naturally introduces changes in both cartilage matrix and chondrocyte function that predisposes to OA development. With age, the number of proteoglycans and the size of aggregates decreases⁶⁶ and the covalent crosslinking of type II collagen increases due to accumulated advanced glycation end products (AGEs)⁶⁷. The combination of the two results in a stiffer cartilage matrix with inferior mechanical properties to withstand compressive loads. In addition, aged chondrocytes also show a natural decline in synthetic function, and reduced sensitivity to growth factors such as insulin-like growth factor-1 (IGF-1)⁶⁸ and TGF- β ^{69,70}. Like other aged cells, chondrocytes also exhibit signs of senescence, with telomere shortening and increased staining for β -galactosidase activity^{71,72,73}. Mobasher et al. coined the term chondrosenescence to define the age-dependent deterioration of chondrocyte function highlighting changes in calcium signaling, ion channels, and mitochondrial dysfunction in oxidative stress response⁷⁴. Recently, both chondrocyte apoptosis^{75,76} and autophagy⁷⁷ have also gained traction as essential contributors to OA cartilage pathology, but it remains unclear whether age alone results the dysfunction of these cellular programs prior to OA. Caramez et al. have demonstrated a protective role of autophagy in normal cartilage, which becomes dysregulated with age and in a surgically-induced OA model⁷⁸. These types of cellular programming could account for the observation that cellularity in articular cartilage declines with age⁷⁹. Since apoptosis and autophagy are detected in early stages of OA⁸⁰, they remain potential therapeutic targets for preventing the onset of OA.

Subchondral Bone and Osteophytes

Other than cartilage degradation, abnormal bone modeling also occurs in OA. Subchondral bone plate thickening⁸¹ and osteophyte formation⁸² are dominant features of OA pathology and can be detected on plain radiographs. However, the mechanisms behind these two bone changes are thought to be very different.

The subchondral bone plate is the cortical bone directly beneath the calcified cartilage layer. Due to the close proximity of the subchondral bone to the overlying cartilage, both biochemical and mechanical crosstalks between these tissues have been thoroughly investigated⁸³. Pan et al. used fluorescein-labeled tracer perfusion and photobleaching techniques to show that small nutrients and signaling molecules can diffuse between articular cartilage and the subchondral bone⁸⁴. Older studies have also detected structural defects and signs of vascular invasion that connects subchondral bone to articular cartilage^{85,86}. Bone marrow lesions that can be detected on MRI are also more localized to areas of severe cartilage damage⁸⁷. These studies debunk the previous notion that calcified cartilage serves as an

impenetrable barrier for nutrients and biochemical signals between the two structures⁸⁸. Mechanical loading also directly affects both cartilage and subchondral bone, causing microcracks and splitting at the interface. Under repetitive microinjuries and mechanical weakening of the overlying cartilage, subchondral bone responds to the altered stimulus by initiating a faulty repair process. Although the overall bone volume appears to increase (sclerosis) as part of the repair process, mechanical testing of the sclerotic subchondral bone plate suggest a weaker structure with lower bone mineral density⁸⁹. Whether this faulty repair process is driven by cytokine signaling from hypertrophic chondrocytes or inflamed synoviocytes or abnormal mechanical loading, evidence has accumulated that subchondral bone osteoblasts are also dysfunctional. Primary human osteoblasts derived from OA subchondral bone show elevated alkaline phosphatase activity⁹⁰, osteocalcin⁹⁰, IFG-1⁹¹ and reduction in parathyroid hormone (PTH) receptors⁹². Cytokines, prostaglandins and growth factors produced from these sclerotic osteoblasts can further target chondrocytes and exacerbate the degenerative process in the overlying cartilage^{93,94}. These close interactions and interplay between cartilage and subchondral bone have led to the well-accepted concept of a bone-cartilage or osteochondral unit^{95,96,97}, in which the perturbation of one structure ultimately affects the function of the other.

Osteophytes are cartilaginous-bony outgrowths that are often localized to the periphery of the joint near the junction between cartilage and bone. The term osteophyte also encompasses the term chondrophyte, which refers to outgrowths that are predominantly composed of cartilage matrix. Unlike subchondral bone, it is unclear whether osteophytes have a functional role or if they develop secondary to other degenerative changes in the joint. One hypothesis is that osteophytes counter the mechanical instability in a diseased joint by pushing against slackened ligaments or limiting range motion^{98,99}. However, conflicting evidence also suggests that osteophytes develop independently from other changes in the joint. For instance, in both mouse and dog models of OA, osteophyte formation can be detected as early as 2-3 days after OA induction^{100,101}. Nevertheless, a number of clinical studies have confirmed a greater association with disease severity based on the presence and size of the osteophyte alone^{102,103,104}. Osteophytes are thought to derive from mesenchymal progenitor cells in the periosteum or synovium in response to abnormal mechanical loads¹⁰⁵. Although a number of different characterization¹⁰⁵, scoring criterion¹⁰⁶ and classification¹⁰⁷ of osteophytes have been performed, it remains a challenge to histologically assess osteophytes in humans and to correlate it with other degenerative changes. Nevertheless, osteophytes can contribute to joint pain through invasion of nerves through the marrow-like cavity and limit movement in OA

patients, so therapies that inhibit their formation could still relieve symptoms and maximize function.

Synovial Inflammation and Proinflammatory Cytokines

In healthy joints, the synovium is responsible for producing lubricin and hyaluronic acid (HA). They are the major components of the synovial fluid, which help protect cartilage¹⁰⁸, provide a frictionless surface¹⁰⁹ and regulate chondrocyte activity^{110,111}. When the synovium becomes inflamed, inflammatory cytokines and proteolytic enzymes are released into the synovial fluid and can drive chondrocyte catabolism. Synovitis is detected in both early and late OA¹¹² and is thought to contribute to both pain^{113,114} and OA progression¹¹⁵. Historically, OA is not considered an inflammatory arthritis like RA due to a lack of immune cells in the synovial fluid and synovium, but the effects of proinflammatory cytokines on OA pathology has increasingly become evident¹¹⁶. Several key catabolic cytokines that are upregulated in OA include interleukin-1beta (IL-1 β), tumor necrosis factor-alpha (TNF- α), interleukin-6 (IL-6) and interleukin-8 (IL-8)^{117,118}.

The impact of IL-1 β activity in the joint is extensive and detrimental, partly because chondrocytes, osteoblasts and synoviocytes can all produce and respond to it during inflammation. *In vitro* culture of human chondrocytes shows that IL-1 β is a potent inhibitor of cartilage matrix synthesis by reducing type II collagen and aggrecan and increasing proteolytic enzymes like MMP-3 and MMP-13^{119,120,121}. Furthermore, the cell surface receptors for IL-1 β are increased in both OA chondrocytes¹²² and synovial fibroblasts¹²³, implying an increased sensitization to the catabolic effects of IL-1 β . IL-1 β also has a significant impact on regulating other cytokines and growth factor signaling. IL-1 β can stimulate the production of IL-6¹²⁴ and IL-8¹²⁵, which further tips the balance of cartilage matrix proteins towards catabolism and enhances the inflammatory process. IL-1 β can also counter the anabolic effects of TGF- β signaling by increasing the inhibitory protein, SMAD7 and reducing TGF- β receptor expression¹²⁶.

TNF- α , like IL-1 β , is also a major cytokine involved in OA pathogenesis. Because they share the same downstream signaling pathway that leads to NF κ B activation⁶³, TNF- α also inhibits chondrocyte synthesis of type II collagen¹²⁷ and proteoglycans¹²⁸. They can also modulate mitochondrial function¹²⁹ and increase production of reactive oxygen species^{130,131}. Compared to IL-1 β , TNF- α is less effective and less potent at inducing an inflammatory response and does not cause significant proteoglycan loss *in vivo*¹³². However, a combination of

these two cytokines is found to be synergistic at recruiting leukocytes to the synovium¹³². Another study also found that TNF- α and IL-1 β inhibits the migration of chondrogenic progenitor cells *in vitro*, highlighting a new role for these cytokines to impair the cartilage healing process¹³³.

The production of IL-6 and IL-8 are most likely a consequence of IL-1 β activity¹³⁴ but can also be induced by advanced glycation end products¹³⁵. While these cytokines share similar effects such as promoting cartilage catabolism^{136,137} and recruiting inflammatory cells to the synovium^{137,138}, other conflicting evidence exists about their exact role. For instance, knocking out IL-6 resulted in more advanced OA with age or in a collagenase-induced OA model¹³⁹. A possibility is that IL-6 could have some proanabolic and anti-inflammatory effects in early OA but may alter with age or at different stages of the disease. IL-6 is also thought to be an important cytokine in regulating osteoblast physiology¹⁴⁰. Application of nonphysiological loads on osteoblasts derived from osteophytes induces both IL-6 and IL-8 production, suggesting that osteophytes could contribute to OA pathology through an inflammatory process¹⁴¹.

4. Clinical Trials of Potential OA Drugs

It is clear that many overlapping signaling pathways and joint structures are involved in OA (Figure 1.3). Through the use of genetically-modified mice, many potential targets for DMOADs have been proposed. These targets range from modulating chondrocyte behavior (catabolism, anabolism, metabolism, and differentiation), to remodeling subchondral bone and inhibiting synovial inflammation. Unfortunately, very few of these have yet to progress to larger animals or preclinical human trials. While the lack of a specific enough small molecule drug could be a limiting factor, unimpressive clinical results have also deterred the translation of our mechanistic understanding of OA to clinical therapies.

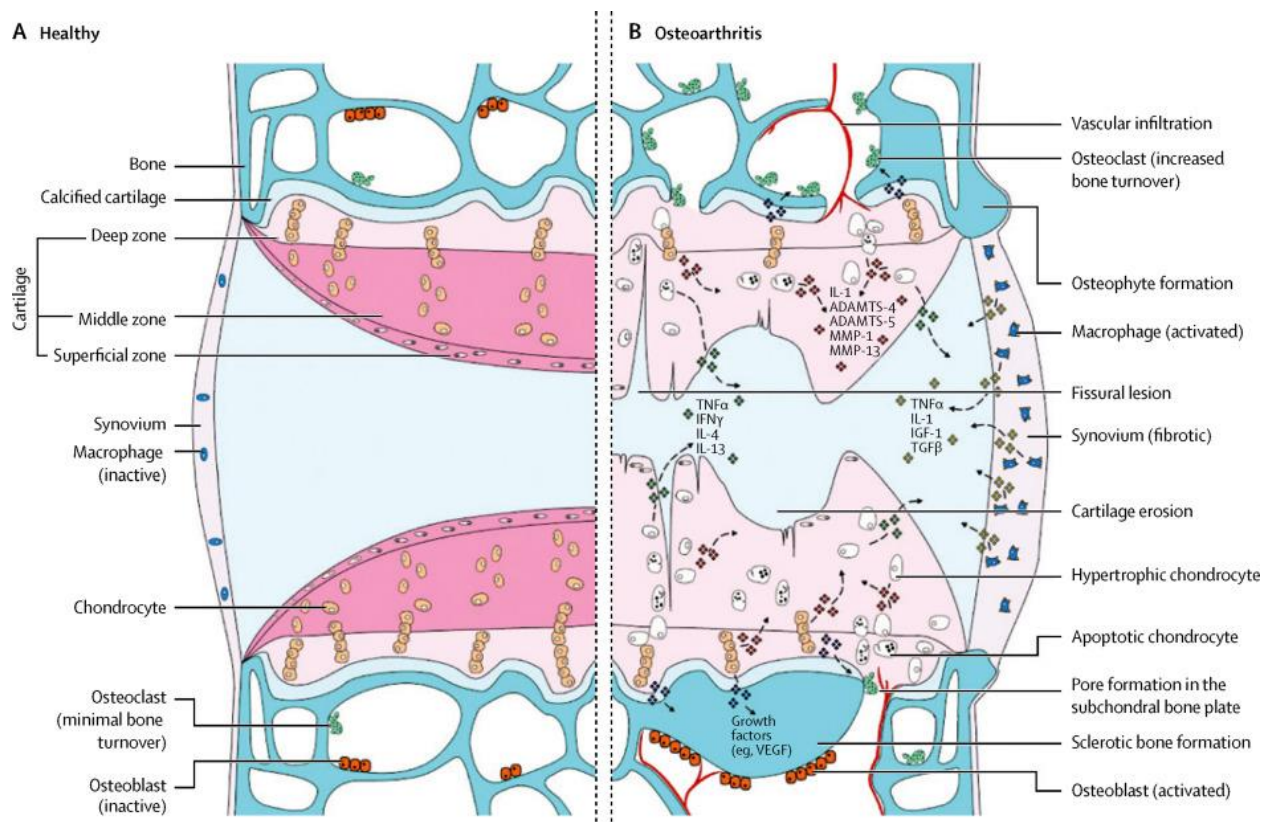


Figure 1.3 Overview of signaling pathways and structural changes in the development of OA.

ADAMTS=a disintegrin and metalloproteinase with thrombospondin-like motifs. IL=interleukin. MMP=matrix metalloproteinase. TNF=tumour necrosis factor. IFN=interferon. IGF=insulin-like growth factor. TGF=transforming growth factor. VEGF=vascular endothelial growth factor. Figure is reproduced with permission from Glyn-Jones S, Palmer AJ, Agricola R, Price AJ, Vincent TL, Weinans H, Carr AJ. Osteoarthritis. *Lancet*. 2015 Jul 25;386(9991):376-87. [http://www.thelancet.com/journals/lancet/article/PIIS0140-6736\(14\)60802-3/abstract](http://www.thelancet.com/journals/lancet/article/PIIS0140-6736(14)60802-3/abstract)

One major setback has been the lack of clear evidence that anti-inflammatory biologics can modulate OA progression in humans. It is well-established that proinflammatory cytokines like TNF- α and IL-1 β are key mediators of chondrocyte dysfunction and cartilage loss. Blocking IL-1 β activity in animal OA models also showed chondroprotective effects^{142,143}. However, human clinical trials comparing IL-1 receptor antagonists to placebo showed some pain relief in knee OA but no improvement in function as determined by the Western Ontario and McMaster Universities Osteoarthritis Index (WOMAC) scores¹⁴⁴. In another study, human monoclonal antibody to IL-1 receptor type I also showed a non-significant but numerical improvement in pain¹⁴⁵. Further optimization in dosing strategy or extending the half-life of the protein could yield different clinical results. Also, inhibitors of IL-1 β may also be more effective in a subset of OA patients with more severe pain and signs of inflammation.

On the other hand, there is an increasing effort from the clinical side to use existing small molecule drugs or biologics to target known degenerative changes in the joint. For

instance, many drugs used for the treatment of osteoporosis are being investigated as potential treatment for OA. Since subchondral bone remodeling in OA parallels osteoporosis in that it results in a mechanically weak bone with low mineral density, antiresorptive agents like bisphosphonates are being evaluated as a potential DMOAD¹⁴⁶. The disease modifying effects of bisphosphonates was demonstrated in a surgically-induced OA rat model¹⁴⁷, but not in studies using a spontaneous OA guinea pig model^{148, 149}. Several human prospective randomized clinical (RCT) trials showed that risedronate reduced markers of cartilage degradation like CTX-II and NTX-1 but with no improvement in WOMAC scores or structural changes^{150,151}. Clinical benefit was observed in one study, showing that maintaining low levels of CTX-II with risedronate for six months lowered risk of radiographic progression at 24 months¹⁵². Another drug that is used to treat severe osteoporosis in other countries but not the US is strontium ranelate. Clinical trials using strontium ranelate showed clinically meaningful improvements in pain as well as joint function¹⁵³, but the drug's risk for cardiovascular events such as myocardial infarction and venous thromboembolism should be carefully addressed.

Statins, which are a class of cholesterol lowering drugs, are also hypothesized to be a potential DMOAD by regulating metabolically-induced inflammation in OA¹⁵⁴. Since existing data associating statin use with incidence of OA are inconclusive^{155,156}, a prospective randomized clinical trial evaluating atorvastatin on OA progression is currently ongoing in Australia¹⁵⁷. Other drugs that have been tested in humans but failed to reach a meaningful clinical endpoint include doxycycline^{158,159}, vitamin D supplementation¹⁶⁰, and salmon calcitonin¹⁶¹.

5. Spontaneous and Induced Mouse Models of OA

Basic science research investigating potential molecular targets for DMOADs rely on genetically-modified mice to tease out the molecular signals involved in OA. While no OA mouse model fully recapitulates the human OA exactly, the similarities in disease manifestation are sufficient to uncover potential modulators. Mice colonies are relatively easy to maintain and expand and are much more affordable to achieve statistically significant results than larger animals. Ninety-nine percent of mouse genes match to the human genome¹⁶², and the shorter lifespan of mice makes them ideal for conducting age-related studies. Over the years, a number of different strategies have been developed to study OA progression in mice. They can be divided into spontaneous and induced models, with the latter being subdivided into non-surgical and surgical interventions.

Mice strain with spontaneous OA.

Many inbred mice show a natural tendency to develop OA with age, but the incidence and severity of the disease varies widely with the strain, highlighting the importance of genetic risk factors in OA development. The STR/ort strain is the most commonly studied mouse for spontaneous OA and shares the same degenerative joint changes as humans¹⁶³. The parental CBA strain, which does not develop spontaneous OA, serves as an effective control. While the advantage of such a model is that it mimics the slow progression of primary OA in humans, it is also more susceptible to varying outcomes of incidence and severity and requires a larger number of animals to power a study¹⁶⁴. Other phenotypes such as obesity¹⁶⁵, hepatomas, and altered metabolism (hypercholesterolemia, hyperlipidemia, anemia)¹⁶⁶ that are not observed in the CBA strain can also confound the interpretation of specific causal relationships in this OA model. Since the STR/ort strain results in predictable and distinct stages of OA development, it could be beneficial for evaluating new therapeutic agents. However, the duration of treatment ranging from 8-30 weeks could be a discouraging factor¹⁶⁷.

Genetically modified mice with OA-like symptoms

The ease of manipulating the mouse genome has led to numerous transgenic mice that develop an OA-like phenotype. In most cases, this involves knocking out a gene or knocking in a constitutively active gene that is suspected to be involved in OA development. Because the exact phenotype is not predictable, extensive biochemical and histological characterization is necessary to understand the exact pathology and determine whether it relates to OA. Several cartilage-specific genes that accelerate a spontaneous OA-like phenotype include knockouts of type IX collagen¹⁶⁸, peroxisome proliferator-activated receptor gamma (PPAR γ)¹⁶⁹, von Hippel–Lindau gene (Vhl)¹⁷⁰, and constitutive expression of genes like MMP-13¹⁷¹. In cases where no age-dependent OA phenotype is observed such as in TGF- β receptor¹⁷², fibroblast growth factor receptor 1 (FGFR-1)¹⁷³ or ADAMTS-4 and -5^{174,175} knockout mice, other strategies to induce ‘secondary’ OA are required.

Non-surgical induction of OA

Non-surgical induction of OA typically refers to intraarticular injection of a chemical agent like monosodium iodoacetate (MIA) developed by Kalbhen¹⁷⁶ or a catabolic agent like collagenase. An advantage of using these injections is the ability to induce OA in any joint, and

they can easily be applied to other non-rodent species. MIA is an inhibitor of glycolysis and is thought to initiate OA rapidly through its cytotoxic effect on chondrocytes. Histological analysis of knee joints a week after single injection of MIA shows severe chondrocyte death and collapse of cartilage structure, but synovial inflammation and subchondral bone changes were less apparent¹⁷⁷. Due to its non-physiological mechanism and accelerated OA phenotype, the use of MIA for studying OA progression is no longer favored. More recently, MIA was used in mice¹⁷⁸ and rats^{179,180} to evaluate OA pain as measured by tactile allodynia, asymmetric weight bearing and forced ambulation.

Unlike MIA, collagenase-induced OA has a latency period in which proteoglycan synthesis is maintained during the first month, followed by progressive degradation of the cartilage structure¹⁸¹. The differences in timing and severity of affected structures suggest a difference in etiology between these two methods. Collagenase indirectly causes joint instability by damaging type I collagen and increases the laxity of ligaments and tendons surrounding the joint¹⁸². On the other hand, like MIA, collagenase fails to induce a strong inflammatory response in the synovium, with symptoms resolving within 1 week and a lack of IL-1 activity thereafter¹⁸³. Therefore, while much more gradual at inducing OA, collagenase may not reflect some of the major cytokines players involved in human OA.

Although not as popular among researchers, non-invasive injury is another non-surgical induction of OA that is gaining interest over the years. These include intra-articular fracture of the tibial subchondral bone¹⁸⁴, cyclic tibial compression loading¹⁸⁵, and anterior cruciate ligament (ACL) rupture via tibial compression¹⁸⁶. A major advantage of this type of OA model is to mimic the mechanical traumas seen in human joints such as motor vehicle accidents or in sports-related ACL tears. These aseptic techniques allow assessment of early inflammatory and cellular response and avoid the skin incision and capsulotomy, which are required for surgically-induced models¹⁸⁷. Because these methods are still in their infancy, emphasis should be placed on reproducibility, proper controls and correlation to human OA.

Surgical induction of OA

Surgical induction of OA combines joint destabilization, intraarticular inflammation and abnormal contact between cartilage surfaces to reflect a post-traumatic state. Surgical models were initially developed in larger animals such as the anterior cruciate ligament transection (ACLT) in dogs¹⁸⁸ and the partial meniscectomy in rabbits¹⁸⁹. These techniques were later applied to small animals like rats¹⁹⁰ and guinea pigs¹⁹¹. Compared to non-invasive injuries,

surgical injury models are more precise in that they create specific cuts and damage to ligament(s) and/or the meniscus. However, gaining access inside the joint is an additional burden to the animal. Furthermore, performing the surgery often requires proper training and practice with microsurgical tools and the reproducibility among researchers is a concern.

The earliest surgical induction of OA in mice was described by Visco et al. using a partial medial meniscectomy and medial collateral ligament transection¹⁹². Using this technique, Clements et al. showed that loss of IL-1 β and IL-1 β -converting enzyme led to an accelerated OA after surgery¹⁹³. This was soon followed by Kamekura et al. who demonstrated that the severity of OA progression after surgery can be modulated by the severity of the injury (i.e. number of transected ligaments and involvement of the meniscus)¹⁹⁴. In their study they focused on ACLT and how the addition of other ligament transection and/or meniscectomy accelerated the OA phenotype post-surgery (Figure 1.4). The combination of these different surgical procedures allows assessment of different stages of OA without needing to wait for disease progression.

In comparison to ACLT, Glasson et al. proposed a new surgical instability model that involves destabilization of the medial meniscus (DMM) by transecting the meniscotibial ligament (shown in green in Figure 1.4)¹⁹⁵. Their results show that DMM results in a mild OA phenotype with a reproducible cartilage lesion in the center of the medial tibial plateau. Moreover, the peripheral nature of the meniscotibial ligament makes the surgery much easier to perform than ACLT. Over the years, the DMM model has become a gold standard for studying OA onset and progression in many transgenic mice¹⁹⁶. Potential therapeutic agents such as rapamycin¹⁹⁷, resveratrol¹⁹⁸, proteasome inhibitor MG132¹⁹⁹ and kartogenin²⁰⁰ have all been demonstrated to inhibit OA progression in the DMM model.

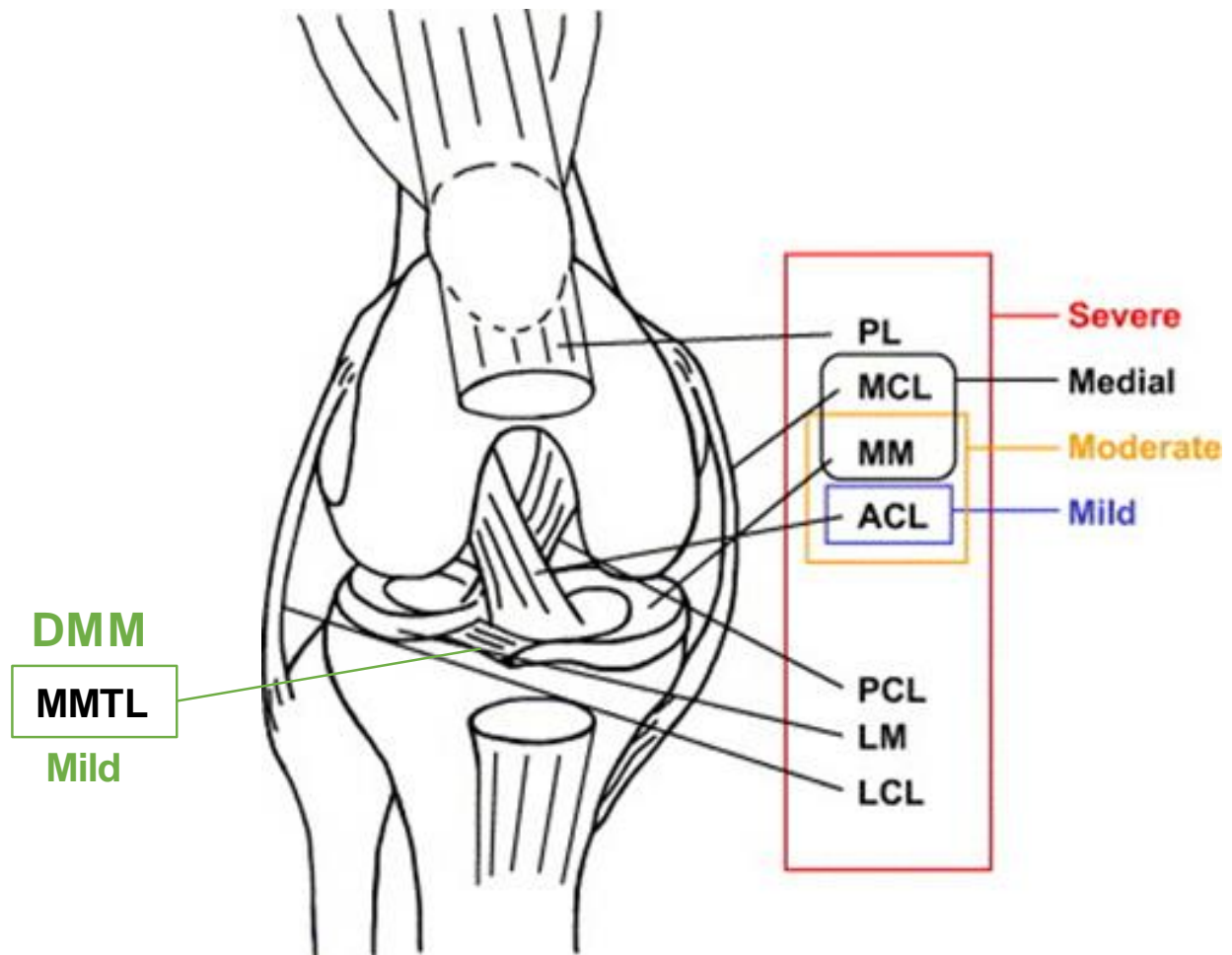


Figure 1.4 Diagram of mouse knee and the combination of ligament transections and meniscectomy needed to induce different severity of OA.

PL=patellar ligament. MM=medial meniscus. LM=lateral meniscus. MCL=medial collateral ligament. LCL=lateral collateral ligament. ACL= anterior cruciate ligament. PCL=posterior cruciate ligament. MMTL=medial meniscotibial ligament. DMM=destabilization of the medial meniscus surgery. Figure is adapted from Kamekura S, Hoshi K, Shimoaka T, Chung U, Chikuda H, Yamada T, Uchida M, Ogata N, Seichi A, Nakamura K, Kawaguchi H. Osteoarthritis development in novel experimental mouse models induced by knee joint instability. *Osteoarthritis Cartilage*. 2005 Jul;13(7):632-41.

6. Tissue Engineering Strategies to Repair Articular Cartilage Defects

Post-traumatic OA and Articular Cartilage Damage

OA that develops after a documented incident resulting in articular fracture, cartilage or meniscal damage is termed post-traumatic OA. Approximately 12% of all symptomatic OA is estimated to be post-traumatic OA²⁰¹. Even though the progression to OA after an injury is poorly documented, patients who develop post-traumatic OA are on average 10 years younger

than those who develop primary OA²⁰¹. This gap between joint injury and OA onset is a potential window of opportunity for medical therapy to intervene.

However, treating articular cartilage damage is a clinical challenge due to the lack of innate repair mechanisms. Cartilage lesions are categorized as non-structural (alterations in composition of matrix proteins), partial thickness, full thickness (subchondral bone surface is exposed), or osteochondral (if the subchondral bone is also damaged)²⁰². Unlike the degenerative changes seen in OA, chondral defects are usually focal, well-defined and surrounded by healthy tissue. These defects are often a result of blunt-force trauma experienced during sports or accidents²⁰³. Regardless of whether the defect heals spontaneously or heals through bone marrow stimulation (microfracture)²⁰⁴, the result is a type I collagen-rich fibrocartilage that does not confer the same mechanical or lubricating properties as hyaline cartilage. Eventually, fibrocartilage also degrades and progressive damage originating from the initial lesion will accelerate OA development²⁰⁵. Therefore, the ideal treatment for cartilage lesions is still to promote cartilage regeneration²⁰⁶ or at the very least, to inhibit progressive damage by resurfacing the defect with a matrix similar in composition and mechanical strength to hyaline cartilage.

Cartilage Tissue Engineering

Tissue engineering is an interdisciplinary approach to replace or regenerate tissue using a combination of cells, biomaterials and/or bioactive molecules²⁰⁷. Whether there is a limited healing capacity or a defect in the repair process (caused by disease or trauma), tissue engineering attempts to overcome these challenges by enhancing innate repair processes, facilitating the growth of new tissue *in situ*, or delivering a tissue-like structure that was grown *ex vivo*. For cartilage tissue engineering, this often involves progenitor cells that recapitulate the developmental process of new cartilage formation²⁰⁸, biomaterials that exhibit mechanical strength similar to native cartilage or function as a bioactive template for regenerative processes, or pre-assembled chondral/osteochondral-like constructs that is implanted and integrated with neighboring tissue²⁰⁹. The immune privileged site of cartilage and the misconception that it is a relatively homogenous structure led many to believe that the success of cartilage tissue engineering was inevitable. Early work by Freed et al. showed that bovine chondrocytes seeded on a synthetic porous scaffold *in vitro* and *in vivo* produced a cartilage-like ECM (dominated by type II but not type I collagen)²¹⁰. Since then, many new biomaterials have been developed,

alternative cell types such as stem cells have been investigated, and fundamental biology relating to chondrogenesis and chondrogenic differentiation have been uncovered.

Despite these advances in research, over two decades have passed and the only clinical progress for cartilage repair is in autologous chondrocyte implantation (ACI) that Brittberg et al. pioneered²¹¹. To effectively translate cartilage tissue repair research to clinical therapies, many challenges and unanswered questions need to be addressed²¹². Some of these involve 1) determining the cell type most suitable for producing hyaline cartilage but which can also be expanded to sufficient quantity²¹³, 2) scaling up scaffolds without compromising nutrient diffusion²¹⁴, 3) determining whether recapitulating zonal architecture of cartilage is necessary for long-term function and stability²¹⁵, 4) facilitating integration of neocartilage with native tissue²¹⁶, and 5) overcoming regulatory restrictions on introducing new cell-biomaterial constructs in humans^{217,218}.

Natural versus Synthetic Hydrogels

Hydrogel is an attractive material for cartilage tissue engineering due to its innate water absorbing capacity that is reminiscent of native cartilage. The ability of hydrogels to encapsulate cells within a 3D network can also maintain their spherical morphology and prevent dedifferentiation²¹⁹. Hydrogels derived from both natural and synthetic polymers have been explored for cartilage tissue engineering and each has its own advantages and disadvantages.

The inspiration behind natural polymer-based hydrogels is to mimic macromolecules found in native cartilage, such as collagen^{220, 221}, hyaluronic acid (HA)²²², and glycosaminoglycans (GAGs)²²³. As a result, these macromers are inherently biocompatible and possess many bioactive cues that assist in directing encapsulated cells' behavior. Even though covalent chemical modifications of these macromers are often required to create a gelation reaction through photopolymerization²²⁴ or click chemistry²²⁵, the degree of modification is often poorly controlled and characterized. Other disadvantages of these natural hydrogels are their mechanically weak structure and their poorly controlled rates of degradation²²⁶.

On the other hand, hydrogels derived from biocompatible synthetic polymers such as poly(ethylene) glycol are versatile and can be easily manipulated to achieve different mechanical or chemical properties or 3D printed into different shapes and structures. The incorporation of ester-containing polymers such as polyglycolic acid (PGA) and polycaprolactone (PCL) also introduce tunable rates of degradation into the hydrogel to hypothetically match the formation of neotissue from encapsulated cells. While the advantage of

being biocompatible renders these polymers biologically inert, these hydrogels are often combined with growth factors²²⁷ or native cartilage macromolecules in order to enhance their bioactivity²²⁸.

Cell Types

Since chondrocytes are the only cells that reside in cartilage and are solely responsible for producing and maintaining cartilage ECM, it is intuitive to use them for cartilage repair. Currently, ACI is the only FDA-approved cartilage repair technique that has shown promise for producing hyaline-like matrix. The procedure involves harvesting autologous chondrocytes from a non-weight bearing location, expanding them *in vitro*, then implanting the cells mixed with a collagen-rich solution and covering the defect site with a periosteal autograft²¹¹. The main advantage of autologous chondrocytes is the lack of immune rejection from the host, but harvesting chondrocytes requires another surgical procedure and the donor site can lead to additional morbidity in patients²²⁹. Due to the low number of chondrocytes at time of harvest, *in vitro* expansion of these cells is required to achieve sufficient quantity for a larger defect site. However, primary chondrocytes tend to 'dedifferentiate' or lose their chondrogenic phenotype when expanded in 2D tissue culture plates (TCPS)²³⁰ and will most likely lead to fibrocartilage after implantation.

In order to overcome the limitations of autologous chondrocytes, an alternative cell type for cartilage tissue repair is the stem cell. A potential source of stem cells in adults is the bone marrow. Bone marrow stromal cells (BMSC), sometimes referred to as mesenchymal stem cells (MSC), were first isolated by Freidenstein et al.²³¹ and later characterized to show trilineage differentiation into adipocytes, osteocytes and chondrocytes²³². Successful repair of an osteochondral defect in rabbits was performed by Wakitani et al. using autologous BMSCs and a collagen gel²³³. They demonstrated successful tissue repair with BMSCs differentiating into chondrocytes and undergoing endochondral ossification to restore the subchondral bone. More importantly, their results suggested that *in vitro* expansion of BMSCs did not lead to a loss of differentiation potential. Many tissue engineering studies soon followed to investigate BMSCs growth and differentiation with many biomaterials²³⁴ and in combination with growth factors such as TGF- β ^{235,236,237} and BMP²³⁸ to aid in differentiation and matrix production. Other properties of BMSC that aid in tissue repair process include hypoimmunogenicity²³⁹, immunosuppression²⁴⁰ and chemotaxis²⁴¹.

Although research interest in stem cells has grown exponentially, it is unclear whether the tissues grown from stem cells are any different than those grown from chondrocytes. A small study by Nejadnik et al. compared cartilage repair using autologous chondrocytes or BMSCs and showed that both groups had similar tissue composition and comparable improvement in patient function²⁴². However, patient age appears to affect outcomes measures in the chondrocyte group, but not in the BMSC group, suggesting that age may impair chondrocyte function more easily than stem cells. While the replacement of autologous chondrocytes with BMSCs seem inevitable in the future due to accessibility of bone marrow, multilineage potential, and simplification of surgical procedure, many challenges still remain for BMSCs. For one, the precise control of BMSC differentiation is critical for cartilage repair since over differentiation could result in a hypertrophic phenotype²⁴³ or an undesired cell type. Isolation of BMSCs through plastic adherence results in a heterogeneous population that can also affect culture expansion and differential potential²⁴⁴. Cell surface markers are heavily studied to help enrich for a more homogenous stem cell population²⁴⁵ but the ideal profile for BMSCs has yet to reach consensus among researchers.

Biochemical, Mechanical and Other Cues that direct Chondrocyte Behavior

Hydrogels derived from synthetic polymers are biocompatible but at the same time also bioinert. In order to enhance the healing properties of cells delivered within them, bioactive molecules are often incorporated to prompt cell differentiation or augment matrix production. Bioactive molecules can range from proteins like cytokines and growth factors²⁴⁶ to smaller chemical molecules, peptides²⁴⁷ or nano-sized particles^{248,249,250}. Growth factors such as TGF- β ²⁵¹, BMP²⁵², IGF-1²⁵³, and fibroblast growth factor (FGF)²⁵⁴ are frequently co-delivered with hydrogels to enhance chondrogenesis. Native biomacromolecules such as chondroitin sulfate and hyaluronic acid are also thought to be prochondrogenic due to their unique chemical composition that facilitates cell-matrix interaction and enriches secreted growth factors. Peptides containing the arginine-glycine-aspartic Acid (RGD) motif are also frequently tethered onto biomaterials to enhance cell attachment via integrin binding. Even though RGD motifs can facilitate chondrocyte attachment and proliferation, evidence also suggests that too much incorporation can alter their rounded morphology and lead to decreased ECM production²⁵⁵.

Dynamic mechanical loading also play a critical role in modulating chondrocyte behavior. Given that the joint experiences stresses from 10-20 MPa on a daily basis, deformation of cartilage and the chondrocytes is essential to distribute the load and reduce contact stress²⁵⁶.

Mechanical loads, either applied directly²⁵⁷ or in the form of hydrostatic pressure²⁵⁸, have been shown to modulate chondrocyte metabolism and matrix synthesis. They are also frequently used to enhance tissue engineered cartilage constructs *ex vivo* via a bioreactor²⁵⁹. Mechanical stimulation can also be combined with anabolic growth factors for synergistic effects²⁶⁰. Along the same lines, the interaction between material and chondrocytes can also induce mechanical signal transduction or alter metabolic activity in order to direct chondrocyte behavior. Chondrocytes cultured on stiffer materials produce less ECM than those cultured on softer matrices^{261,262}. However, one study also suggests that chondrocytes prefer an optimal material stiffness (~0.5 MPa) for chondrogenesis²⁶³, highlighting the need to establish sufficient structural support for chondrocytes at time of implant. Furthermore, this mechanical integrity of the scaffold will need to be maintained during competing processes of ECM matrix production and scaffold resorption.

Finally, oxygen tension also plays a role in chondrocyte behavior. Since cartilage is avascular, chondrocytes reside in a hypoxic environment with oxygen levels ranging from 7% near the surface to 1% near the subchondral bone²⁶⁴. Chondrocytes cultured in a hypoxic environment (5%) shows enhanced chondrogenesis and reduced catabolic gene expression compared to normoxic conditions (20%)²⁶⁵. This is most likely due in part to reduced nitric oxide (NO) production²⁶⁴, a mediator of proinflammatory cytokines in the joint, and upregulation of HIF-1 α ²⁶⁶, which directly affects chondrocyte metabolism, matrix production and differentiation²⁶⁷.

7. Overview of Dissertation

OA is a significant burden on an aging population and contributes to reduced quality of life and increased healthcare spending. Because no current DMOADs exist, there is a desperate need to identify new targets and therapies that can delay the onset or progression of OA and postpone joint replacement.

This dissertation examines two parallel strategies to promote translational therapies for OA. Chapter II investigates whether Smad ubiquitin regulatory factor 2 (Smurf2), an E3 ubiquitin ligase, is required for OA pathogenesis and whether it is a viable target for DMOADs. Since Smurf proteins (Smurf1 and Smurf2) have been identified as a modulator of Smad proteins in TGF- β signaling, it was hypothesized that knock down of Smurf2 could perturb the behavior of chondrocyte and/or osteoblast phenotype *in vivo*. In addition, Smurf2 has been implicated as a regulator of senescence and could potentially modulate age-dependent factors that drive OA

pathogenesis. Skeletal characterization of Smurf2-deficient (MT) mice were compared with wild-type mice in an age-dependent manner and in a surgically-induced OA model. MT primary chondrocytes were also characterized to determine if the balance between cartilage matrix synthesis and degradation under chondrogenic and proinflammatory environments were perturbed compared to WT mice. Young MT mice showed milder cartilage OA damage after DMM surgery compared to age-matched WT. However, this protective effect was diminished in the older mice. MT primary chondrocytes expressed higher levels of chondrogenic mRNA compared to WT *in vitro*, but the difference was not detected at the protein level. These results highlight a potential role of Smurf2 to modulate OA but suggest that age-related factors or proteins with redundant Smurf2 function may limit the therapeutic efficacy of Smurf2 inhibition alone.

Due to the differences observed in cartilage degradation between young and old mice after DMM, Chapter III takes a deeper look at the structural changes in the knee joint post DMM with respect to both age and sex. Using a combination of histology and microCT, this chapter highlights how age modulates the structural changes of different tissue compartments in response to DMM surgery. The susceptibility of female mice to DMM-induced OA is also increased with age but compared to male mice, they remain protected up to 18 months of age. These results supplement existing knowledge about DMM-induced OA in mice but also question the validity of such a model to identify disease modifying targets that is translatable to primary OA in humans.

In Chapter IV, we turn towards tissue engineering strategy of repairing articular cartilage lesions. Because unrepaired focal articular cartilage lesions increase the risk of developing OA early, promoting hyaline cartilage formation in these defect sites using a cartilage tissue engineering approach could delay the onset of OA. A challenge with using synthetic hydrogels as a scaffold is balancing the mechanical strength to resist compressive loads without compromising nutrient transport and inhibiting chondrogenesis of encapsulated cells. This chapter investigates whether incorporation of synthetic chemical residues into a bioinert hydrogel could enhance its mechanical properties and promote matrix production by encapsulated chondrocytes. Covalent incorporation of small anionic or zwitterionic chemical residues in a polyethyleneglycol-based hydrogel improved its stiffness and resistance to fluid flow; however, at a certain incorporation content, the resulting stiffer environment also exerted a dominant negative effect on matrix production. These results suggest that modulating the biosynthesis of chondrocytes with biochemical signals may requires a concurrent reduction in

conflicting mechanotransduction signaling, emphasizing the concurrent need for controlling degradation to promote new cartilage formation.

In the final chapter, key findings of this dissertation are summarized and their impact on future work relating to OA therapy is highlighted.

Chapter II: Skeletal Characterization of Smurf2-Deficient Mice and In Vitro Analysis of Smurf2-Deficient Chondrocytes

1. Introduction

Transforming growth factor- β (TGF- β) signaling consists of multiple secreted ligands such as bone morphogenic proteins (BMPs), TGF- β s, activins, inhibins, and growth and differentiation factors (GDFs) that regulate many cellular processes including proliferation, differentiation and apoptosis. Its involvement in limb formation is tightly regulated in order to ensure proper development and maintenance of bone and cartilage tissues²⁶⁸. For instance, TGF- β signaling is essential for joint homeostasis by promoting cartilage matrix synthesis²⁶⁹ and preventing chondrocytes from undergoing terminal differentiation²⁷⁰. Aberrations in the TGF- β /BMP signaling have thus been associated with many skeletal disorders such as osteoporosis, heterotopic ossifications, and osteoarthritis (OA)^{271,272}. TGF- β 1 and TGF- β 3 are shown to be diminished in human and mouse OA cartilage, respectively^{273,274}, and transgenic mice that lose TGF- β signaling in cartilage recapitulate an OA-like phenotype^{70,275,276}.

One way in which TGF- β /BMP signaling is regulated is through the ubiquitin system. Ubiquitination is a post-translational modification that requires the step-wise effort of E1 activating enzymes, E2 conjugating enzymes and E3 ubiquitin ligases. Ubiquitinated proteins are typically known to be targets for proteasomal degradation²⁷⁷; however, non-degradative roles have also been reported which can alter a protein's function²⁷⁸ or its localization²⁷⁹. Smad ubiquitin regulatory factor 1 and 2 (Smurf1 and Smurf2) are E3 ubiquitin ligases that share high homology and have been shown in various cell types to regulate TGF- β /BMP signaling²⁸⁰. They inhibit TGF- β signaling by promoting the degradation of R-Smads (Smads 1, 2 and 3) and TGF- β receptors^{280,281}.

Based on mouse models, Smurf1 has been implicated in various signaling pathways associated with bone development and function²⁸². Smurf1-deficient mice are phenotypically normal at birth, but exhibit an age-dependent increase in cortical bone mass due to sensitization of Smurf1-deficient osteoblasts to BMP²⁸³. Smurf2 has been shown to be upregulated in cartilage explants from OA patients²⁸⁴. Using a transgenic mouse model, Wu et al. demonstrated that overexpression of Smurf2 in articular chondrocytes results in chondrocyte hypertrophy and accelerated cartilage degradation²⁸⁴. The potential of Smurf2 to trigger spontaneous cartilage degradation raises the questions as to what roles Smurf2 has during normal cartilage development and maintenance and whether aberrant expression of Smurf2 is

required for OA development. Smurf2-deficient mice^{285,286} are born at the expected Mendelian ratio with no obvious phenotypic abnormality, but have an increased incidence of tumor formation at 15–20 months compared to wild-type (WT). To our knowledge, there has been no in-depth characterization of age-dependent changes in bone and cartilage in mice with reduced Smurf2 expression.

Here, we used a Smurf2-deficient mouse model generated by gene trapping²⁸⁵ to investigate whether reduced Smurf2 expression affects normal skeletal development and aging and whether it affects pathological conditions such as post-traumatic OA. Specifically, we characterized femoral cortical bone, vertebral trabecular bone, knee subchondral bone and knee articular cartilage of skeletally mature young (4 months old) and old (21 ± 1.3 months) Smurf2-deficient (MT) mice and their WT counterparts by quantitative microcomputed tomography (microCT) analyses and semi-quantitative histological scoring of articular cartilage (Figure 2.1A). In addition, we assessed the severity of OA symptoms of WT vs. MT mice in both age groups in response to surgical destabilization of the medial meniscus (DMM) (Figure 2.1B). Lastly, we utilized primary immature chondrocytes isolated from WT and MT mice to assess how Smurf2 deficiency affects chondrogenic and catabolic gene expression as well as Smurf2 and Smurf1 protein expression in 2D culture after treatment with TGF- β 3 or proinflammatory cytokine IL-1 β .

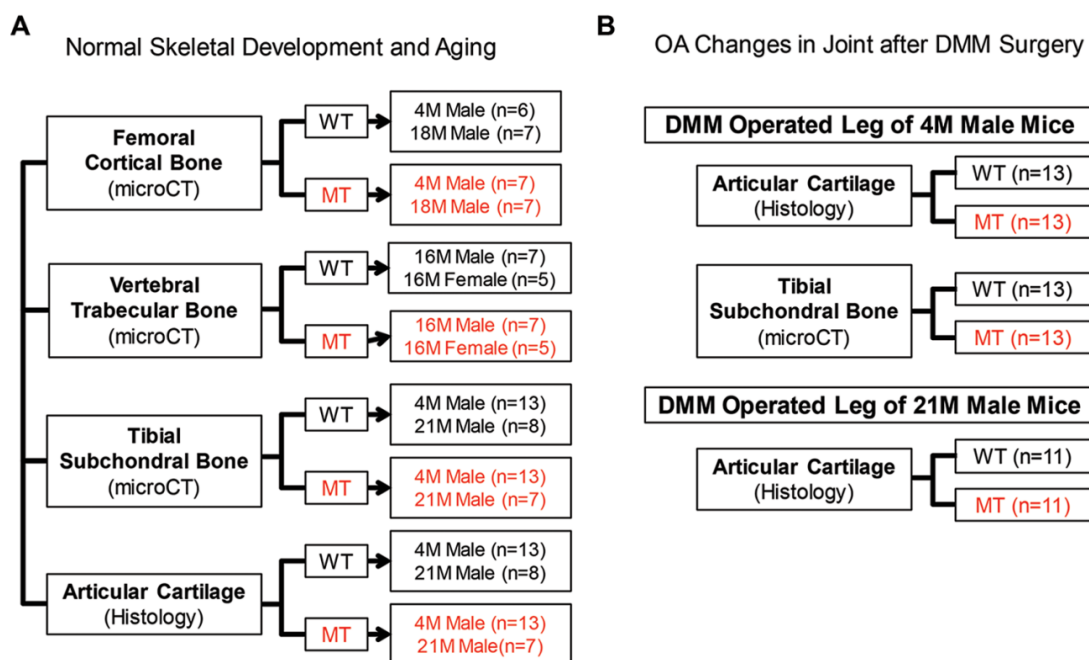


Figure 2.1 Summary of experimental design for skeletal characterization

2. Materials and Methods

Breeding of Smurf2-deficient and WT Mice

A previously reported Smurf2-deficient mouse model generated by gene trapping (on a C57BL/6 background)²⁸⁵ that was developed in the Zhang lab at University of Massachusetts Medical School (Worcester, MA) was used for the study. WT and MT mice were generated by crossing mice heterozygous for the trapped Smurf2 allele. For isolation of primary chondrocytes, homozygous mice were bred to produce sufficient neonates of the same genotype. Adult mice and neonates were euthanized by carbon dioxide asphyxiation followed by either cervical dislocation (adults) or decapitation (neonates). All mice were housed in a fully accredited Animal Care facility and the animal handling and surgical procedure were approved by the University of Massachusetts Medical School Institutional Animal Care and Use Committee (IACUC).

Bone Marrow Stromal Cells (BMSC) Isolation

Hind legs were harvested from skeletally mature 4-month-old WT and MT mice. Excess muscles were trimmed off and one end of the tibiae and femur was cut. Adopting a published method²⁸⁷, bone marrow (BM) plugs were isolated by inserting a 25-gauge syringe needle into the uncut end of the long bones and flushing with serum-free α -MEM. The BM plugs were mechanically disrupted using a pipettor and filtered through a 70- μ m mesh to remove debris. Red blood cells were lysed by mixing with an equal part of sterile water for <10 sec followed by a 1:5 dilution in 1 \times PBS. Cells were pelleted at 400g for 10 min and resuspended in complete culture medium (α -MEM with 20% hyclone FBS, 1% L-glutamine, and 1% pen/strep). The total cell suspension was plated on two p100 plates and media were changed twice a week.

Immature Murine Articular Chondrocyte (iMAC) Isolation

Following a published protocol²⁸⁸, iMACs were isolated from 5- to 7-day-old neonates. Cartilage from the knee and ankle joints was harvested, pooled, and subjected to a 60-min digestion in type II collagenase (Worthington) solution (3mg/mL in high glucose DMEM with 1% pen/strep) at 37°C under agitation. The cartilage pieces were then transferred to a diluted collagenase solution (0.5mg/mL) and incubated for 5–6 hours at 37°C under moderate agitation. The solution with residual fragments was mixed to yield a single cell suspension and filtered through a 70- μ m nylon mesh. The chondrocytes were pelleted at 400g for 10 min, washed in PBS and

then resuspended in DMEM/F12 with 10% FBS. The cells were plated at a density of 2.5×10^4 cells/cm² and cultured for 4–6 days before subsequent in vitro treatments and analyses. The chondrogenic nature of these cells was confirmed by positive Alcian Blue staining for cartilage ECM and the expression of chondrogenic gene which decreased with multiple passaging.

Whole Tissue Dissection

The hind legs from 4 months old WT and MT were harvested and each leg was dissected into 1) muscles surrounding the tibia and femur, 2) knee joint including the patella, ligaments and the tibial and femoral articular ends, and 3) mid-shaft tibia and femur with intact bone marrow. The spleen was harvested as a control where Smurf2 is known to be highly expressed in the WT. All specimens were immediately frozen in liquid nitrogen, powdered using a mortar and pestle, and stored at -80°C until time for protein or RNA isolation.

Western blot for BMSCs, iMACs, and musculoskeletal tissues

Total cell lysates from Passage 0 BMSCs and iMACs were extracted using RIPA buffer (50mM Tris pH 7.5, 150mM NaCl, 1% Triton X, 1mM EDTA, 0.1% SDS, 0.5% Na-deoxycholate) supplemented with a protease inhibitor cocktail (Roche). For protein isolation from whole bone, joint, and skeletal muscle, powdered specimens were resuspended in RIPA. Protein lysates (25–60µg) were separated by SDS-PAGE mini-protean gels (Bio-Rad) and transferred to nitrocellulose membranes. Membranes were probed using primary antibodies against Smurf2 (Abcam, ab53316, 1:1000), Smurf1 (Abcam, ab117552, 1:2000), Col2 (Millipore, MAB8887, 1:2000), Sox9 (Millipore, AB5535, 1:1000), GAPDH (Sigma, G8795, 1:5000), tubulin (Sigma, T6074, 1:5000) and goat secondary antibodies against rabbit (Santa Cruz, 1:5000) and mouse (Santa Cruz, 1:10,000) IgG and then visualized using a chemiluminescent substrate (Pierce).

RT-PCR for Smurf2 mRNA levels in whole bone and cartilage tissues

Powdered tissues were resuspended in TRIzol reagent (Life Technologies) and vortexed at room temperature for 15–20 min. Insoluble components were removed by centrifugation (12,000g, 10 min). RNA was purified using Direct-zol RNA MiniPrep (Zymo Research) according to manufacturer's instructions and RNA concentration was determined using a Nanodrop 2000 spectrophotometer (Thermo Scientific). Total RNA (1 µg) was reverse-transcribed using

SuperScript III First-Strand Synthesis Kit (Life Technologies) according to manufacturer's instructions. PCR reactions were conducted on a GeneAmp PCR system 2700 (Applied Biosystems) under the following conditions: 94°C for 3 min, followed by 35 cycles at 94°C for 20 sec, 58°C for 30 sec, 72°C for 1 min, and a final extension at 72°C for 10 min. PCR products were subjected to electrophoresis on a 1% agarose gel and visualized by ethidium bromide staining. RT-PCR primer sequences: Smurf2 (Fwd: 5'-AACCGTGCTCGTCTCTCTTC-3', Rev: 5'-ATGAAGTCATTCCCCAGCAC-3'); GAPDH (Fwd: 5'-AGGTCGGTGTGAACGGATTTG-3', Rev: 5'-TGTAGACCATGTAGTTGAGGTCA-3').

Preparation of skeletal tissues for microCT and histology

For analysis of knee joints by microCT and histology, hind legs were harvested from skeletally mature young (4 months old) and old (21 ± 1.3 month old) male mice, tied to a toothpick in a fully extended position, and fixed in 10% neutral buffered formalin for 2–3 days at 4°C before being scanned and subsequently decalcified for histology. For analysis of femoral cortical bone and vertebral trabecular bone, hind legs from 4 and 18 month old mice and lumbar vertebrae from 16 month old male and female mice were harvested and fixed in 10% neutral buffered formalin for 2–3 days at 4°C before being scanned by microCT and subsequently decalcified for histology.

Quantitative MicroCT analyses

All skeletal tissues were scanned on a Scanco microCT 40 scanner (Scanco Medical, Brüttisellen, Switzerland) at a 10- μ m voxel resolution. Cortical bone analysis was performed by evaluating 50 slices (volume of interest/VOI) from the midshaft (10 micron spacing, flanking the midpoint between growth plates of the femur) for bone volume, cortical thickness, and bone mineral density. Vertebral bone analysis was performed on either the L4 or L5 vertebrae and the region of interest (ROI) was defined by the entire trabeculae within the body of the vertebra excluding the cortical bone. The bone volume/tissue volume (BV/TV), trabecular thickness, trabecular spaces, and bone mineral density were determined using Scanco's trabecular bone evaluation that is based on distance transformations (Direct-No model method). For subchondral bone analysis, the medial and lateral condyles of the proximal tibia epiphysis were analyzed separately. The ROI was defined by the bone between the calcified cartilage and the growth plate. The bone volume/tissue volume (BV/TV), trabecular thickness, trabecular spaces,

and bone mineral density were calculated using the same trabecular bone evaluation method as the vertebrae. For subchondral bone analysis after DMM surgery, only the medial condyle of the tibia was evaluated and osteophytes were excluded from the ROI.

Knee Histology and Semi-Quantitative Scoring of Articular Cartilage

Formalin-fixed hind legs were decalcified for 14 days in 18% EDTA and frontally embedded in paraffin blocks. Blocks were cut using a Reichert-Jung 2030 microtome to produce 5µm thick sections. Sections were deparaffinized then stained with Weigert's iron hematoxylin/fast green/safranin-O (Sigma). To systematically compare knee articular cartilages, a minimum of five equally spaced sections spanning the knee joint were analyzed using a modified published semi-quantitative scoring criterion²⁸⁹. Articular cartilage with loss of staining or superficial structural damage was referred to as mild OA (scores of 0.5 and 1), while fibrillations and erosions with increasing depth and width below the superficial layer and extending past the tidemark were referred to as moderate (scores of 2 and 3) or severe OA (score of 4). Sections with majority of the subchondral bone exposed or only a small portion of articular cartilage intact were categorized as very severe OA (scores of 5 and 6). The medial femoral and tibial articular cartilages of each knee section were blindly scored by 7 trained examiners. The scores from each examiner were averaged and the average scores for the femoral and tibial cartilage were plotted separately on the same graph for semi-quantitative comparisons.

Surgical Induction of OA by Destabilization of Medial Meniscus (DMM)

DMM, a well-established surgical model for inducing OA¹⁹⁵, was performed on 2 month old and 19 ± 1.3 month old male mice. Briefly, the mice were anesthetized using 2% isoflurane in oxygen, and the surgical site was sterilized before a medial parapatellar incision was made to expose the joint cavity. The meniscotibial ligament was identified and transected under a stereomicroscope. Joint capsule and overlying skin were sutured in layers using 7-0 PGA sutures. Buprenorphine (0.05mg/kg, 3 times a day) and cefazolin (20mg/kg, twice a day) were injected subcutaneously immediately post-operation (post-op) and for 2 more days thereafter. Mice were allowed to move freely in cages immediately after the operation. At 2 months post-DMM, the mice were euthanized and their hind legs were harvested and prepared for µCT and histology analyses as described above.

Quantitative RT-PCR (qPCR) of Primary Chondrocytes

iMACs were isolated from WT and MT mice as described above. Cells were seeded at 2.5×10^4 cells/cm² and cultured in expansion medium (5% FBS in DMEM/F12) for 4 days on tissue culture polystyrene (TCPS). Cells were then treated with 10 ng/mL of TGF- β 3 (R&D Systems) or 5 ng/mL of IL-1 β (R&D Systems) for 24 hours. RNA was isolated, purified and reverse-transcribed as described above. qPCR samples were prepared using Power SYBR Green Master Mix (Applied Biosystems) and analyzed using a 7500 Real-Time PCR System (Applied Biosystems). Gene expression of Sox9, Col2, Acan, Col1, MMP-3, MMP-9, MMP-13, and ADAMTS5 were normalized to β -actin levels. Data were plotted as fold-change relative to those of untreated WT. Primer sequences are summarized in Table 2.1.

Table 2.1 Sequences of primers used for quantitative RT-PCR.

Gene	NCBI Ref Seq	Forward Primer Sequence 5'-3'	Reverse Primer Sequence 5'-3'	Primer Size (bp)
β -Actin	NM_007393.3	CGAGCGGTTCCGATGC	TGGATGCCACAGGATTCCAT	69
SOX9	NM_011448.4	AGGAAGCTGGCAGACCAGTA	CGTTCTTCACCGACTTCCTC	193
COL2	NM_031163.3	GATCACCTCTGGGTCCTTGTT	TCCTCTGCGATGACATTATCT	222
ACN	NM_007424.2	AGTGGATCGGTCTGAATGACAGG	AGAAGTTGTCAGGCTGGTTTGA	105
COL1	NM_007742.3	AACGAGATCGAGCTCAGAGG	CACGAAGCAGGCAGGGCCAA	213
MMP-3	NM_010809	AGTCTACAAGTCTCCACAG	TTGGTGATGTCTCAGGTTCC	152
MMP-9	NM_013599.3	TAGCTACCTCGAGGGCTTCC	GTGGGACACATAGTGGGAGG	147
MMP-13	NM_008607.2	AGACCTTGTTTGCAGAGCACTAC	CTTCAGGATTCCC GCAAGAGT	70
ADAMTS5	NM_011782.2	CGAAGAGCACTACGATGCAG	TGGAGGCCATCATCTTCAAT	144

doi:10.1371/journal.pone.0148088.t001

Statistical Analysis

Statistical analyses were performed using Prism (Graphpad Software, Version 6.0). MicroCT data were presented as the mean \pm standard deviation and the statistical analyses were performed using 2-way ANOVA followed by Tukey's post-hoc test. Knee histological scores were plotted as a dot plot with the median and interquartile range, and the statistical analyses were performed with either Kruskal-Wallis with Dunn's multiple comparison test (for age and genotype-dependent changes) or the Mann-Whitney rank-sum test (response to DMM surgery). Distribution of the histological scores from post-DMM WT and MT knees were compared using Kolmogorov-Smirnov test. qPCR results are presented as a mean \pm standard deviation of three separate chondrocyte isolation experiments for each genotype and the statistical analysis was performed using unpaired t-test for each treated and untreated condition. Quantifications of WB bands were normalized to WT expansion medium control and averaged among three replicates. A value of $p < 0.05$ was considered statistically significant.

3. Results

Characterization of Smurf2 Expression in skeletal tissues

To study the role of Smurf2 in skeletal tissues, we began by examining the levels of Smurf2 expression in these tissues. The level of Smurf2 protein in knee joints, cortical bones/bone marrow, and skeletal muscles of C57BL/6 WT mice was undetectable compared to levels in the spleen by western blot (Figure 2.2A). Using RT-PCR, we confirmed that the total mRNA levels of Smurf2 extracted from these skeletal tissues were much lower than in the spleen, but all MT tissue examined showed reduced Smurf2 mRNA expression compared to WT, as expected (Figure 2.2B). We also examined Smurf2 expression in bone marrow stromal cells (BMSC) and immature murine articular chondrocytes (iMAC) isolated from MT and WT mice, and found that Smurf2 protein levels are significantly reduced in both MT primary cells (Figure 2.2C).

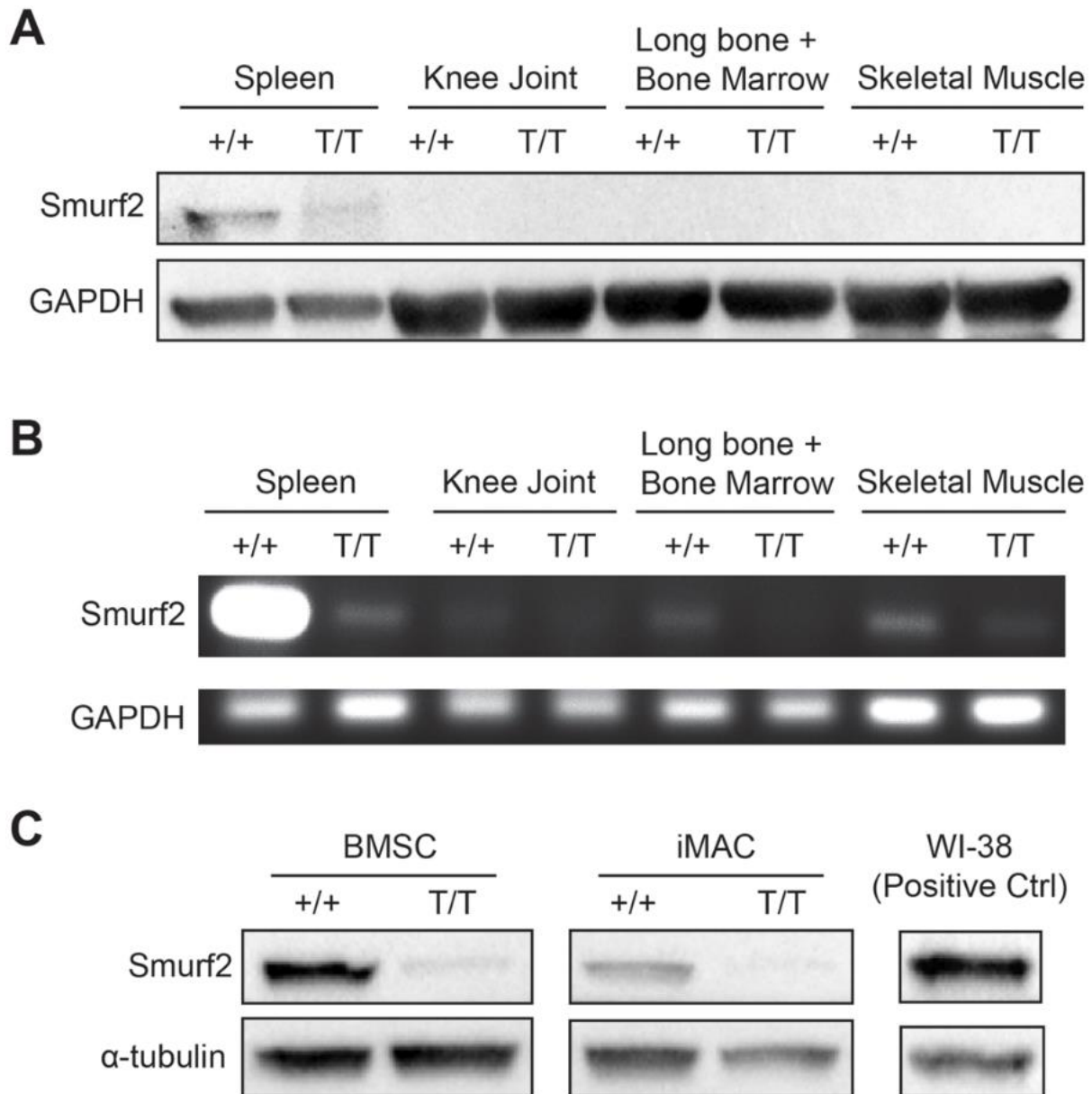


Figure 2.2 Smurf2 protein and gene expressions in WT (+/+) and Smurf2-deficient MT (T/T) skeletal tissues and primary cells.

(A) Protein expression of Smurf2 in various skeletal tissues from healthy 4 month old male WT and MT mice. Spleen, where Smurf2 is highly expressed, is included as a positive control. (B) Smurf2 mRNA expression in various skeletal tissues compared to spleen in 4 month old male WT and MT mice. (C) Protein expression of Smurf2 in bone marrow stromal cells (BMSC, passage 0) isolated from 4 month old WT and Smurf2-deficient MT mice and immature articular chondrocytes (iMAC, passage 0) isolated from WT and MT neonates.

Smurf2-deficient mice exhibit normal age-dependent cortical and trabecular bone phenotypes

Using microCT, we examined changes in mid-shaft femoral cortical bone between WT and MT mice at 4 months and 18 months of age. Although a slight drop in bone mineral density

(BMD) was observed with advanced age, these changes were not statistically significant. No significant difference between WT and MT mice at a given age was detected (Figure 2.3A). Due to its high surface area to bone matrix volume ratio, trabecular bone undergoes more rapid remodeling and is associated with more prominent bone loss with age than cortical bone²⁹⁰. We therefore assessed the vertebral trabecular bone in 16 month old mice using microCT to reveal potential remodeling abnormality between genotypes. To account for the effect of estrogen deficiency on bone remodeling, these analyses were performed in a sex-specific manner (Figure 2.3B and 2.3C). Regardless of genotype, the vertebral trabecular bone of old female mice exhibited lower BV/TV and higher trabecular thickness and trabecular spaces than their male counterparts. These sex-specific differences were not statistically different between WT and MT mice.

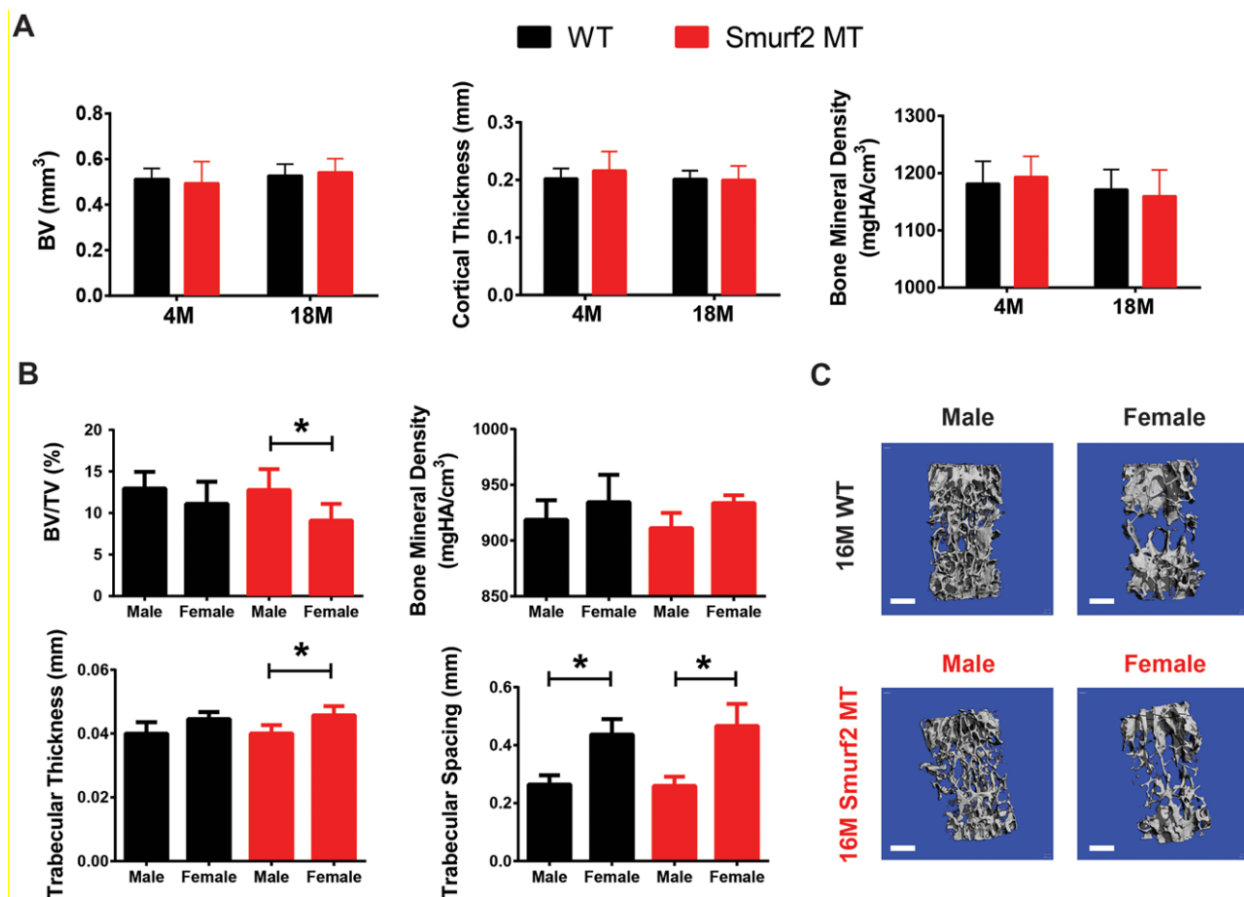


Figure 2.3 Age- and sex-specific cortical bone and trabecular bone analyses of WT and Smurf2-deficient MT mice.

(A) Mid-shaft cortical bone analysis of male WT and MT femurs from 4 month (WT: n = 6; MT: n = 7) and 18 month old (WT and MT: n = 7) mice. (B) Sex-specific trabecular bone analysis of lumbar vertebrae from 16 month old WT and MT mice (Male: n = 7; Female: n = 5). (C) Representative 3D reconstruction of contoured vertebral trabecular bone. Scale bar = 500 μ m.

Smurf2-deficient mice exhibit normal knee joint phenotype

Qualitative comparison of histological sections of WT and MT knee joints did not reveal any gross developmental or age-related abnormalities within the growth plates, menisci, or synovia (data now shown). In order to characterize the structural changes in knee articular cartilage that would reflect spontaneous OA development with age, we adopted a published semi-quantitative knee histological scoring system²⁸⁹ and assigned each score an overall OA severity (Figure 2.4A). Since lateral tibial articular cartilage tends to be thinner with less distinct zonal architecture²⁹¹, we focused our analyses on the medial side. Using this scoring system, we detected age-dependent changes in the articular cartilage from normal to mild OA in the medial tibial and femoral condyles in both the WT ($p = 0.0011$) and MT ($p < 0.0001$) mice, but no statistically significant difference was detected between them at a given age (Figure 2.4B). The main differences observed between the two age groups ranged from general loss of proteoglycan staining to mild superficial fibrillations as reflected by the median scores of 0.64 (0.35–0.72) and 0.57 (0.41–0.67) in the 21 month old WT and MT groups, and 0.26 (0.14–0.36) and 0.14 (0.06–0.26) in the young 4 month old WT and MT groups, respectively.

We then investigated whether age-dependent changes in the tibial subchondral bone were different between WT and MT. Since previous work reported differences in the medial and lateral compartments of the subchondral bone²⁹², we analyzed microCT data in these two compartments separately. Compared to the lateral side, the medial subchondral bone compartment had a higher BV/TV, trabecular thickness and BMD across both age groups and genotypes (Figure 2.4C and 2.4D). The age-dependent loss of trabecular bone within the medial compartment was also apparent as supported by the increase in trabecular spacing, from 0.154 ± 0.011 (WT) and 0.175 ± 0.027 (MT) in the young group to 0.193 ± 0.026 (WT) and 0.229 ± 0.036 (MT) in the old group, respectively. However, no statistically significant differences were detected between WT and MT mice at a given age.

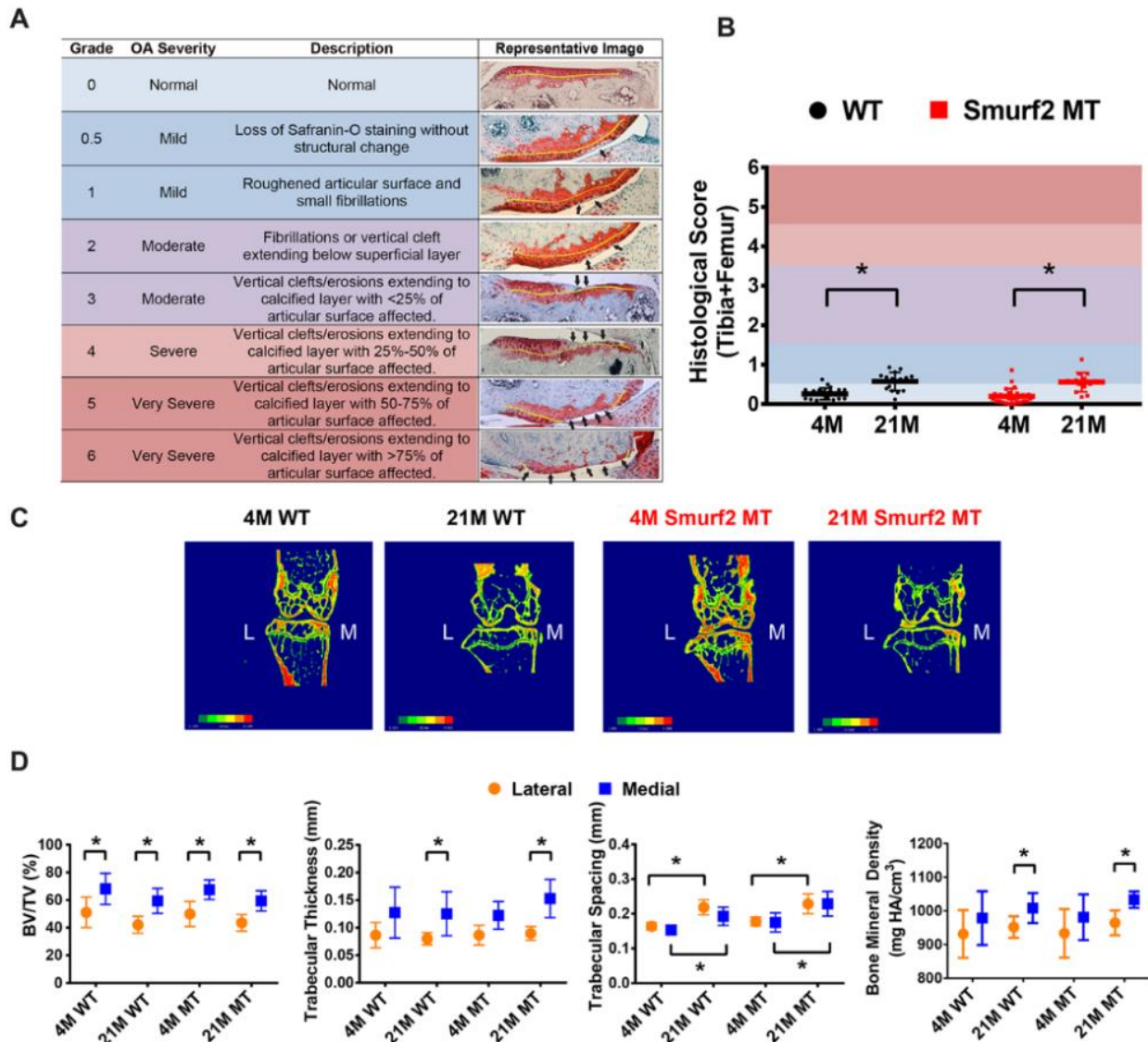


Figure 2.4 Age-specific knee joint phenotypes of male WT (+/+) and Smurf2-deficient MT (T/T) mice.

(A) Normal and osteoarthritic joint articular cartilage histology scoring along with representative safranin O-stained cartilage sections. Yellow line indicates tidemark; Black arrows denote loss of staining, fibrillations, or erosions. (B) Combined histology scores of femoral and tibial articular cartilage of 4 month old WT ($n = 13$), 4 month old MT ($n = 11$), and 21 month old WT ($n = 11$), and 21 month old MT ($n = 11$). (C) Representative microCT images of bone mineral density color mappings of mid-frontal knee sections from young and old WT and Smurf2 MT mouse knees. Red indicates higher BMD while green indicates lower BMD. (D) Quantitative comparisons of the lateral and medial subchondral bone analyses between 4 month (WT: $n = 9$; MT: $n = 11$) and 21 month (WT: $n = 10$; MT: $n = 8$) WT and MT mice. * $p < 0.05$.

Young Smurf2-deficient mice develop milder OA in knee articular cartilage compared to WT mice after DMM surgery

DMM is a well-established surgical-induced model of OA in mice that mimics the slow progression of human OA following traumatic knee injury¹⁹⁵. To determine whether Smurf2

deficiency affects the pathological development and progression of OA or alters the repair mechanisms in response to knee injury, we performed DMM surgery on 2 month old male WT and MT mice and evaluated their knee articular cartilage by histological scoring after 2 months. Histological sections from the medial side of the DMM-operated knees revealed cartilage erosions extending below the superficial layer and past the tidemark in the WT mice, while mainly loss of proteoglycan staining and superficial fibrillations were observed in the MT DMM knees (Figure 2.5A). This difference resulted in a post-DMM median histological score of 1.85 (0.91–3.80) for WT and 1.00 (0.59–1.78) for MT, both of which were significantly higher than the respective un-operated contralateral controls ($p < 0.0001$) and significantly different from each other ($p < 0.01$) (Figure 2.5B). We also observed a profound difference in the distribution of the post-DMM histology scores between WT and MT, which was verified using the Kolmogorov-Smirnov test ($p = 0.043$). The difference in the distribution of cartilage scores between WT and MT knees in response to DMM is best reflected by categorizing the OA severity of each scored specimen (Figure 2.5C). Specifically, while all WT mice developed knee OA 2 months after DMM, with 69.2% of the articular cartilage exhibiting moderate (42.3%) to severe/very severe (26.9%) OA phenotypes, 69.2% of the articular cartilage from MT mice knees developed either mild OA (50.0%) or remained normal (19.2%). Only 30.8% of the MT mice exhibited a moderate OA cartilage phenotype at 2 months after DMM, and none exhibited severe or very severe OA symptoms.

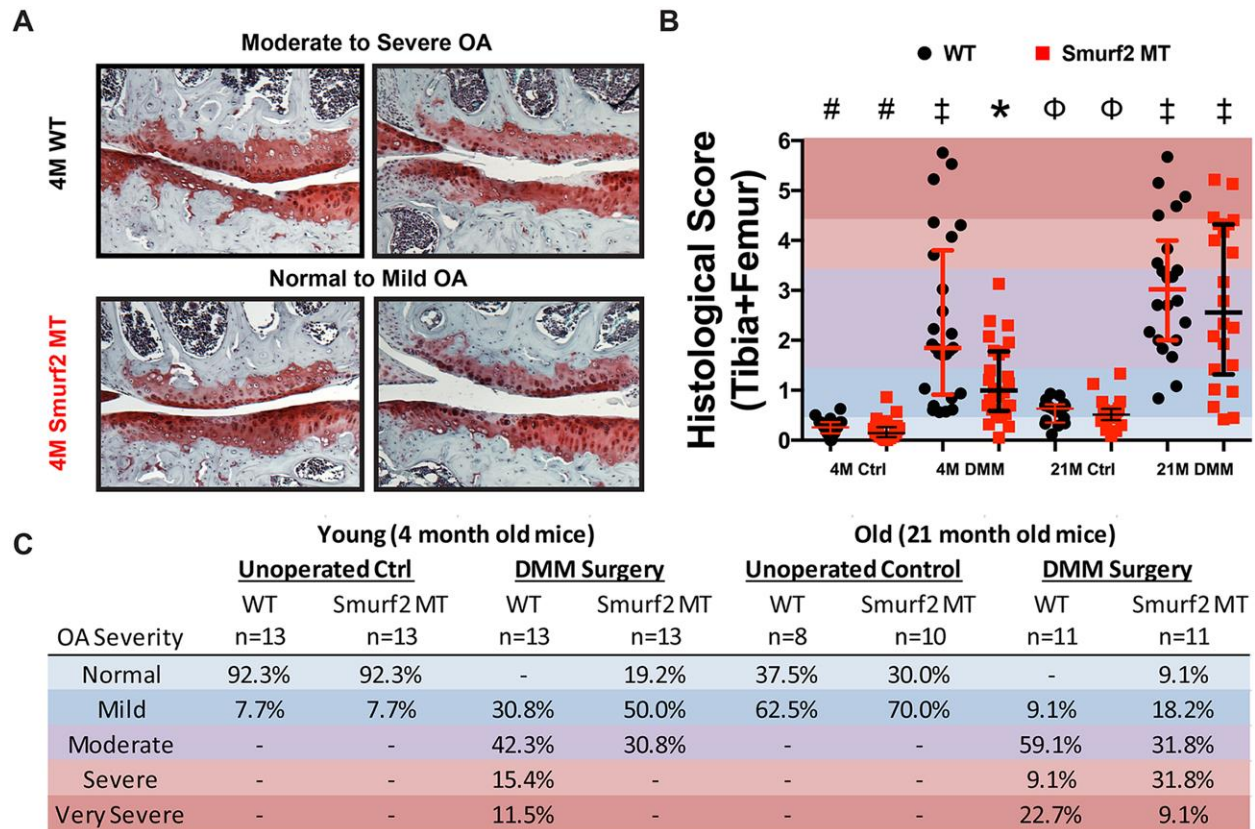


Figure 2.5 Differential severity of knee joint articular cartilage erosions in young (4 month) and old (21 ± 1.3 month) male WT and Smurf2-deficient MT mice after DMM surgery.

(A) Representative images of safranin O-stained articular cartilage sections from the medial compartment of WT and MT knees 2 months post-DMM surgery. (B) Semi-quantitative histology scores of the femoral and tibial articular cartilage of DMM knees vs un-operated controls (n = 13 for 4 month; n = 11 for 21 ± 1.3 month). The average femoral and tibial articular cartilage scores for each joint were plotted separately on the same graph. Groups with the same symbol are not statistically significant (p > 0.05) based on mean ranks. (C) Distribution of DMM knee scores for WT and MT based on OA severity.

Since sclerosis of the subchondral bone has been detected in mice after DMM surgery, we evaluated whether Smurf2-deficiency affected the degree of sclerosis. Representative images of WT and MT DMM knees revealed increased bone mineral density localized in the medial femoral condyle and the tibial plateau at 2 months after DMM (Figure 2.6A). Quantitative analysis of the medial subchondral compartment of the tibia (Figure 2.6B) showed an increasing trend in trabecular thickness in both WT and MT. The concurrent loss of trabecular space is more apparent in the MT mice. The changes in BMD detected before and after DMM surgery in either genotype was not statistically significant, likely due to the large standard deviation among the WT subchondral bone in response to DMM.

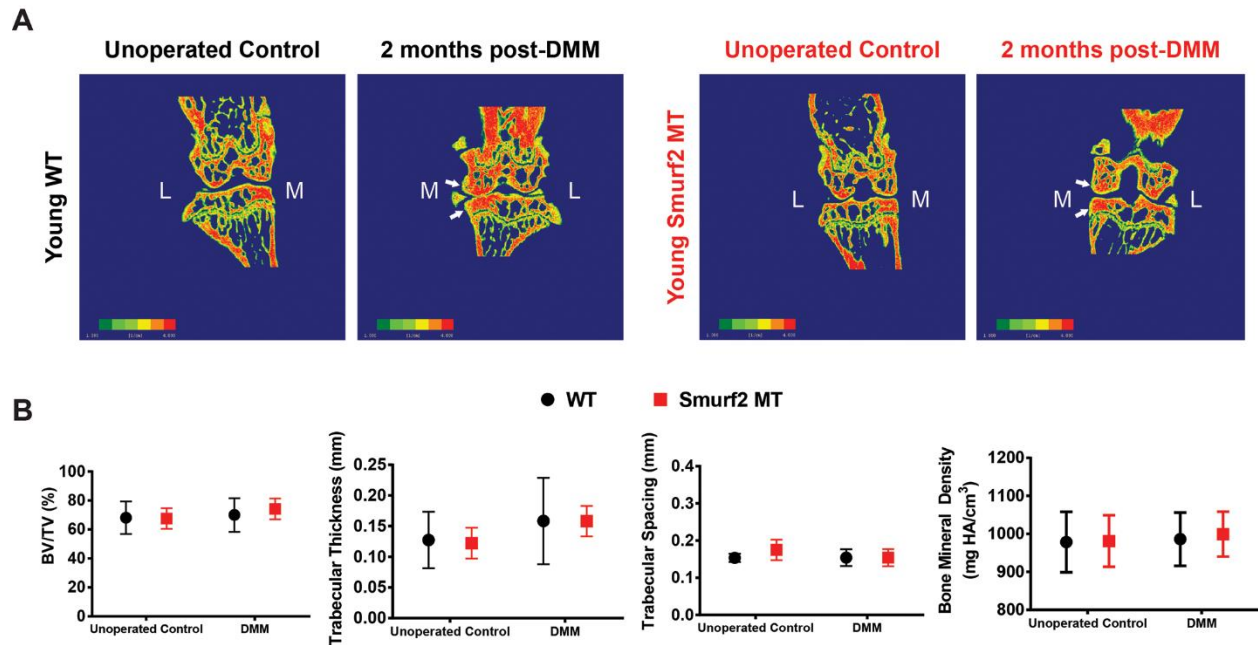


Figure 2.6 Knee joint subchondral bone analyses in 4 months old male WT and Smurf2-deficient MT mice upon surgical induction of OA by DMM.

A) Representative microCT bone mineral density (BMD) color mapping of medial compartment of 4 month old male mice knees 2 months post DMM. White arrows = areas with increased bone mineral content; L = lateral; M = medial; red indicates higher BMD while green indicates lower BMD. B) Quantification of subchondral bone change in medial compartment of tibial plateau after DMM reflecting trends of increased BV/V, trabecular thickness and decreased trabecular spaces. WT: n = 9; MT: n = 11.

Ageing increases severity of OA in both WT and MT knees but the subset of mice exhibiting normal or mild OA is still greater in MT

Since age is a risk factor for OA development, we performed DMM surgery on older (19 ± 1.3 month) Smurf2-deficient mice to examine whether the attenuated OA cartilage phenotype observed at 4 months may be sustained with age. Histological scores of the older knees 2 months post-DMM revealed that ageing increased the overall severity of OA symptoms for both WT ($p < 0.05$) and MT mice ($p < 0.001$) (Figure 2.5B and 2.5C). The median post-DMM histological scores for the older mice were 3.02 (2.00–4.00) for WT and 2.56 (1.32–4.32) for MT, but the reduction in OA severity in MT was not statistically significant ($p = 0.460$) based on mean ranks comparison. Unlike the 4 month old mice, the distribution of histological scores was also similar between the old WT and MT mice as verified by the Kolmogorov-Smirnov test ($p = 0.621$). It is interesting to note, however, the subset of mice exhibiting normal or mild OA articular cartilage symptoms post-DMM at such an advanced age was still greater in the MT mice (27.3%) than in the WT mice (9.1%).

Smurf2-deficient chondrocytes display elevated chondrogenic gene expression in 2D culture compared to WT

To examine how Smurf2 deficiency might affect chondrocyte function in a chondrogenic or pathological environment in 2D culture, we isolated iMACs from WT and MT mice and compared the gene expression of key anabolic and catabolic genes in the presence of a chondrogenic factor, TGF- β 3, or a proinflammatory cytokine, IL-1 β . MT chondrocytes showed trend of higher levels of chondrogenic gene expression (Sox9, Col2, and Acan) than WT with and without addition of TGF- β 3 (Figure 2.7). In the presence of IL-1 β at 5 ng/mL, an overall decrease in the expression of chondrogenic genes Sox9, Col2, and Acan and an increase in the expression of catabolic genes MMP-3, MMP-9, MMP-13 and ADAMTS5 were observed in both WT and MT. It is worth noting that the trend of higher levels of chondrogenic genes in MT than WT persisted even under the inflammatory conditions, with the higher Sox9 expression in MT being statistically significant. Although there was no consistent trend in the expression of catabolic genes between WT and MT iMACs, there was a statistically significant difference in MMP13 and ADAMTS5 expression between WT and MT upon IL-1 β treatment. The level of Col1, a marker for chondrocyte dedifferentiation, was similar across all conditions between genotypes. We were unable to detect Col10 expression in iMACs from either genotype after 40 cycles.

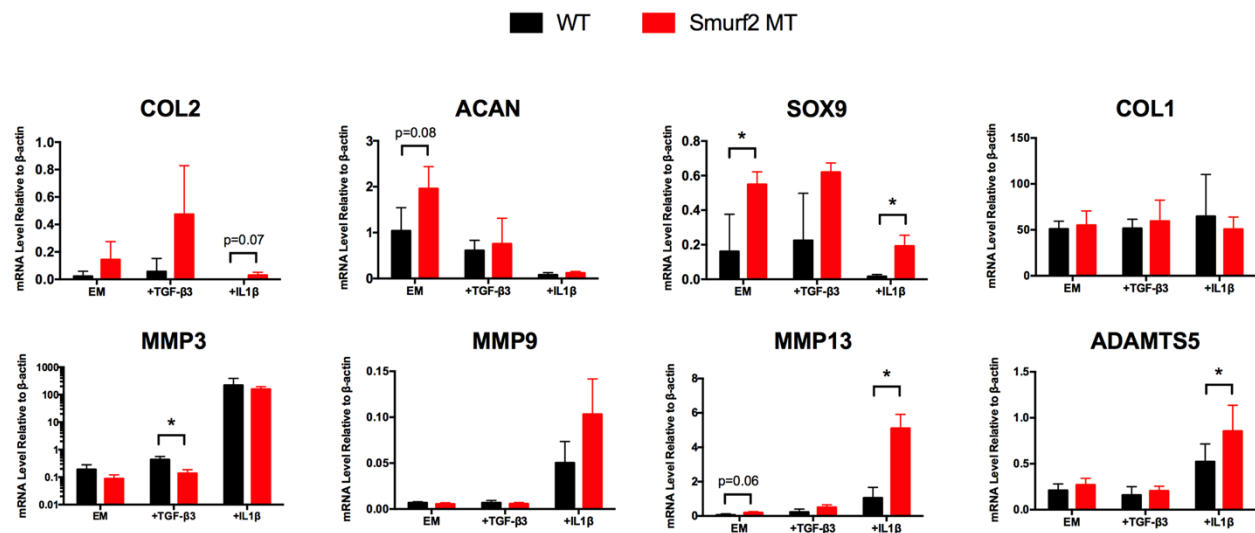


Figure 2.7 Quantitative gene expression analyses of key anabolic and catabolic markers in WT and MT iMACs. Cells were cultured as a monolayer on 2D tissue culture polystyrene for 4 days and treated with either 10 ng/mL of TGF- β 3 or 5 ng/mL of IL-1 β for 24 hours. Data are reported as the mean \pm standard deviation of three separate chondrocyte isolations for each genotype. EM = Expansion Media, * $p < 0.05$ (p values approaching significance are noted on the graph).

TGF- β 3 and IL-1 β modulates Smurf1 and Smurf2 expression in iMACs in vitro

To determine whether Smurf2 and Smurf1 protein levels are perturbed in chondrogenic or pathological conditions, we detected their expressions in WT iMACs after TGF- β 3 or IL-1 β treatment by western blot. Treatment of WT iMACs with TGF- β 3 caused a dose-dependent increase in Smurf2 while treatment with IL-1 β resulted in a dose-dependent decrease (Figure 2.8A). Even though the treatment of iMACs with TGF- β 3 widened the difference in Smurf2 between WT and MT, the difference in protein expression of Col2 and Sox9 between WT and MT was not as apparent (Figure 2.8B). Smurf1, which shares high homology with Smurf2, appeared slightly elevated in MT iMACs compared to WT after TGF- β 3 treatment, but quantification of the intensities of these bands was not statistically significant (Figure 2.9).

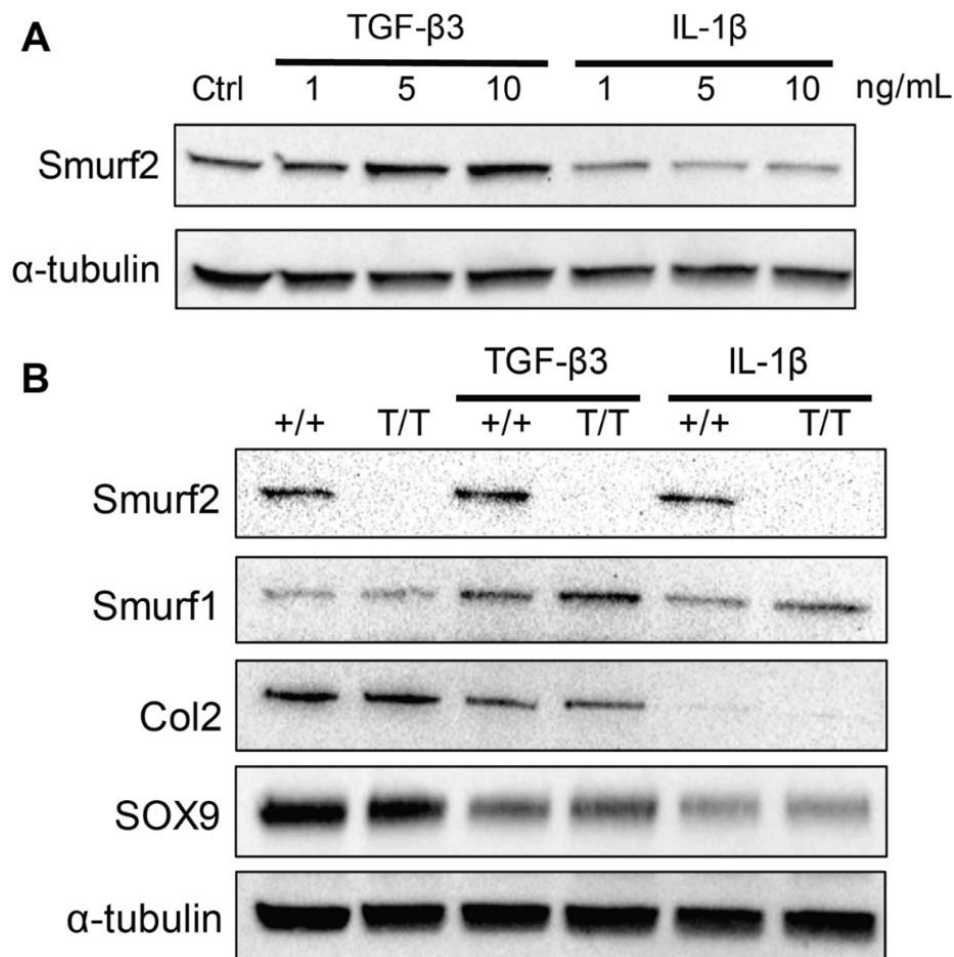


Figure 2.8 Smurf protein expression changes upon 24-h treatment of TGF- β 3 and IL-1 β .

A) WT chondrocytes show dose-dependent increase of Smurf2 protein with 24-h TGF- β 3 treatment and dose-dependent decrease with 24-h IL-1 β treatment. B) No compensatory increase of Smurf1 protein levels was detected between WT (+/+) and Smurf2-deficient MT chondrocytes (T/T) with and without treatment of TGF- β 3 (10 ng/mL) or IL-1 β (0.1 ng/mL). Type 2 collagen levels were also similar between WT and MT chondrocytes across all conditions.

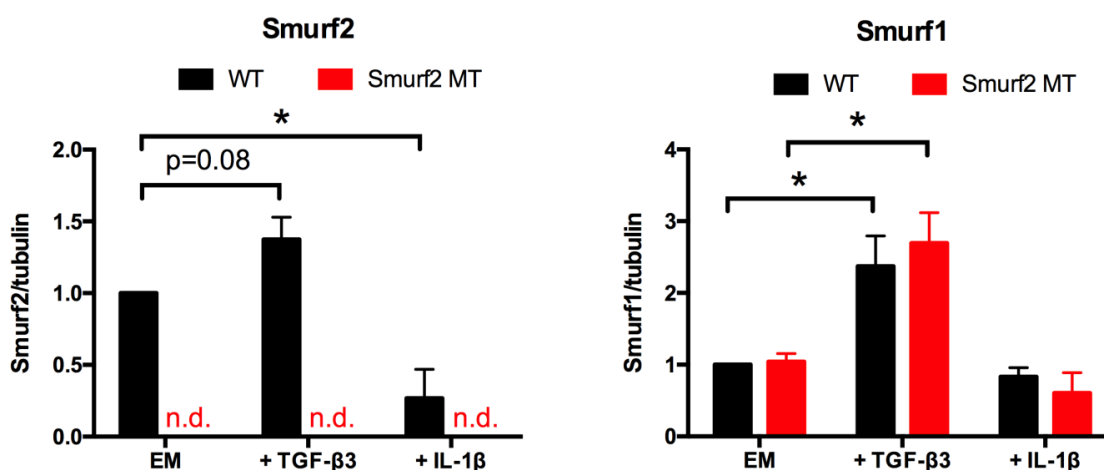


Figure 2.9. Western blot quantification of Smurf2 and Smurf1 proteins in WT and MT iMACs.

Protein bands for Smurf2 and Smurf1 bands were quantified and normalized to WT iMAC in expansion media (EM). Quantification was based on the average of three separate experiments with different WT and MT pairs. n.d. = not detected.

4. Discussion

In this study, we characterized bone and joint phenotypes of Smurf2-deficient mice as a function of age because Smurf1 and Smurf2 have been implicated in regulating bone and cartilage function, respectively. Using microCT and histological analyses, we compared age-dependent changes in femoral cortical bone, vertebral trabecular bone (sex-specific), tibial subchondral bone, and knee articular cartilage between WT and Smurf2-deficient MT mice. We found that the reduction of Smurf2 expression did not impact the normal development and maintenance of bone and cartilage throughout adulthood, and the observed bone and cartilage changes as a function of age are consistent with previous reports on aged WT C57BL/6 mice^{291,293,294,295}.

Since the overexpression of Smurf2 in chondrocytes was reported to trigger spontaneous OA²⁸⁴, we subjected skeletally mature 2 month old Smurf2-deficient mice to DMM surgery and examined whether their development of OA is mitigated compared to WT. We observed that at 2 months post-DMM, MT mice were less susceptible to pathological development of OA compared to WT. Based on our OA severity categorization criteria, the majority of articular cartilage from WT DMM knees developed moderate to severe OA (69.2%; characterized by significant cartilage fibrillations and erosions extended beyond the tidemark and into subchondral bone), while the majority of articular cartilage from MT DMM knees was normal or developed only mild OA (69.2%). More remarkably, none of the articular cartilage

from MT DMM knees developed severe OA. In contrast, none of the articular cartilage from WT knees was normal 2 months after DMM, and a subset of them developed severe to very severe OA (26.9%). The presence of subchondral bone sclerosis and osteophyte formation has long been associated with human OA knees. However, it remains controversial whether subchondral bone changes are an etiology of OA or whether they reflect a bone remodeling process that reacts to the deteriorating overlying cartilage²⁹⁶. From our study, we did not detect any significant changes in subchondral bone sclerosis (Figure 2.6) or osteophyte formation between genotypes by 2 months post-DMM, suggesting that the subchondral bone remodeling process induced by DMM is not entirely dependent on Smurf2 expression or the integrity of the overlying cartilage.

Given that the impact of Smurf2 on cartilage progressed with age and that Smurf2 deficiency has been implicated in inhibition of cellular senescence²⁸⁵, we questioned whether the protective effect of Smurf2 deficiency against OA development after DMM surgery may persist with age. Histological scores of the joint articular cartilage showed that aging caused both WT and MT mice to develop more severe OA after DMM surgery, with an increase of the median score for the 21 month old WT (3.02 vs. 1.85) and MT (2.56 vs. 1.00) when compared to 4 month old counterparts. Nevertheless, we found that the subset of joint cartilage that remained normal or exhibited only mild OA phenotype post-DMM was still greater among old MT than WT, suggesting that some degree of protective effect may still persist at this age. Because the majority of the specimens do develop moderate to severe OA, a larger sample size is necessary to demonstrate the significance of this subset between old WT and MT. Altered biomechanics due to weight changes, impaired bone and cartilage repair, and homeostasis due to aging can all potentially mask the protective effect of Smurf2 deficiency on OA development. Overall, the ability of Smurf2 inhibition to delay, alleviate or prevent OA symptoms in the multi-tissue compartments of the joint, particularly at advanced age, requires further investigation.

Taking advantage of this Smurf2-deficiency mouse model, we isolated immature articular chondrocytes from newborn mice and asked how Smurf2 deficiency affects the expression of common chondrogenic and catabolic genes upon culture treatment with TGF- β 3 or IL-1 β . The pro-inflammatory cytokine IL-1 β is known to shift the balance of chondrocytes from matrix synthesis towards degradation and has been used to emulate an inflammatory OA environment *in vitro*^{297,298}. We found that MT chondrocytes trended toward a higher mRNA level of chondrogenic genes including Sox9, Col2, and Acan compared to WT with and without TGF- β 3 treatment. As expected, IL-1 β treatment of the chondrocytes globally suppressed chondrogenic genes and upregulated the catabolic genes that we examined. The general trend

of higher chondrogenic gene expression in the MT than WT was maintained even under proinflammatory conditions, with the difference in Sox9 being statistically significant and that of Col2 approaching significance. The differences observed between WT and MT iMACs at the mRNA level, however, did not translate directly to the protein level. We found no difference in Col2 protein expression and Sox9 protein expression was only slightly higher in the MT iMACs treated with TGF- β 3 compared to WT. Interestingly, both Col2 and Sox9 expression seem to decrease after 24 hour treatment with TGF- β 3 compared to untreated cells. We confirmed that this increase in chondrogenic gene expression was not due to differences in the degree of dedifferentiation between WT and MT in vitro by demonstrating that Col1 expression was similar across all experimental conditions. On the contrary, there was no consistent trend in the expression of catabolic genes examined (MMP-3, -9, -13 and ADAMTS5) between WT and MT. Compared to WT iMACs, MT iMACs had statistically significant lower expression of MMP3 upon TGF- β 3 treatment, but higher expression of MMP-13 and ADAMTS5 after IL-1 β treatment. In the absence of TGF- β 3 or IL-1 β , no significant differences in any catabolic genes were detected. Incidentally, we found that both TGF- β 3 and IL-1 β modulated Smurf2 levels in WT iMACs in a dose-dependent manner. TGF- β 3 also increased Smurf1 levels, and the increase was higher in MT chondrocytes than in WT, suggesting a potential but weak compensatory mechanism by Smurf1 in Smurf2-deficient iMACs. Whether TGF- β 3-induced increase of Smurf1 and Smurf2 affects the phosphorylation of intracellular R-Smads or the stability of TGF- β receptors or other downstream effector proteins remain to be determined.

Despite previous reports demonstrating Smurf proteins to modulate the TGF- β /BMP signaling^{299,300} and the importance of this pathway in bone and cartilage development^{301,302,303}, the lack of an obvious skeletal phenotype in MT mice during normal development and aging as elucidated by this study has a few implications. It suggests that a high level of Smurf2 expression may not be required for bone and cartilage development and that the low levels of Smurf2 present in the MT mice may be sufficient to maintain normal physiological activities. In addition, Smurf1 may have redundant functions that can compensate for the reduced Smurf2 levels during normal development and aging, and account for the moderate and weak protection against OA development observed in young and old Smurf2-deficient mice, respectively.

There are a few limitations of our study. First, it is unclear whether reduced Smurf2 expression functions to delay the onset of OA and/or hinders its progression. We have not identified the exact stress signals produced by DMM that can trigger Smurf2 activity or stimulate its expression beyond physiological levels, which could help establish a molecular basis of how Smurf2 drives OA pathogenesis. Second, besides articular cartilage and subchondral bone,

other joint tissue compartments involved in OA pathogenesis such as synovium, muscles and bone marrow were not examined in this study. Third, the use of immature articular chondrocytes, driven by their ease of isolation, to compare the chondrogenic potential of WT and MT cells may not be ideal. Not only is the population of iMACs heterogenous with varying degrees of differentiation, but their response to exogenous growth factors and cytokines may be different from the chondrocytes residing in mature articular cartilage. Tissue-specific Smurf2-deficient cells (e.g. obtained via conditional knockouts) may be more accurate at revealing the potential cellular contributors within the multi-tissue joint compartment to the protective OA phenotype observed in MT mice after DMM. Lastly, to unequivocally establish the redundant function of Smurf1 and Smurf2 in chondrocytes, validation by simultaneous knock down experiments would be desired.

In summary, we show that while loss of Smurf2 in mice has no physiological impact on bone and cartilage development and aging, its ability to attenuate OA symptoms after DMM surgery in 4 month old mice indicate a potential role in regulating the pathological development of OA. Whether Smurf2 inhibition alone is sufficient to be a therapeutic target for OA remains unclear since the protective effect of Smurf2 in older mice is markedly reduced compared to the younger age group. The enhanced chondrogenic gene expressions in MT iMACs compared to WT suggest a potential for greater cartilage matrix deposition, but the optimal condition to facilitate its translation into meaningful enhancements in cartilage regeneration remain to be identified.

5. Acknowledgments

In addition to the author, the following individuals contributed to the work described in this chapter:

- Eric S. Veien performed a subset of the DMM surgeries on the young mice.
- April Mason-Savas processed all the tissue samples for histology and stained the slides.
- Members of the Song lab (Tera Filion, Artem Kutikov, Pingsheng Liu, Jordan Skelly, Jie Song, Jianwen Xu, and Jing Zhang) assisted in scoring histological sections.
- Stacey Russell performed microCT scans for all the tissue sample.

Chapter III: Age-dependent Changes in the Articular Cartilage and Subchondral Bone of C57BL/6 Mice after Surgical Destabilization of Medial Meniscus

1. Introduction

Age is the primary risk factor for developing osteoarthritis (OA), a chronic, degenerative joint disease that is characterized by progressive loss of articular cartilage and subchondral bone changes. While joint space narrowing, subchondral bone sclerosis and osteophyte formation are all clinical signs of OA, the temporal nature of these changes and how they contribute to OA etiology are still an ongoing debate^{304,305}. More recently, the notion that articular cartilage and subchondral bone should be viewed as a single unit due to their proximity and evidence of biomechanical and molecular signaling crosstalk has gained traction^{96,306,307}. Osteophytes have also been regarded as a compensatory response to mechanical weakening of the degrading cartilage¹⁰⁰, but existing evidence remains limited. Therefore, understanding how bone and cartilage structures change during OA progression as a function of age is essential to better understand OA pathology, elucidate key cellular and molecular players, as well as to develop disease modifying drugs.

Murine OA models are invaluable tools for both basic and translational research due to the ease of manipulating mouse genome. OA can be induced in murine articular joints by collagenase injection³⁰⁸, surgical destabilization¹⁹⁴, or non-invasive injury techniques¹⁸⁷. Surgical destabilization of the medial meniscus (DMM) results in gradual deterioration of articular cartilage and subchondral bone changes, and is thought to recapitulate the progression of human OA pathology^{174,195}. Although DMM emulates post-traumatic OA by nature, murine DMM models have been broadly used by many studies to identify disease-modifying OA targets such as FGF1³⁰⁹, progranulin³¹⁰, IGF-II³¹¹, DKK1³¹², DDR2³¹³, Hif2alpha⁵¹ and ADAMTS5³¹⁴. Recently, our lab has shown that Smurf2-deficiency mitigates cartilage degradation following DMM surgery; however, this benefit is reduced with advanced age³¹⁵. In order to elucidate how age impacts the efficacy of various therapies for DMM-induced OA, it is critical to understand age-dependent changes in articular cartilage and subchondral bone after joint destabilization.

Most DMM-induced OA studies entail surgery on 2–3 month old male mice and analyze their OA phenotypes 1–2 months later. While 2 month old mice are considered skeletally mature adults, their skeletal tissues continue to undergo significant changes well beyond 2 months. For instance, C57BL/6 mice femurs do not reach their maximum length until 6 months of age, and osteoporotic changes in the trabecular bones are not apparent until 6–12 month in females and

over 12 months in males²⁹⁴. Aged mice also undergo significant weight changes, where it almost doubles by 12 months due to body fat accumulation²⁹⁴. Such age-related skeleton and body mass changes may reflect more accurately the biochemical and mechanical environment of human OA joints of middle-aged and older populations. Understanding how aged mice respond to DMM differently can enhance the translatability of this murine model to human OA. In addition, young (~4 M) female mice were found to be less prone to developing OA following DMM compared to their male counterparts³¹⁶, but whether the perceived protective effect of sex hormone persists over age is unclear.

While prior human studies^{317,318,319} have established correlations among articular cartilage erosions, subchondral bone sclerosis and osteophyte formation, whether and how age impacts such structures in the mouse DMM OA model has not been carefully investigated. Previous studies that evaluated the effects of age on DMM-induced OA only examined young mice with 1 month age difference prior to DMM²⁹¹ or focused their study on differences in gene expressions³²⁰. This study aims to understand how different tissue compartments in the knees of wild-type C57BL/6 mice from different age groups respond to DMM surgery by using cartilage histology scoring and quantitative micro-computed tomography (microCT) analyses of subchondral bone plate thickness and osteophyte formation. In addition, we also evaluate whether female hormones continue to provide protective effects on DMM-induced OA by comparing joint phenotype differences between middle-aged males and females at 2 months post-DMM.

2. Materials and Methods

Animals

Wild-type C57BL/6 mice were used in this study. The mice were divided into three age groups corresponding to 4 month old (4 M, male), 12 month old (12 M, male and female) and 18–22 month old (19 M+, male; 18 M and 21 M, female) mice at 2 months post-DMM surgery. All mice were housed in a fully accredited Animal Care facility. All procedures and experiments were approved by the University of Massachusetts Medical School Institutional Animal Care and Use Committee (IACUC), and performed in accordance with the relevant guidelines, regulations and approved IACUC protocol.

DMM Surgery

Surgery was performed on the right knee of mice at 2 months (male, n = 13), 10 months (male, n = 11; female, n = 11), 17–20 months (male, n = 11), and 19 months (females, n = 4) as previously described on page 29.

Histology Analysis

The operated and unoperated knees were harvested, processed for histology, and sections were scored as described on page 28-29. In this study, we focused our analysis on the medial tibial plateau since it is known to be more susceptible to damage after DMM³¹⁴ and we confirmed that it is indeed the case even in the 19M+ age group. Furthermore, we avoided femoral condyle analysis as we found that it revealed less consistent results with changes in cartilage and the subchondral bone due to its greater degree of rotation.

microCT Analysis

Mice knees from each age group (4 M male, n = 9; 12 M male, n = 8; 12 M female, n = 7; 18 M female, n = 3; 19 M+ male, n = 7; 21 M female, n = 3) were scanned on a microCT using parameters described on page 28. To determine subchondral bone plate thickness, the cortical bone of the medial tibial plateau was contoured to exclude the calcified articular cartilage and any portion that is part of an osteophyte. The thickness was calculated using Scanco's trabecular bone evaluation (Direct method). Color maps of the thickness were generated from the contoured subchondral bone plate of the operated and unoperated knees. Only well-demarcated osteophytes that projected outward from the subchondral bone of DMM operated knees were contoured and quantified for total osteophyte tissue volume (TV) and bone volume fraction (BV/TV). 3D reconstruction of the knees was carried out to visualize topographical changes on the bone surface as well as the extent of bony outgrowths as a function of age, gender and DMM. Quantitative microCT data were presented as mean \pm standard deviation.

Statistical Analysis

All statistical analysis was performed using GraphPad Prism version 7.0 (La Jolla, CA). Analysis of the histological scores was performed using Mann-Whitney non-parametric t-test. Analysis of

all microCT data was performed using 2-way ANOVA and Tukey's multiple comparisons test. P-value < 0.05 was considered significant.

3. Results

Severity of cartilage loss after DMM surgery was exacerbated in older male mice.

Cartilage histological scores of the medial tibiae from DMM-operated and unoperated contralateral knees of male mice from three different age groups revealed that the severity of OA cartilage 2 months post-DMM was significantly higher in the 12M and 19M+ group than in the 4M group (Figure 3.1A and 3.1B). The median histological scores of unoperated knees for the 4M, 12M and 19M+ groups were 0.18 (0.11–0.33), 0.33 (0–0.33) and 0.67 (0.33–0.75), respectively, consistent with very mild, non-structural spontaneous OA cartilage changes with age. The median histological score of the DMM knees in the 4M, 12M and 19M+ groups was 1.8 (0.81–2.4), 4.2 (3.8–4.5) and 3.4 (2.2–4.7), respectively. Representative images of the articular cartilage in unoperated contralateral knees showed only progressive loss of safranin-O/fast green staining but minimal structural change with age, with superficial fibrillations only observed in some of the 19M+ group. By contrast, the articular cartilage of DMM-operated knees showed increasing severity of cartilage erosion beyond the tidemark with age (Figure 3.1B).

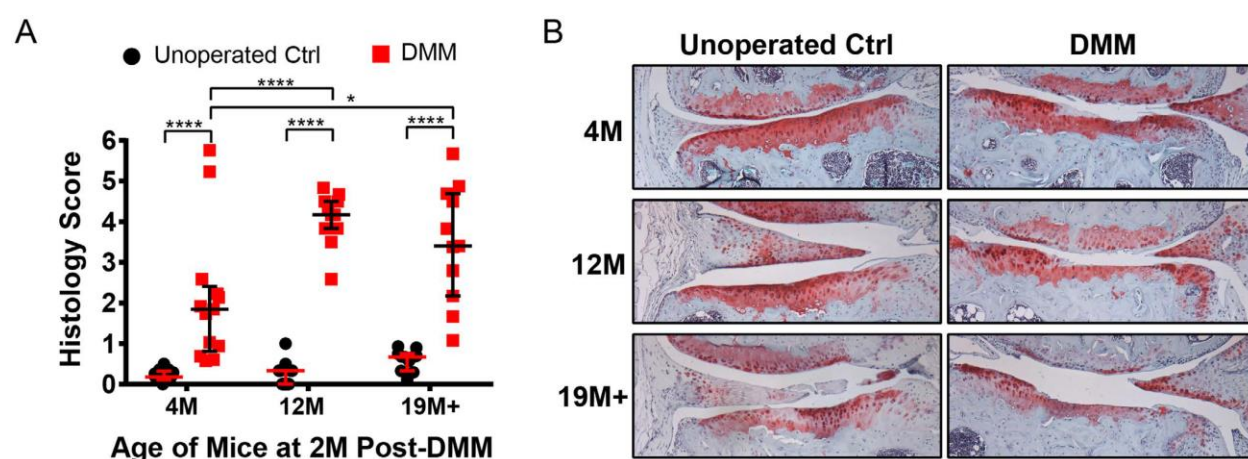


Figure 3.1 Age-dependent changes in articular cartilage degradation of male mice 2M post-DMM

(A) Histological score of the tibial articular cartilage of unoperated and DMM operated knees of male mice from different age groups. Individual scores are plotted along with median score and interquartile range. *p-value < 0.05, ****p-value < 0.0001; (B) Representative safranin-o/fast green stained histological sections of the articular cartilage of unoperated and DMM operated knees of male mice from different age groups.

Subchondral bone plate thickening after DMM surgery was greater in older male mice

The subchondral bone plates of operated knees increased in thickness 2 months after DMM surgery compared to unoperated contralateral knees regardless of age (Figure 3.2A). The difference in thickness between the operated and unoperated knee was significant in the 12 M and 19 M+ groups. The 4 M group followed a similar upward trend, but the increase was not statistically significant. In the unoperated control knees, the thickness of the subchondral bone plates was comparable across all age groups. Color maps of the subchondral bone plate thickness confirmed that the 4 M age group exhibited a similar range of thickness between operated and unoperated knees, but in the 12 M and 19 M+ groups, the thickness significantly increased post-DMM (Figure 3.2B).

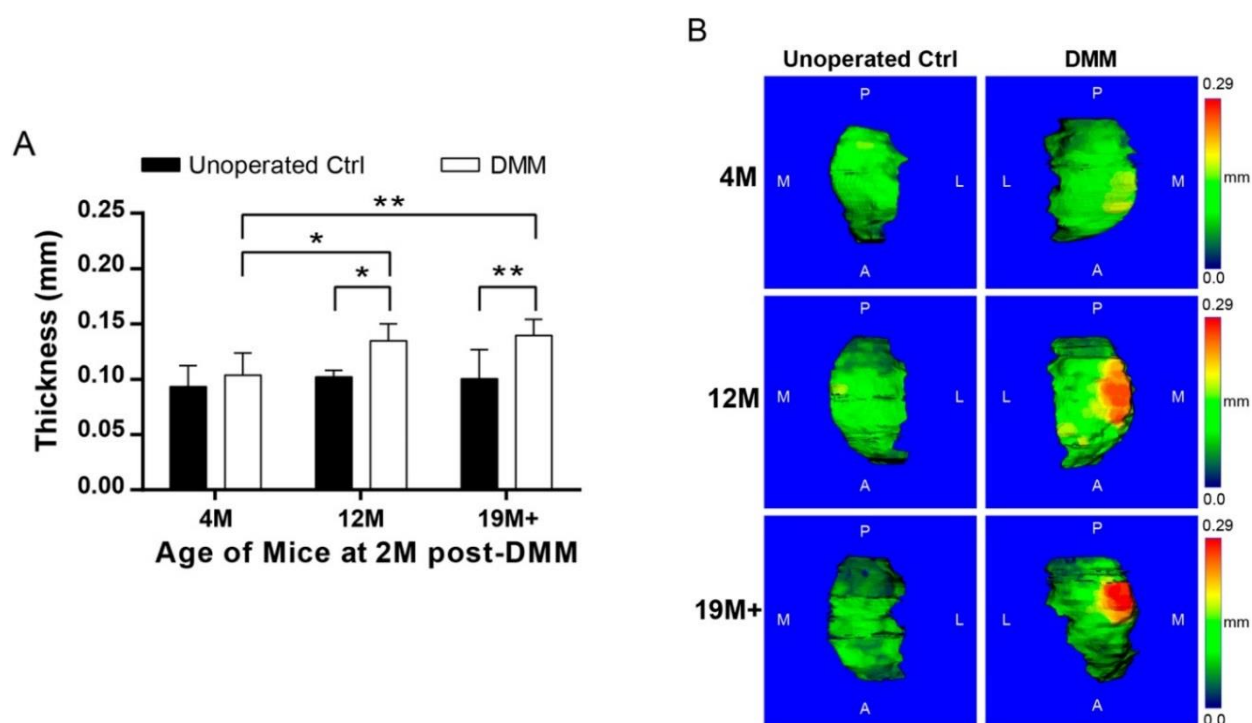


Figure 3.2 Age-dependent changes in subchondral bone plate thickness of male mice 2M post-DMM

(A) Quantification of tibial subchondral bone plate thickness of DMM operated and unoperated contralateral knees of male mice from different age groups. *p-value < 0.05, **p-value < 0.01; (B) Representative color maps of subchondral bone plate thickness of DMM operated and unoperated contralateral knees from each age group. Color map legend is scaled to the maximum thickness detected in the 19 M+ group. A = anterior, P = posterior, M = medial, and L = lateral.

Bone volume fraction of osteophytes after DMM was significantly higher in older (19 M+) male mice

Osteophytes were detected on all of the DMM operated knees regardless of age, although two knees from the 4 M age group showed only superficial bony outgrowths and were not quantified. None of the unoperated knees showed signs of osteophyte formation, except for one knee in the 19 M+ age group. Quantification of the osteophyte total tissue volume (TV) revealed a trend of increasing size with age, but this was not statistically significant (Figure 3.3A, left). The bone volume fraction (BV/TV) of osteophytes was significantly higher in the 19 M+ group compared to the other age groups, while no difference in bone volume fraction was observed between the 4 M and 12 M age groups (Figure 3.3A, right). Representative histological images of the osteophyte, as demarcated by a black dashed line, showed a progressive increase in osteophyte size and disappearance of cartilaginous regions and marrow-like cavities with age (Figure 3.3B). 3D reconstruction of the microCT images allowed visualization of the bone surface topographical changes between DMM operated and unoperated knees (Figure 3.3C). The 4 M unoperated tibia had an even textured surface and a distinct ossification groove that marks the perichondrial ring of the growth plate. In contrast, the 4 M DMM operated knee showed extensive superficial bone thickening that obscured the ossification groove. A few roughened patches (indicated by unfilled arrows) were also observed in the distal femur. In the 12 M group, the ossification groove was less visible in the unoperated tibia than the younger mice while the DMM operated tibia showed extensive bone thickening, prominent rough patches (especially in the distal femur, indicated by unfilled arrows) and appearance of distinct bone projections (indicated by filled arrows). In the 19 M+ group, signs of rough patches were observed both before and after DMM while far more pronounced osteophyte projections were observed post DMM.

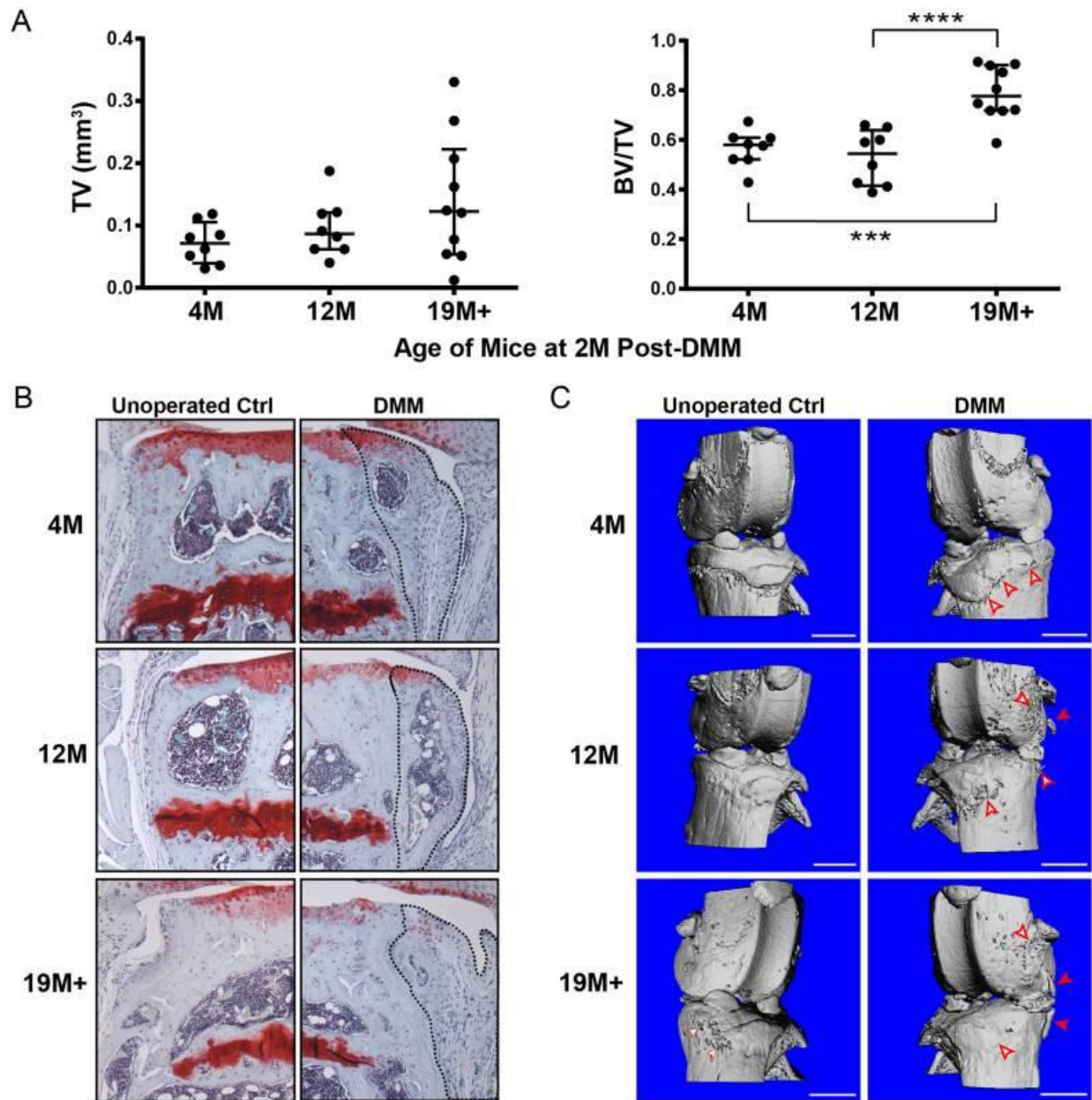


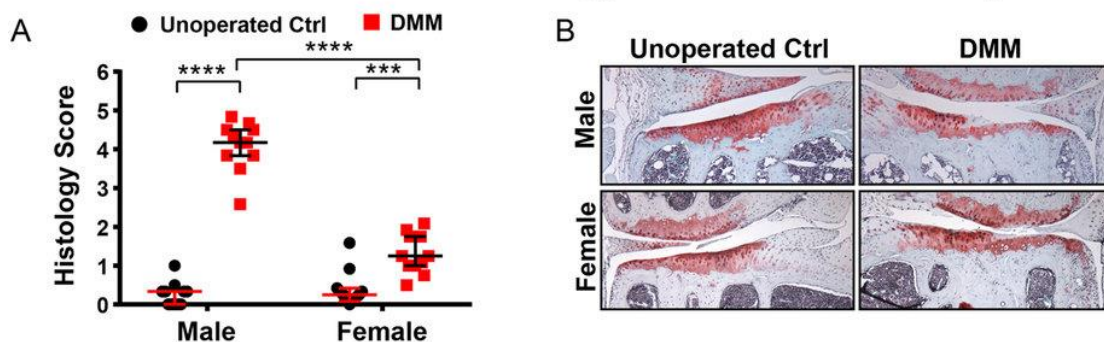
Figure 3.3 Age-dependent changes in osteophyte size and quality of male mice 2M post-DMM

(A) Total tissue volume (TV) and bone volume fraction (BV/TV) of contoured osteophytes in DMM operated knees of male mice from different age groups. *** $p < 0.001$, **** $p < 0.0001$; (B) Representative safranin-O/fast green stained histological sections of the DMM operated knees in male mice from different age groups, with osteophytes contoured by dotted lines; (C) Representative 3D reconstructed microCT images revealing distinct surface topographical changes of the knee post-DMM in male mice from different age groups. Open red arrows indicate areas of superficial roughening and/or thickening of bone surface that were not observed in the unoperated knee. Filled red arrows indicate osteophyte protrusions away from subchondral bone surface which were more prominent in the 19 M+ age group. Scale bar = 1 mm.

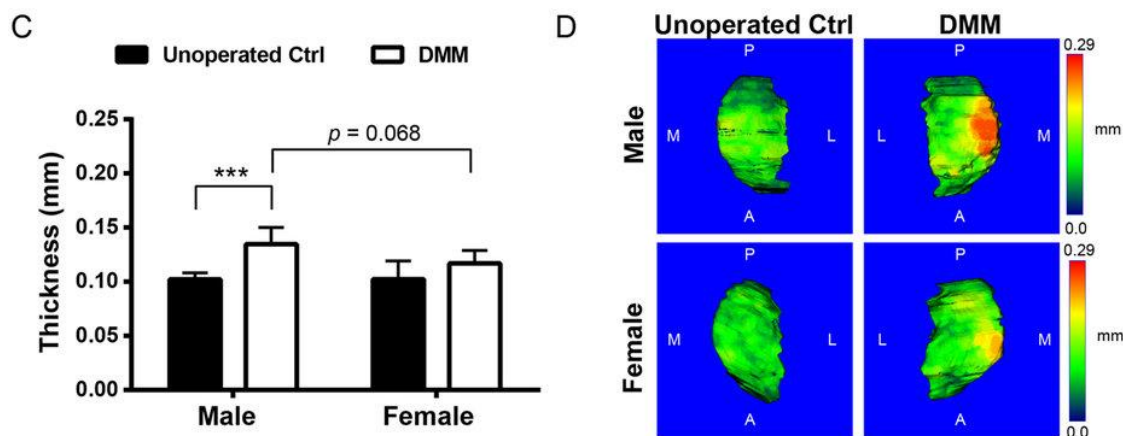
Female mice developed milder OA post-DMM compared to males in the 12 M age group

Female mice from the 12 M group developed milder OA than their male counterparts (Figure 3.4A). The median histological score of the articular cartilage from unoperated female knees was 0.25 (0.08–0.42) compared to a score of 0.33 (0.00–0.33) in the males, reflecting normal cartilage structures for both sexes (Figure 3.4B). In the DMM operated female knees, the median histological score was 1.3 (1.0–1.8) compared to the operated male knees of 4.2 (3.8–4.5). Histological images showed that the articular cartilage damage was primarily limited to superficial fibrillations and loss of safranin-O/fast green staining in the 12 M female post-DMM, while the male operated knees showed more severe cartilage erosions down to the calcified cartilage (Figure 3.4B). The degrees of subchondral bone sclerosis between 12 M male and female DMM operated knees were also very different despite similar bone plate thickness in the unoperated knees. No statistically significant increase in subchondral bone plate thickness was observed in the females while significant thickening was observed in the males after DMM (Figure 3.4C). Color maps of bone thickness showed a distinct localization of the thickened region in the subchondral bone plate of the male operated knee while the spatial variation of subchondral bone plate thickness between unoperated and operated knees remained similar in the 12 M female (Figure 3.4D). Finally, smaller osteophytes were detected in 12 M female DMM operated knees ($TV = 0.028 \pm 0.014 \text{ mm}^3$) compared to males ($TV = 0.096 \pm 0.047 \text{ mm}^3$) (Figure 3.4E), but the bone volume fraction of the osteophytes were comparable between the two sexes (Figure 3.4F). Histology also confirmed smaller osteophytes in the female DMM knees, which were also characterized by the presence of marrow-like cavities (Figure 3.4G). 3D reconstruction of the microCT images detected visible projections of osteophytes extending out from the subchondral bone (Figure 2.4H, indicated by filled arrows) in DMM operated males but not in the females.

Semi-Quantitation and Histology of Tibial Articular Cartilage



Quantitation and Color Mapping of Subchondral Bone Plate Thickness



Quantitation, Histology and μ CT Visualization of Osteophyte Formation

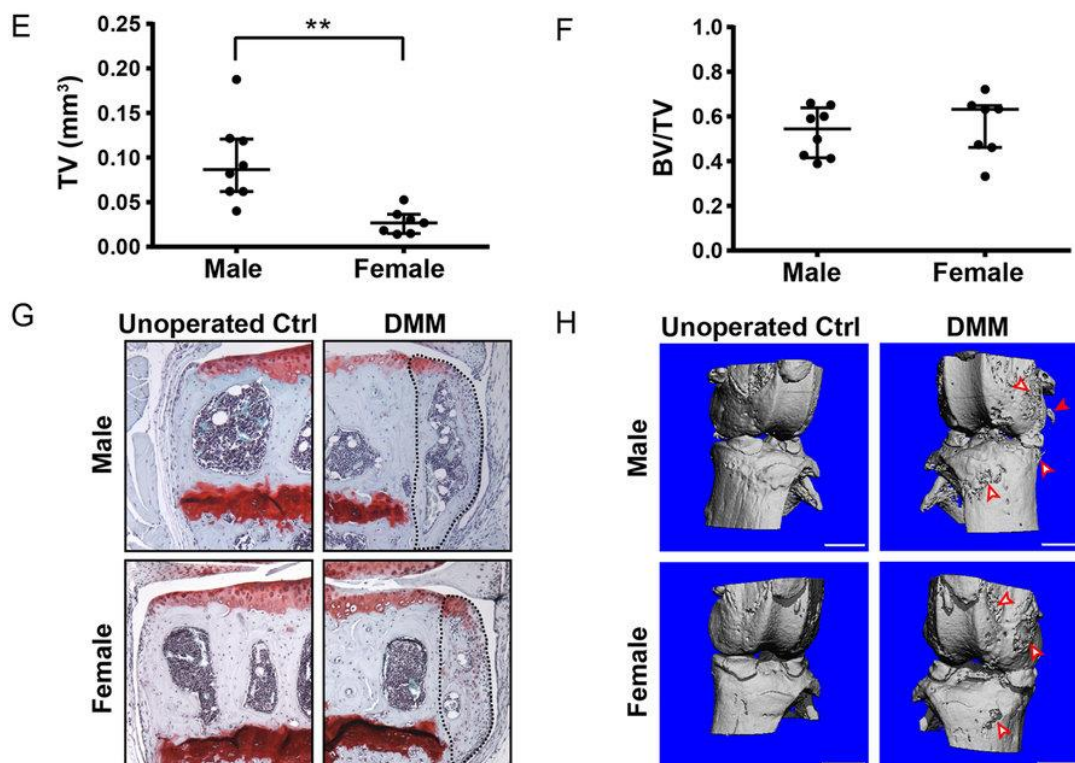


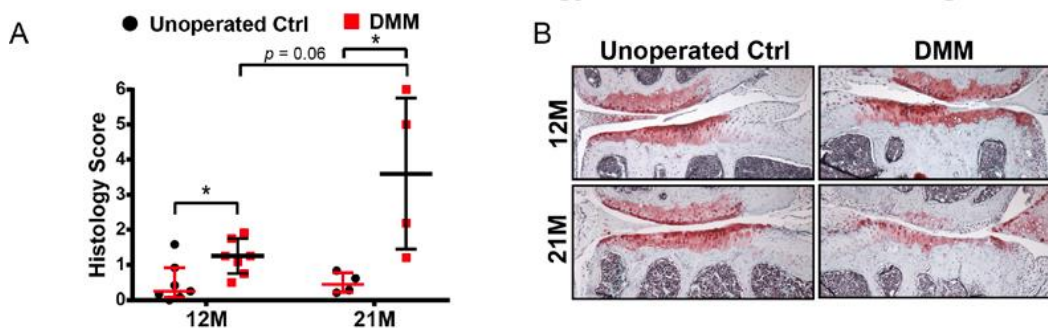
Figure 3.4 Comparison of different tissue compartments of the joint between 12M male and 12M female mice 2M post-DMM

(A) Histological score of the tibial articular cartilage from unoperated and DMM operated knees of male vs. female mice from the 12 M age group. Individual scores are plotted along with median score and interquartile range. ***p-value < 0.001, ****p-value < 0.0001; (B) Representative safranin-O/fast green stained histological sections of the articular cartilage of unoperated and DMM operated knees of male vs. female mice from the 12 M age group; (C) Quantification of tibial subchondral bone plate thickness of DMM operated and unoperated contralateral knees of male vs. female mice from the 12 M age group. **p-value < 0.01; (D) Representative color maps of subchondral bone plate thickness of DMM operated and unoperated contralateral knee of male vs. female mice from the 12 M age group. Color map legend is scaled to the maximum thickness detected in the 19 M+ age group. A = anterior, P = posterior, M = medial, and L = lateral; (E) Total tissue volume (TV) and (F) bone volume fraction (BV/TV) of contoured osteophytes in DMM operated knees from male vs. female mice from the 12 M age group. **p < 0.01; (G) Representative safranin-O/fast green stained histological sections showing the presence of osteophyte (dashed line) in the DMM operated knees in male vs. female mice from the 12 M age group; (H) Representative 3D reconstructed microCT images showing distinct surface topographical changes of the knee post-DMM in male vs. female mice from the 12 M age group. Open red arrows indicate superficial roughening and/or thickening of bone surface. Filled red arrows indicate osteophyte protrusions away from subchondral bone surface. Scale bar = 1 mm.

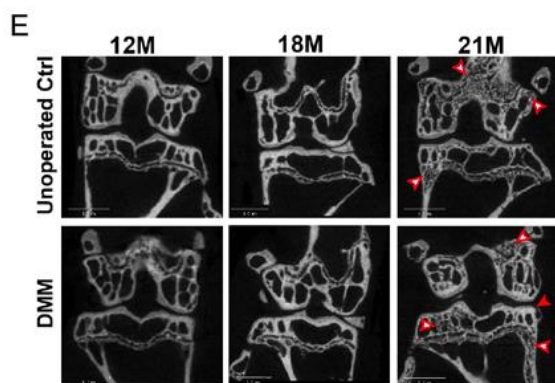
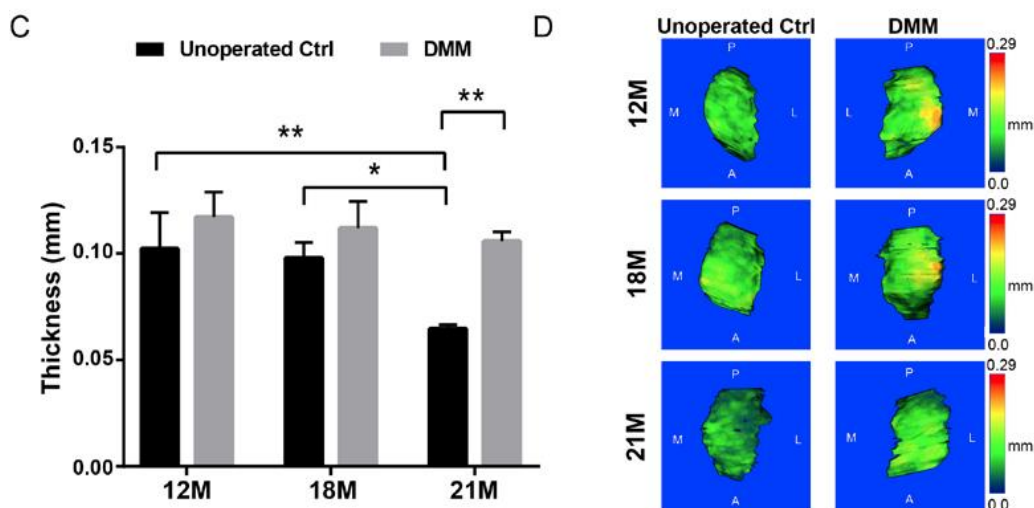
With advanced age, female mice showed signs of severe OA and subchondral bone changes post-DMM

Of the female mice at 21 M (n = 4) that underwent DMM surgery, two showed signs of severe OA cartilage with scores of 5.0 and 6.0 while the other two had scores of 1.2 and 2.2, which were comparable to the scores from the female 12 M group post-DMM (Figure 3.5A and 3.5B). The difference in subchondral bone plate thickness with and without DMM surgery was also significant for female mice in the 21 M (n = 3) group but not in the 12 M (n = 7) or 18 M (n = 3) groups (Figure 3.5C). Color mapping showed that the overall subchondral bone changes with and without DMM were very mild compared to male counterparts (Figure 3.5D) and that the difference observed in the 21 M group was a result of severe osteoporosis in the unoperated control (Figure 3.5E). The sizes of the osteophytes detected in the DMM-operated knees were comparable across all female age groups (Figure 3.5F), but the BV/TV of the osteophytes was highest post-DMM in the 18 M group (Figure 3.5G).

Semi-Quantitation and Histology of Tibial Articular Cartilage



Quantitation and Color Mapping of Subchondral Bone Plate Thickness



Quantitation of Osteophyte Formation

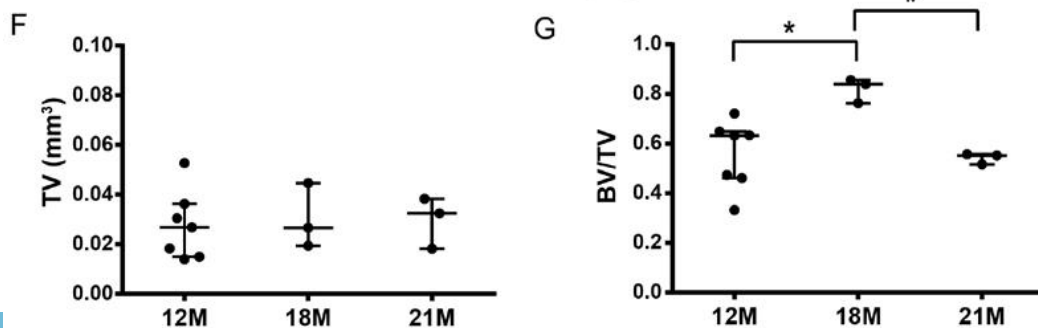


Figure 3.5 Age-dependent changes in different joint structures of female mice 2M post-DMM

(A) Histological scores and (B) representative safranin-O/fast green stained histological sections of the tibial articular cartilage from unoperated and DMM operated knees of female mice from the 12M and 21M age groups. Individual scores are plotted along with median score and interquartile range. * $p < 0.05$; (C) Quantification and (D) representative color maps of tibial subchondral bone plate thickness of DMM operated and unoperated contralateral knees of female mice from the 12M, 18M and 21M age groups. * p -value < 0.05 , ** p -value < 0.01 ; Color map legend is scaled to the maximum thickness detected in the male 19M+ age group. A = anterior, P = posterior, M = medial, and L = lateral; (E) μ CT images of longitudinal cross sections of DMM operated and unoperated contralateral knees of female mice from 12M, 18M and 21M. Open arrows indicate areas of osteoporosis and closed arrow indicates region of enhanced bone remodeling after DMM surgery. (F) Total tissue volume (TV) and (G) bone volume fraction (BV/TV) of contoured osteophytes in DMM operated knees of female mice from the 12M, 18M and 21M age group. * $p < 0.05$.

4. Discussion

Multiple tissue compartments within the knee undergo significant structural changes during OA development. Using C57BL/6 mice from 3 age groups, we determined that articular cartilage and subchondral bone respond to DMM differently with age. The DMM surgery, popularized by Glasson et al.¹⁹⁵, is considered a minimally invasive surgery that mimics human OA following meniscal injury. However, most murine OA studies that perform DMM do not adequately address age-related perturbations in joint mechanics or cellular processes. Results from this study reaffirm that age is an important factor in dictating how various compartments in the mouse joint respond to DMM-induced OA and should be considered in determining the translatability between murine OA models and human OA.

Subchondral bone plate sclerosis and articular cartilage degeneration are both hallmarks of mouse³¹⁴ and human OA³²¹. We showed that in male mice, the thickening of DMM-induced subchondral bone plate accompanied increased severity of degradation in the overlying cartilage. However, between 12 M and 19 M+ groups, we did not observe significant differences between the degrees of cartilage degradation and subchondral bone thickening. Interestingly, although the 12 M and 19 M+ groups both weighed significantly more than the 4 M group, no significant further increase in body weight from 12 M to 19 M+ was detected (data not shown). Whether the observed age-related changes can be attributed to altered joint mechanics (driven by weight gain or reduced physical activity) or by age-related cellular metabolism and function requires additional studies. Given the need for more reproducible murine models to study OA³²², our results suggest that performing DMM surgery on middle-aged male mice (12 M group) could be advantageous in producing more uniform and reproducible OA phenotypes than in younger mice (2 M group). The 19 M+ group also developed more severe cartilage degradation post-DMM than the 4 M group, but the histology scores were not as uniform as the 12 M group.

Possible reasons include the wider age range (19 to 22 months at time of analysis) within this group and other unexplored comorbidities that accompany advanced age.

Osteophyte formation was detected in all DMM operated knees regardless of age, but the size and shape varied. Among the three age groups, the size of the osteophyte post-DMM trended up with age but the increase was not significant (Figure 3.3A, left). The size³²³ and direction³²⁴ of the osteophyte have been associated with the degree of cartilage erosion, but this correlation was not evident from our data. No significant differences in the size or bone volume fraction of osteophytes was observed between 4 M and 12 M age groups where the greatest difference in cartilage and subchondral bone plate changes were detected. The direction of the bony outgrowths was also confined to the horizontal axis and never in the vertical axis, which is common in advanced human OA. Overall, our data with aged male mice do not support a strong correlation between the extent of osteophyte formation/remodeling and the degrees of articular cartilage erosion or subchondral bone plate thickening. This finding is in line with previous observations that osteophytes can develop in the absence of overt cartilage damage^{100,106} and in some animal models is visible a few days after joint injury¹⁰¹. Nevertheless, it is still possible that cartilage and the subchondral bone plate affect osteophyte development through soluble factors. Interestingly, we found that the bone volume fraction of the osteophytes in the 19 M+ age group was significantly higher than those in the younger age groups, consistent with more extensive bone remodeling/faster bone turnover reported within more mature osteophytes^{105,107}. The appearance of central ossification coupled with fewer cartilaginous regions and marrow-like cavities in the 19 M+ osteophyte was also consistent with more extensively remolded bone found in later stages of osteophyte development¹⁰⁷. While higher bone turnover in the subchondral bone has been associated with advanced stages of human OA^{325,326,327}, further studies are necessary to understand the relationship among different stages of osteophytes and OA progression.

Sex hormones play a significant role in OA severity in the murine DMM model, where young 4.5 M males develop more severe OA than age-matched females³¹⁶. Given the more consistent OA phenotype in 12 M males, we examined whether sex differences in DMM-induced OA severity persisted at this age. We found that at 12 M, female mice continue to develop milder OA compared to age-matched males, characterized by less articular cartilage degradation, less subchondral bone sclerosis, and smaller osteophytes. This milder OA in the 12 M females also reflects the same association between cartilage erosion and subchondral bone plate thickening found in males. Since C57BL/6 female mice produce litters up to 15 months of age³²⁸, the amount of circulating estrogen in 12 M females may be sufficient to still

protect against more severe OA in spite of their increasing osteoporosis risks and weight gains²⁹⁴. It should be noted, however, the weight factor cannot be ruled out from the observed sex-specific differences as 12 M female mice weighed significantly less than 12 M male counterparts (data not shown).

Although not the focus of this study, examination of the contralateral unoperated joint controls revealed that spontaneous OA due to age was very mild in nature. The age-induced OA changes were characterized with mainly progressive loss of safranin-O staining of the articular cartilage but no significant structural perturbations (superficial fibrillations only observed in some of the 19 M+ group). We also did not observe significant changes in subchondral bone with age except for the very old (21 M) females where a reduction in subchondral bone mineral density consistent with osteoporosis was observed.

There are several limitations in this study. First, we validated the efficacy of our DMM procedure with sham operation controls (opening and closing of skin and joint capsule) in the 2 M aged groups prior to the study where OA was only found in DMM-operated but not sham-operated joints (comparable to non-operated control), but such validation was not performed in the other older age groups. It should be noted, however, that the limited literature³²⁰ on relatively old mice demonstrated no difference between sham and unoperated control in 12 M male mice. In addition to articular cartilage and subchondral bone, synovial inflammation also plays a role in OA development¹¹⁶ and is also age-dependent²⁹¹. Detecting markers of inflammation in the synovial fluid or in the serum could provide insight into age-related difference in the degree or onset of joint inflammation. Finally, the observation that females were still protected from DMM-induced OA at 12 M begs the questions as to whether such protection diminishes in even older females. Since this was not the initial focus of our study, we used only a limited number of aged female mice to preliminarily evaluate the structural joint changes in much older (18 M and 21 M) females. We observed severe cartilage erosions in some 21 M females while others showed only mild cartilage erosions similar to those seen in the 12 M age group. This suggests that the protective effect of sex hormone may have started to decrease at 21 M. It was only in the 21 M female group that we observed significant differences in subchondral bone plate thickness between DMM operated and unoperated knees, which we attribute to the severe thinning of the subchondral bone prior to DMM due to osteoporosis. For future comprehensive studies investigating the role of sex hormone in OA development in old female mice, it would be valuable to extend the examination beyond 2 months post-DMM, as others have shown that sex hormone protection against DMM-induced OA in younger females could subside after 12 weeks³²⁹.

In conclusion, we showed that the increasing severity of DMM-induced cartilage degradation as a function of age was accompanied with more pronounced subchondral bone plate thickening and, to a lesser extent, the increasing size of osteophytes. Our findings support previous work³³⁰ that utilizes non-invasive monitoring of subchondral bone changes as an accurate method for evaluating OA severity longitudinally. Future work combining contrast-enabled microCT quantitation³³¹ of cartilage changes with subchondral bone plate thickness changes could help establish better temporal correlations between these two structures during OA development. Our study supports the view³³² that age is an important factor in dictating structural changes (accelerated cartilage loss coupled with subchondral bone plate sclerosis and enhanced osteophyte maturation) post-DMM. Accordingly, we suggest that therapeutic effects of potential disease modifying OA targets observed in young adult mice using DMM-induced OA should also be validated in older mice. Our data also suggest that DMM-induced OA in older 12 M mice is more reproducible and may be more relevant than 4 M mice for identifying and translating potential disease modifying OA targets to human therapy.

5. Acknowledgments

In addition to the author, the following individuals contributed to the work described in this chapter:

- Jordan Skelly assisted in scoring histological sections and analyzing microCT results.
- April Mason-Savas processed all the tissue samples for histology and stained the slides.
- Stacey Russell performed the microCT scans for all the tissue sample.

Chapter IV: Anionic and Zwitterionic Residues Modulate the Stiffness of Photo-crosslinked Hydrogel and the Cellular Behavior of Encapsulated Chondrocytes

1. Introduction

Articular cartilage is a highly specialized and organized tissue that lines the ends of long bones and is integral to the function of all diarthrodial joints. Not only does it provide superior lubrication for moving bones but it also possesses the mechanical properties to resist compressive and tensile forces that are essential for weight-bearing and movement. The unique extracellular matrix (ECM) of cartilage is comprised of an interpenetrating network of collagen and negatively charged proteoglycans and contains only one cell type, chondrocytes. Due to its avascular and aneural nature, articular cartilage has very limited regenerative capability. Defects in articular cartilage as a result of traumatic injury fails to heal properly and promote the formation of a mechanically inferior fibrocartilage, predisposing an individual to develop osteoarthritis (OA) and to undergo total knee arthroplasty ten years earlier than the average population^{333, 334}. Various surgical techniques²⁰⁴ have been employed to promote hyaline cartilage regeneration, including osteochondral autograft/allografts, microfracture, and autologous chondrocyte implantation, but none has unequivocally demonstrated long-term efficacy in delaying the onset of OA.

With promising clinical results^{335, 336} and recent FDA approval³³⁷, matrix-assisted autologous chondrocyte implantation (MACI) has gained traction for focal articular cartilage lesion repair, and has inspired more biomimetic scaffold designs to promote ECM deposition. Ongoing strategies have focused on engineering synthetic polymer scaffolds to recapitulate the biochemical and biomechanical environment of native ECM³³⁸. For instance, incorporation of natural hyaluronic acid and chondroitin sulfate in synthetic hydrogels have frequently been employed to stimulate chondrocyte differentiation and promote cartilage matrix production of encapsulated progenitor cells^{339,340,341,342}. The bioactivity of these macromolecules has been attributed to their interaction with cell surface receptors³⁴³ as well as their ability to sequester and enrich secreted endogenous soluble factors within the tissue microenvironment through electrostatic interactions^{344,345}. The prochondrogenic effects of these biomacromolecules on 3D encapsulated chondrocytes and stem cells, however, are difficult to delineate as their incorporation into the synthetic matrices often perturb other properties, such as crosslinking efficiencies and swelling ratios, making it difficult to isolate one effect from the other. Controlled covalent incorporation of small molecule chemical moieties into a synthetic hydrogels has

therefore been explored as an alternative for regulating the fate / metabolism of encapsulated cells.

Previous work^{346, 347} from the Anseth group have shown that covalent incorporation of hydrophobic tert-butyl and phosphate residues in hydrogels promoted adipogenic and osteogenic differentiations of encapsulated stem cells, respectively. Zwitterionic residues, which possess equal numbers of positive and negative charges and are overall charge neutral, have the ability to interact with oppositely charged ionic solutes or oppositely charged epitopes of proteins. We previously showed that zwitterionic residues, when presented in 3-D crosslinked hydrogels, are able to template robust mineralization by attracting oppositely charged precursor ions^{348, 349} or dynamically retain and release growth factors for scaffold-guided bone tissue regeneration³⁵⁰. Whether synthetic hydrogels functionalized with zwitterionic residues may be exploited for cartilage tissue engineering, however, remains unclear.

Another distinct feature of the articular cartilage tissue microenvironment is the osmotic swelling pressure and stiffness imposed by the anionic proteoglycans embedded within the collagen network. Aggrecan, the predominant chondroitin sulfate proteoglycan in articular cartilage, is primarily responsible for affording cartilage its resistance to compression. Specifically, it is the fixed negative charges from sulfated and carboxylated residues of aggrecan that attract counter ions and water, resulting in high osmotic pressure and resistance to compression^{351, 352, 353}. Photo-crosslinked polyethylene dimethacrylate (PEGDMA)-based hydrogel scaffolds are highly hydrophilic and have been widely explored for cartilage tissue engineering. However, augmenting their mechanical properties to better resist compressive forces and fluid flow have been largely limited to shortening PEG chain lengths, increasing covalent crosslinking content, or increasing the overall weight fraction of the polymer^{354, 355, 356}. These modifications, however, also inevitably alter the overall swelling behavior and nutrient transport of the synthetic network. Chemical modification of PEGDMA hydrogels aimed at increasing the stiffness of the hydrogel scaffold without increasing polymer content or significantly perturbing swelling behavior remains largely unexplored.

We hypothesize that strengthening mechanical properties of photo-crosslinked PEGDMA hydrogels could be accomplished via covalent incorporation of small molecule anionic or zwitterionic residues without altering overall polymer content or swelling behavior. In addition, we hypothesize that the incorporation of these residues within a 3D matrix at an appropriate content could help maintain a suitable microenvironment for cartilage matrix deposition by encapsulated chondrocytes. To test this hypothesis, we photo-polymerized 0%, 5% or 10% sulfonate (negatively charged) or sulfobetaine (zwitterionic) functionalized methacrylates (SPMA

and SBMA, Figure 4.1A) with varying contents of PEGDMA while maintaining the overall polymer fraction the same. We then investigated their swelling, mechanical properties as well as the viability and chondrogenic matrix production of encapsulated chondrocytes. The non-degradable nature of the photo-crosslinked PEGDMA network was chosen to eliminate the confounding factor of hydrogel degradation so that the effect of chemically-modified microenvironment may be more readily delineated.

2. Materials and Methods

Polyethylene glycol dimethacrylate (PEGDMA) Synthesis

Synthesis of PEGDMA was adapted from a previously described method³⁵⁷. Briefly, 20g of polyethylene glycol (PEG) with molecular weight of 6,000 Dalton (Sigma) was refluxed at 120 °C to remove water. After cooling, the PEG was dissolved in 150 mL of toluene and 4 molar equivalent of anhydrous trimethylamine (Sigma) and methacryloyl chloride (Aldrich) were added. The mixture was reacted at 35 °C overnight under argon. Triethylamine salt was removed by filtration and the PEGDMA product was precipitated in ice cold diethyl ether (Fisher). Finally, the product was further purified by removing lower molecular weight side products/reagents via dialysis against water at room temperature using a 2,000 Dalton MW cutoff membrane prior to freeze drying. The ¹H NMR spectrum of PEGDMA was consistent with previously published work³⁵⁷.

Hydrogel Preparation

Stock solutions of PEGDMA, 3-sulfopropyl methacrylate potassium salt (SPMA, Sigma) and [2-(methacryloyloxy)ethyl]dimethyl-(3-sulfopropyl)ammonium hydroxide (SBMA, Sigma) were prepared in PBS to a final concentration of 10% (w/v). All hydrogels were prepared by adding 0.05% of VA-086 (Wako) into solutions of PEGDMA and either 0%, 5% or 10% of the SPMA or SBMA stock solution to maintain a final polymer content of 10% (w/v). For mechanical testing, hydrogel solutions (200 μ L) were photo-crosslinked in an 8 mm diameter Teflon mold under 365nm irradiation for 10 min, then fully equilibrated in PBS at room temperature prior to testing. For cell-laden hydrogels, 500,000 cells were mixed with 50 μ L of the polymer cocktail and photo-crosslinked in Teflon molds under 365-nm irradiation for 10 min to achieve a final cell encapsulation density of 10⁷ cells/mL.

Equilibrium Volume Swelling Ratio (ESR_v)

Crosslinked hydrogels were equilibrated in PBS for 72 h with gentle agitation on an orbital shaker at room temperature. The height, h , and diameter, d , of the swelled hydrogel was measured using digital calipers and the final swelled volume (V_s) was calculated as $h\pi(d/2)^2$. ESR_v of each hydrogel in PBS was determined by the formula $ESR_v = (V_s - V_d)/V_d \times 100\%$ where V_d is 50 μ L for all formulations.

Immature Murine Articular Chondrocyte (iMAC) Isolation

iMAC was harvested from wild-type C57BL/6 neonates (4-6 days old) as previously described on page 26.

Human OA Chondrocytes (hAC) Isolation

Discarded tissues from osteoarthritic patients (age 50-70) undergoing total knee arthroplasty were collected and stored in ice cold PBS supplemented with penicillin/streptomycin until processing shortly after. Using a sterilized razor blade, structurally intact articular cartilage from the femoral condyles was shaved off and minced into tiny pieces. The cartilage pieces (3-5 g) were transferred to a 50-mL conical tube with type II collagenase solution (1mg/mL or 300U/mL) and digested overnight at 37 °C on a rotator. Any residual cartilage fragments were removed by filtration through a 70- μ m nylon mesh and the cell suspension was plated at a cell density of $25 \times 10^3/cm^2$. Cells were cultured until 80% confluency before trypsinization and encapsulation in hydrogel. Only passage 1 hACs were used in the study.

Cell Culture Media

Cell-laden hydrogels were cultured at 37 °C with 5% CO₂ in either expansion medium (EM) or chondrogenic medium (CM). EM consisted of 10% FBS (Gibco) and 1% penicillin/streptomycin (Corning) in high glucose DMEM (Invitrogen) while CM consisted of high glucose DMEM supplemented with 40 μ g/mL L-proline (Sigma), 100 μ g/mL sodium pyruvate (Sigma), 1% insulin-transferrin-selenous acid mixture (B&D Bioscience), 100 nM dexamethasone (Sigma) and 10 ng/mL TGF- β 3 (R&D systems). Media were changed three times per week.

Mechanical Testing

The unconfined compressive behavior of each hydrogel formulation (n=3) was examined under strain-controlled mode on a DMA800 (TA Instruments) equipped with a submersion compression fixture. Each hydrogel specimen was submerged in PBS (pH 7.4) and compressed three times to 30% strain at a rate of 20%/min under ambient conditions (20°C). The compressive moduli for each hydrogel were calculated at the strain ranges of 5-10% and 15-20%.

Metabolic Activity of Encapsulated Chondrocytes

The metabolic activity of encapsulated chondrocytes in each hydrogel formulation (n=3) was examined using cell counting kit-8 (CCK-8, Dojindo), which reflects the dehydrogenase activity within viable cells. At each time point, CCK-8 reagent was added to the cell culture medium and incubated for 4 h. Colorimetric analysis of the media was performed at 450nm using a Multiskan FC microplate photometer (Thermo Scientific).

Live/Dead Staining of Encapsulated Chondrocytes.

Viability of encapsulated chondrocytes was examined using a live/dead staining kit (Molecular Probes). Staining of the cell-laden 3D constructs was performed according to manufacturer's instructions with working solutions of 2- μ M calcein AM and 1- μ M EthD-1. The stained hydrogels were placed on a glass bottom dish and imaged using a TCS SP5 II (Leica) confocal microscope. The composite image was created by overlaying 21 images acquired at 5- μ m intervals along the z-axis.

Histochemical staining for GAG

Cell-laden hydrogels retrieved from culture were fixed with 10% neutral buffered formalin overnight, serially dehydrated with ethanol and embedded in glycol methacrylate and sectioned. Each 5- μ m section was stained by toluidine blue to assess the production of sulfated GAG and at least 2 sections, 100 μ m apart, were examined for each construct.

Immunofluorescence Staining for extracellular matrix proteins

Cell-laden hydrogels retrieved from culture were fixed by 10% buffered formalin overnight and then washed thrice in 1% BSA in PBS. Primary antibody against type II collagen (Millipore, MAB8887, 1:200) or type X collagen (eBioscience, 14-9771-80, 1:200) was added to the hydrogels and incubated at 37 °C for at least one hour with mild agitation. Negative controls were incubated in PBS without primary antibodies. The hydrogels were washed thrice again with 1% BSA in PBS. Alexa 488-conjugated goat secondary antibody against mouse IgG (Molecular Probes, 1:200) was added for incubation at 37 °C for 1 hr. Hydrogels were then washed thrice in 0.1% BSA in PBS before being stained with DAPI reagent (Invitrogen) according to manufacturer's instructions. The stained 3D hydrogels were placed on a glass bottom dish and imaged by confocal microscope (Leica) as described above.

Statistical Analysis

One-way ANOVA with multiple comparisons was performed using Prism (GraphPad, version 7) to determine the statistical significance between modified vs. unmodified PEGDMA hydrogel formulations (for swelling ratio, compressive modulus, quantification of encapsulated albumin-FITC and CCK8 quantification at each time point), with p-value less than 0.05 considered significant.

3. Results

Covalent incorporation of anionic or zwitterionic residues into PEGDMA hydrogel significantly enhanced the hydrogel stiffness without perturbing the swelling ratio

Percentage weight fractions of polymers in photo-crosslinked hydrogels are known to affect their compressive moduli and swelling behavior. We sought to isolate the effect of covalently incorporated anionic or zwitterionic residues on the physical and biological properties of PEGDMA by maintaining the total weight fraction of the polymer solution. Specifically, we kept the total polymer fractions constant at 10% (w/v, in PBS containing 0.05w/v% of radical initiator VA-086) by lowering the amount of PEGDMA when 5 or 10wt% of anionic SPMA or zwitterionic SBMA was added (Figure 4.1A). There was no statistically significant difference in equilibrated volume swelling ratios (ESR_v) between any anionic or zwitterionic hydrogels and

the unmodified PEGDMA or among the modified hydrogels (Figure 4.1B). The equilibrated weight swelling ratios (ESR_w) of the modified hydrogels were also statistically comparable to that of the unmodified PEGDMA (14.8 ± 0.4) except for 10% SPMA, which was 13.2 ± 0.1 ($p < 0.05$) (data not shown). In contrast to the unchanged swelling behavior, the compressive moduli of all modified hydrogels were found to significantly increase as the content of covalent incorporation of SPMA or SBMA increased (Figure 4.1C). At the lower compressive strain range of 5-10%, compressive moduli of 5% SPMA and 10% SPMA were found to be 205% and 423%, respectively, relative to unmodified PEGDMA; whereas those of the 5% SBMA and 10% SBMA were increased to 168% and 250%, respectively, relative to unmodified PEGDMA. At the 10% incorporation content, the stiffening effect that the SPMA (16.8 ± 6.6 kPa; $p < 0.0001$) and SBMA (10.0 ± 0.03 kPa, $p < 0.05$) residues imposed on the PEGDMA hydrogel (4 ± 0.2 kPa) was statistically significant. At the higher compressive strain range of 15-20%, the stiffening effect of the covalent incorporation of both the anionic and zwitterionic residues became even more pronounced, with compressive moduli of 5% SPMA (16.7 ± 0.4 kPa, $p < 0.0001$) and 10% SPMA (29.4 ± 1.2 kPa, $p < 0.0001$) nearly 3 and 5 times of that of PEGDMA (5.9 ± 0.3 kPa), respectively. The compressive moduli of 5% and 10% SBMA hydrogels were also increased to 9.9 ± 1.0 kPa and 14.4 ± 1.5 kPa ($p < 0.001$), respectively.

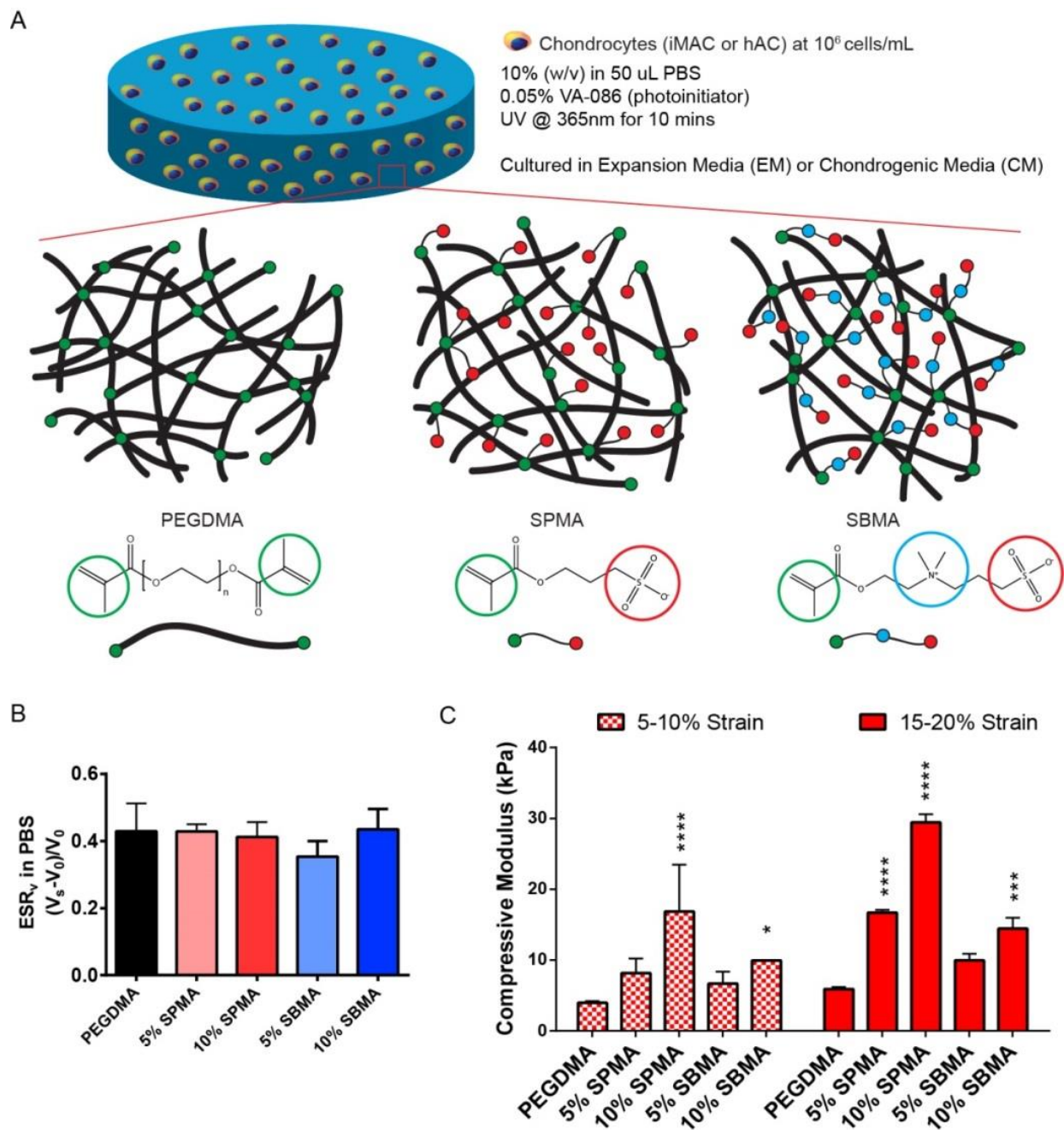


Figure 4.1. Formulations, swelling and compressive behaviors of modified vs. unmodified PEGDMA hydrogels.

(A) Pictorial representation of chondrocytes encapsulated in anionic SPMA and zwitterionic SBMA-modified PEGDMA hydrogel network; (B) Volume swelling ratios (ESR_v) of various hydrogel formulations in PBS (pH 7.4). (C) Unconfined compressive moduli of various hydrogels submerged in PBS (pH 7.4) at strains of 5-10% and 15-20%. * $p < 0.05$, *** $p < 0.001$, **** $p < 0.0001$ compared to unmodified PEGDMA (n=3)

iMACs encapsulated in SPMA hydrogels showed more pericellularly localized proteoglycan and reduced type II collagen expressions in both expansion media and serum-free chondrogenic media cultures.

GAG secretion by iMACs encapsulated within hydrogels was visualized using toluidine blue staining over the course of 10-week culture in expansion medium (10% FBS). While iMACs encapsulated in all the hydrogels showed progressive increases in GAG matrix secretion over time, the staining patterns were quite different (Figure 4.2A). In the SPMA hydrogels, the purple pericellular GAG stains were darker and more compact, while those in the unmodified PEGDMA and SBMA hydrogels were more diffuse and penetrated the surrounding hydrogel matrices. Both the 5% and 10% SPMA hydrogels also showed background staining with toluidine blue as a result of electrostatic absorption of the positively charged dye by the sulfonated residues of SPMA. The GAG production by encapsulated iMACs in serum-free chondrogenic medium was not as robust as in the expansion medium except for those encapsulated in the 10% SPMA construct, which showed similar intense but compact pericellular GAG secretion (Figure 4.2B). Immunofluorescence staining revealed that type II collagen expression by encapsulated iMACs was reduced in the stiffer SPMA hydrogels, with those in 10% SPMA showing the lowest expression (Figure 4.3C). The degrees of chondrocyte hypertrophy, as measured by type X collagen expression, were minimal in all iMAC-laden hydrogel constructs.

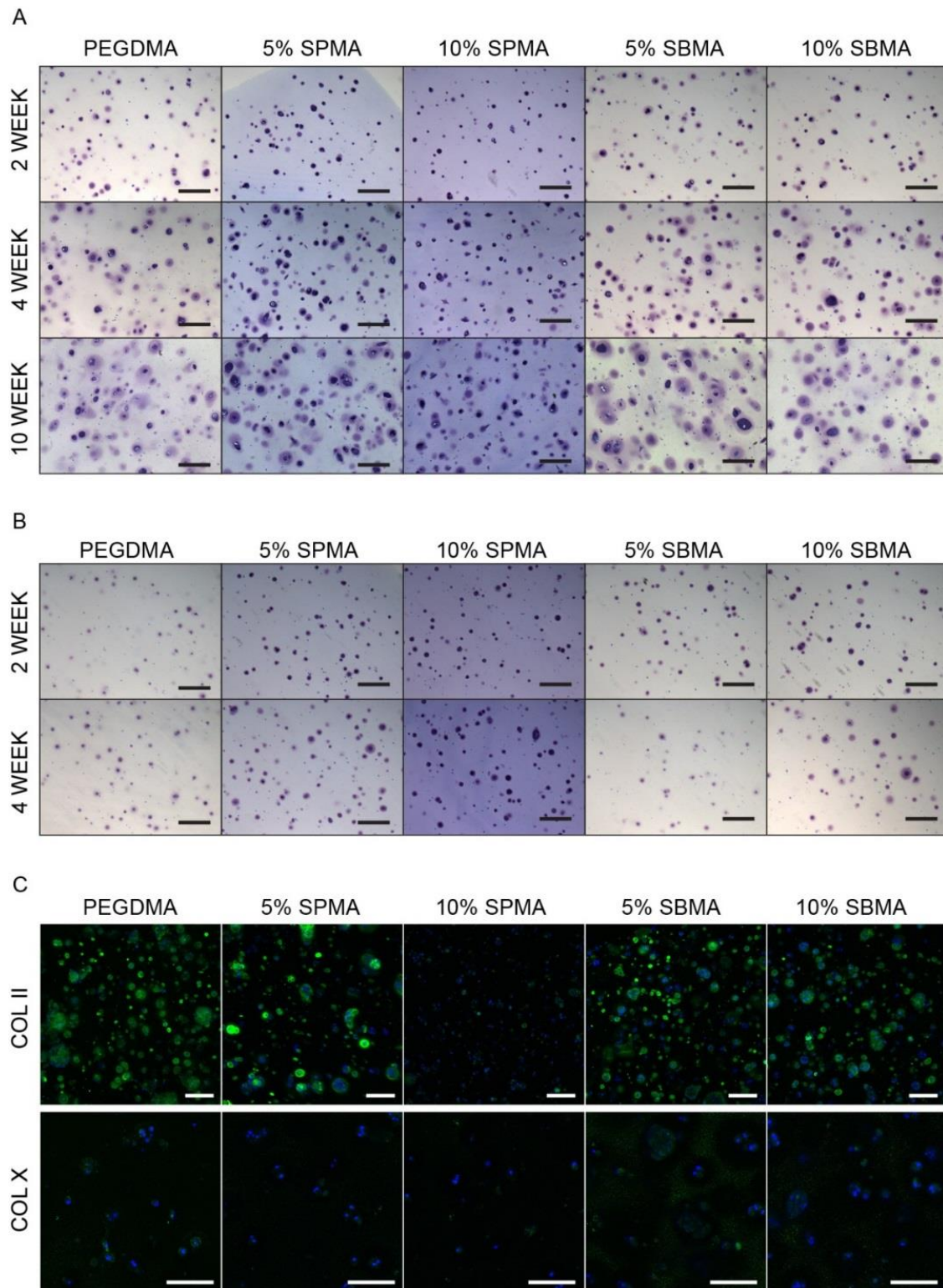


Figure 4.2. ECM production by iMAC in modified vs. unmodified PEGDMA hydrogels.

Toluidine blue-stained histological sections of iMACs encapsulated in various hydrogels and cultured in (A) expansion medium for 2, 4 and 10 weeks and in (B) serum-free chondrogenic media for 2 and 4 weeks. Scale bar = 100 μm (C) Immunofluorescence staining for type II and type X collagen (green) of iMAC-laden hydrogels cultured in expansion medium for 4 weeks. Nuclei were stained with DAPI (blue). Scale bar = 100 μm.

iMACs encapsulated in SPMA hydrogels exhibited reduced metabolism, but not viability, compared to SBMA hydrogels and unmodified PEGDMA hydrogels

Metabolic activity/proliferation of the encapsulated iMACs within each hydrogel formulation was examined using the CCK-8 reagent at various time points. During the first week of culture in expansion medium, encapsulated iMACs were metabolically active and underwent rapid proliferation, with those encapsulated in unmodified PEGDMA and those modified with 5 or 10% zwitterionic SBMA residues proliferating equally well. However, iMACs encapsulated in the 5% and 10% SPMA gave statistically significant lower CCK8 absorbance readings throughout the eight weeks of culture compared to all other formulations (Figure 4.3A and 4.3B). Live/dead cell staining confirmed that the reduced CCK-8 absorbance reading detected within the anionic SPMA formulations was not due to increased cell death, but rather reduced cellular proliferation/metabolism (Figure 4.3C). In all hydrogel formulations, the cell proliferation leveled off during the first two weeks of culture, followed by a slow decline in viable cells. At 8 weeks of culture, reduction in CCK-8 absorbance reading was only significant in the 10% SPMA hydrogels compared to all others.

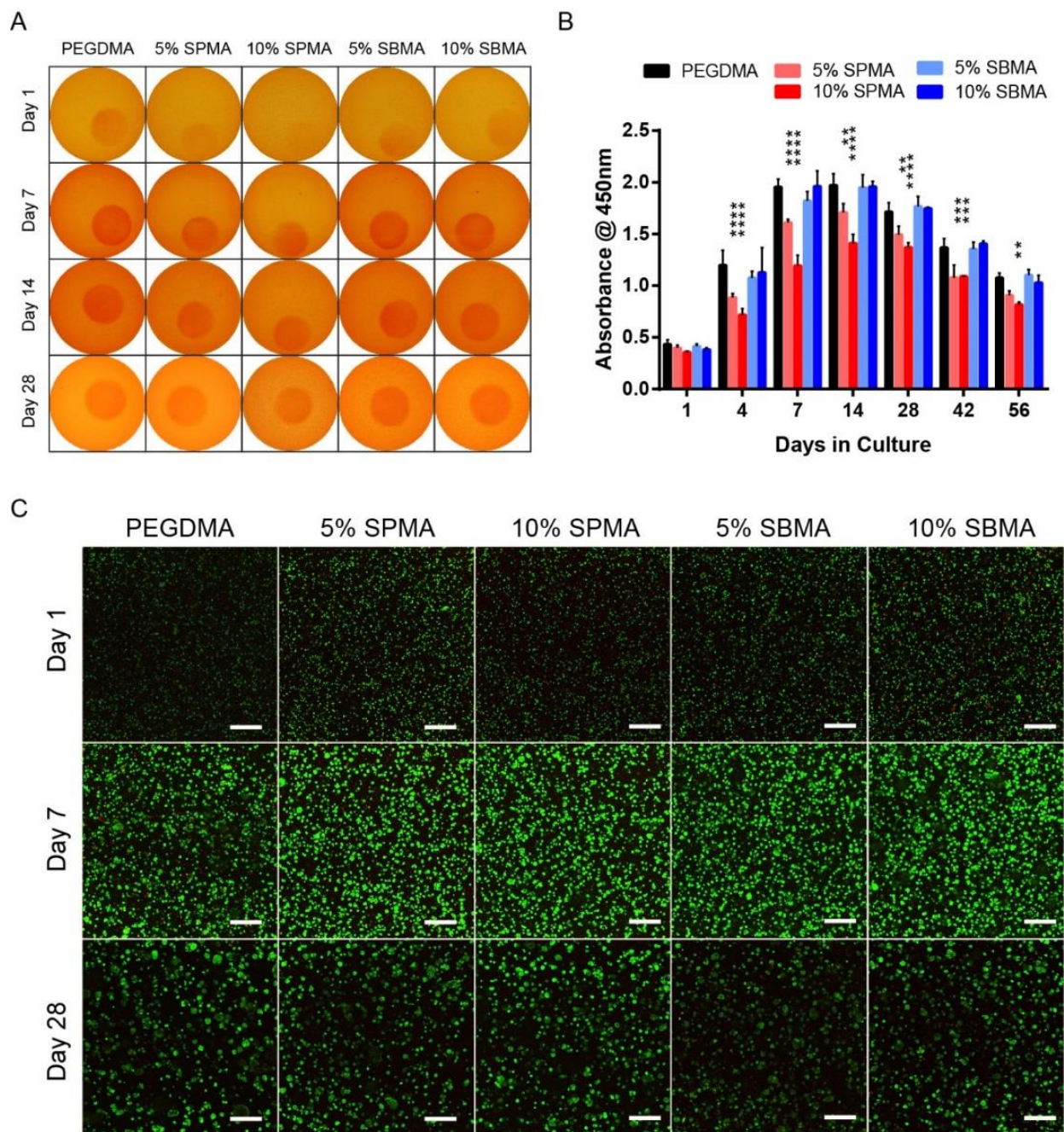


Figure 4.3 Metabolic activity and cell viability of iMACs in modified vs. unmodified PEGDMA Hydrogels. (A) Representative images of iMAC-laden hydrogels after 4 h incubation with CCK8 reagent at various time points in culture. (B) CCK8 quantification of metabolically active cells. $**p < 0.01$, $***p < 0.001$, $****p < 0.0001$ ($n=3$), compared to unmodified PEGDMA at each time point. (C) Live/Dead staining of the iMAC-laden hydrogels at day 1, 7 and 28. Scale bar = 250 μm .

Human OA chondrocytes (hAC) encapsulated in 10% SPMA hydrogels showed reduced/more compact pericellular proteoglycan secretion when cultured in chondrogenic medium.

To determine if the effect of SPMA hydrogels on encapsulated iMACs translates to human cells, we isolated hAC from discarded human OA cartilage. In contrast to iMACs, hACs encapsulated within these hydrogels underwent more robust ECM deposition in serum-free chondrogenic medium than those cultured in expansion medium containing 10% FBS (Figure 4.5A and 4.5B). In chondrogenic medium, the extracellular matrix production of hACs was significantly upregulated, resulting in intense and diffused pericellular GAG staining in the unmodified, zwitterionic SBMA-modified and 5% SPMA-modified PEGDMA. But in the 10% SPMA-modified hydrogels, GAG secretion by hACs was more pericellularly localized (Figure 4.5B). The GAGs secreted by hACs appear to diffuse more readily into the surrounding hydrogel matrices than those secreted by iMACs.

Under chondrogenic conditions, hACs encapsulated in PEGDMA modified with 5% and 10% SPMA and 10% SBMA remained viable but secreted less type II collagen.

The secretion of type II and type X collagens by hACs within various hydrogels was detected using immunofluorescence staining. Type II collagen secretion was the lowest in the presence of 10% SPMA and 10% SBMA modifications (Figure 4.4C). The type II collagen staining was also reduced and appeared more localized around the cell and cell clusters in the 5% SPMA-modified hydrogels compared to the unmodified or 5% SBMA-modified hydrogels. The secretion of type X collagen, a marker of chondrocytes hypertrophy, was minimal across all formulations after 4 weeks of culture.

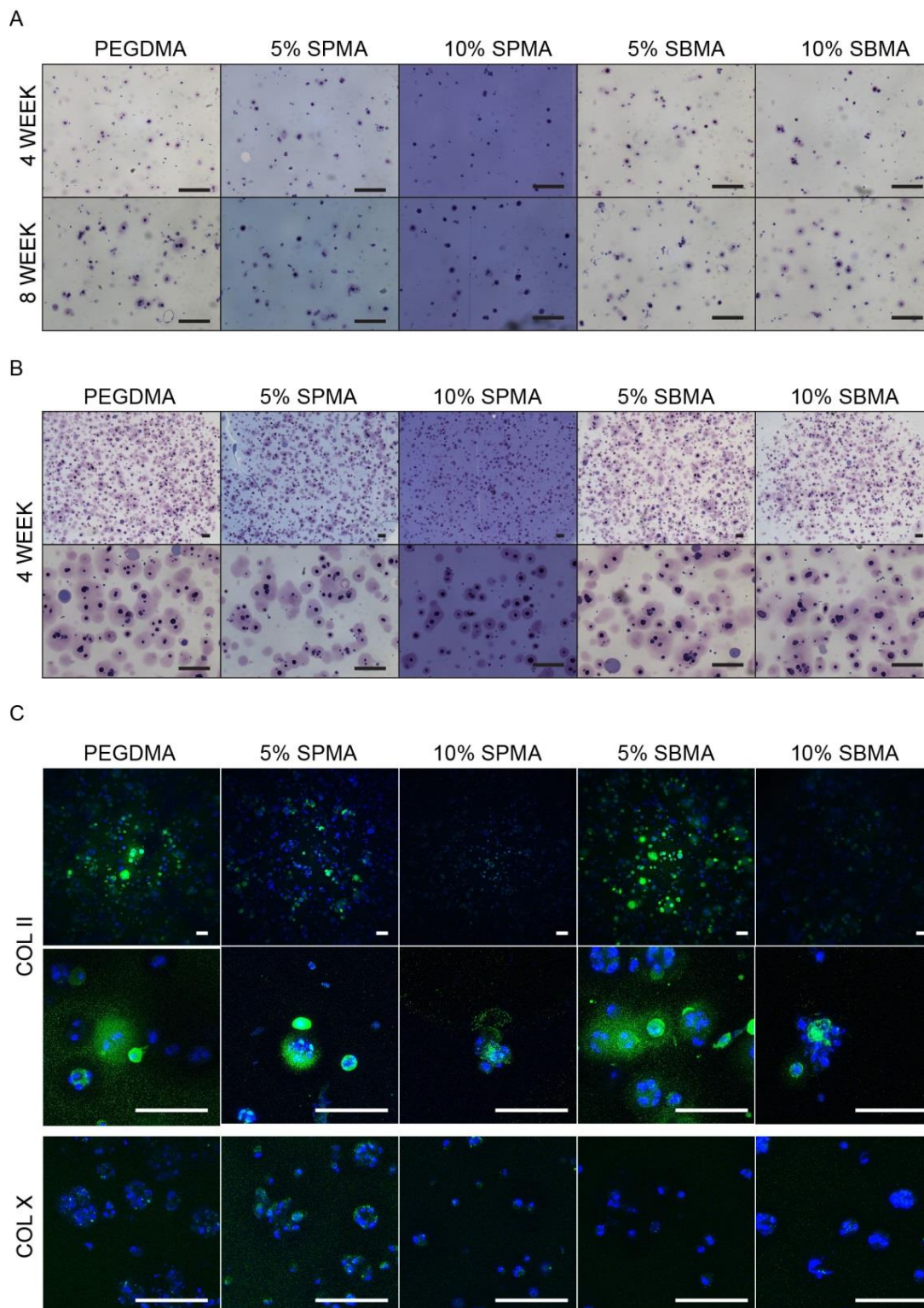


Figure 4.4 ECM production by hAC in modified vs. unmodified PEGDMA hydrogels.

Toluidine blue-stained sections of hACs encapsulated in various hydrogels and cultured for 4 weeks in (A) expansion medium (10% serum) or (B) serum-free chondrogenic medium. Scale bar = 100 μ m. (C) Immunofluorescence staining for type II and type X collagen (green) of hAC-laden hydrogels after 4-week culture in serum-free chondrogenic medium. Nuclei were stained with DAPI (blue). Scale bar = 100 μ m.

4. Discussion

The fixed negative charge density of proteoglycans provides cartilage tissue with the necessary osmotic pressure to withstand compressive forces and limit the expulsion of water. While native glycosaminoglycans such as chondroitin sulfate are often incorporated into the design of cartilage-mimicking hydrogel scaffolds, studies aimed at understanding the effects of fixed charges on both the mechanical properties of the hydrogel and the matrix protein synthesis of encapsulated chondrocytes are lacking. Our study demonstrates that covalent incorporation of small anionic (sulfonate) or zwitterionic (sulfobetaine) chemical residues into non-ionic hydrophilic PEGDMA hydrogel, while maintaining overall polymer content and swelling behavior, can enhance its compressive modulus. In addition, the incorporation of anionic residues can also elicit changes in type II collagen secretion by the encapsulated chondrocytes and how readily the secreted proteoglycans diffuse into the surrounding hydrogel matrices.

While previous studies^{358,359} have shown that sulfonating polymers can affect the storage modulus of the biomaterial, the effect of charge incorporation could not be decoupled from the simultaneous change in its swelling behavior. By maintaining the overall polymer weight fraction at 10% (w/v) across all formulations, we were able to keep the volume swelling ratios (ESR_v) consistent across all hydrogels despite the increase in anionic or zwitterionic residues and the decrease in covalent crosslinking density (due to reduction in PEGDMA). The incorporation of 5 and 10% anionic and zwitterionic residues enhanced the compressive modulus of PEGDMA hydrogels in a SPMA and SBMA content-dependent manner.

In comparison, SPMA incorporation was more effective in enhancing hydrogel stiffness than SBMA incorporation, likely due to more pronounced net electrostatic repulsions among the anionic residues. The incorporation of zwitterionic residues, which are thought to behave like PEG in terms of anti-fouling effects, was also able to enhance the compressive moduli of hydrogels compared to unmodified PEGDMA, although to a lesser extent than SPMA residues. The positive and negative ions in PBS solution are known to disrupt the physical crosslinks formed by dipole-dipole interactions of zwitterionic residues³⁶⁰. This influx of oppositely charged ions into the zwitterionic SBMA-modified hydrogels could be sufficient to create an enhanced osmotic pressure beyond that in the unmodified PEGDMA hydrogel.

Freshly isolated iMACs can undergo robust cartilage matrix protein syntheses in expansion medium and are useful for detecting environmental perturbations presented by encapsulating hydrogels. In 10% SPMA hydrogels, the GAG staining pattern by iMACs were found to be less

diffusive and more confined to the pericellular region compared to other formulations, suggesting that the cells were either secreting less GAGs or that the secreted GAGs were effectively sequestered within the pericellular space by the electrostatic repulsion of sulfonate groups in the surrounding hydrogel matrices.

Due to potential difference in dynamic protein sequestration among these hydrogels, we also assessed how chondrogenic growth medium, which contains a low dose of TGF- β 3 but no FBS, might impact the matrix production of iMACs within these hydrogels. Interestingly, in serum-free chondrogenic medium, we observed a strong reduction in matrix production from iMACs across all the formulations except for 10% SPMA where the GAG staining pattern were comparable to that obtained in expansion medium. This suggests that iMAC matrix synthesis is highly dependent on serum concentrations, but that the presence of SPMA residues could help desensitize iMACs to reduced nutrient content in their local environment. This apparent “shielding” effect may in part be attributed to the higher osmotic pressure in SPMA hydrogels effectively slowing water and nutrient exchange. Published reports have shown that increasing stiffness by way of increasing synthetic matrix crosslinking density inhibits encapsulated chondrocytes’ matrix production through a reduction in cellular metabolism^{355,361}. Our CCK-8 results also confirmed that the metabolic activity of iMACs within the stiffer 5% and 10% SPMA hydrogels was reduced (although proliferation within the first week was observed) compared to those in SBMA-modified or unmodified PEGDMA hydrogels. The molecular mechanisms by which these two distinct stiffening modalities modulate the matrix production of encapsulated cells remain to be elucidated. While we observed a general reduction in type II collagen matrix production in 10% SPMA hydrogels compared to other formulations, we still observed a progressive increase in GAG secretion during 10 weeks of culture. Unlike iMAC, hACs encapsulated within the SPMA or SBMA modified hydrogels produced more cartilage matrix in serum-free chondrogenic medium than in expansion medium, supporting fundamental phenotypic differences between these two primary chondrocytes. Nevertheless, the 10% SPMA-modified hydrogel exerted a similar effect on encapsulated hACs by reducing type II collagen secretion but with limited effect on GAG secretion. The GAG secreted by hAC diffused more readily through the 10% SPMA-modified hydrogels, suggesting that the size or charge density of GAGs produced by human OA chondrocytes may be different from those produced by iMACs. In addition, we also detected differences in type II and type X collagen secretion in 5% SPMA and SBMA hydrogels compared to unmodified PEGDMA hydrogels, suggesting that the metabolic activities of hACs could be tuned by altering the local concentrations of these chemical moieties.

Overall, observations from this study support covalent incorporation of small molecule anionic sulfonate and zwitterionic sulfobetaine residues in sufficient density within PEGDMA hydrogel as a means to enhance the stiffness of the synthetic matrix and the resident time of encapsulated proteins. Stiffer hydrogel resulting from higher content anionic SPMA residue incorporation appear to reduce the metabolic activity of encapsulated chondrocytes analogous to what have been observed with the stiffer substrates derived from highly photo-crosslinked systems^{362,363,364,365}. Whether the magnitude of differences observed between sulfonate and sulfobetaine modifications in this study can be generalized to other anionic and zwitterionic modifications (e.g. carboxylate vs. carboxybetaine, phosphate vs. phosphobetaine) remains determined. Future work should also focus on mechanoregulation of cellular function within these synthetic environment with/without dynamic loading, optimizing the spatial presentation of these chemical cues, and implementing them within a degradable hydrogel system.. Given the significant difference in stiffness among our hydrogels under higher strains, dynamic culture would likely reveal more profound differences in chondrocyte behavior that are not detectable under static conditions. A previous study³⁶⁶ also showed that dynamic loading affects chondrocyte matrix production differently in a neutral versus charged environment. It is also of interest to investigate how the spatial distribution of charges within synthetic hydrogels (e.g. anisotropically presented or clustered charges emulating the densely packed chondroitin sulfate in native cartilage³⁶⁷) may affect the magnitude of their impact on cellular behavior. Finally, temporal control over the degradation of the synthetic matrix is necessary to enable neotissue integration in a timely manner.

5. Acknowledgements

In addition to the author, the following individuals contributed to the work described in this chapter:

- April Mason-Savas processed all hydrogel samples for histology and stained the slides.
- Gregory Molica optimized mechanical testing parameters for the hydrogel.

Chapter V: Discussion and Future Perspectives

1. Summary of Key Findings and Significance of Dissertation Work

The goal of this dissertation was to investigate two strategies that could advance therapies for delaying the onset or progression of OA. The first strategy was to determine whether Smurf2 is a viable target for DMOADs. To do this, Chapter II aimed at determining whether Smurf2 had a role in modulating skeletal tissues under normal development and aging or under a pathological condition such as OA. Primary chondrocytes deficient in Smurf2 were also characterized to determine if any gain of function could be applied towards cell-based therapy for cartilage regeneration. The second strategy was focused on chemical modification of synthetic hydrogels in order to enhance their function for cartilage tissue engineering. Specifically, Chapter IV aimed at incorporating anionic and zwitterionic chemical residues into a PEGDMA hydrogel to improve both its mechanical and chondroinductive properties.

Smurf2 Deficiency Results in Normal Bone Phenotype

The extensive skeletal characterization of WT and Smurf2-deficient MT mice performed in Chapter II suggests that Smurf2 inhibition in bone and cartilage does not cause abnormal skeletal development and aging. This may be attributed in part to the low expression of Smurf2 in skeletal tissue compared to other organs. It should be noted that other mouse models with complete knockout of Smurf2²⁷⁸ also did not report any skeletal abnormalities. Unlike the Smurf1-deficient mice²⁸³, which saw a compensatory increase in Smurf2 levels, we did not detect any compensatory increase of Smurf1 expression in Smurf2-deficient tissues and cells, suggesting a less critical role of Smurf2 in maintaining skeletal homeostasis.

A recent paper published in *Nature Communications* claims that Smurf2 knockout results in a bone loss phenotype, which they attribute to increased receptor activator of nuclear factor kappa-B ligand (RANKL) expression in osteoblasts, driving osteoclastogenesis³⁶⁸. Their result of trabecular bone loss in the lumbar vertebrae at 12 weeks (~3 months) was in stark contrast to the lack of phenotype in our Smurf2-deficient vertebrae even at 16 months. If any correlation between the two mouse models exists, the bone loss should have been more apparent with age. Although the authors attribute the difference in phenotype to residual levels of Smurf2 expression in our gene trap model, we have not been able to detect any Smurf2 protein in the skeletal tissues of our Smurf2-deficient mice.

Smurf2 Deficiency Attenuates OA Development in Young Mice but not Old Mice

Chapter II also showed that systemic knockdown of Smurf2 slowed the progression of cartilage destruction in the knees of young mice after DMM surgery. This modulatory effect indicates that Smurf2 could very well be a potential target for DMOADs. However, the attenuated protection of Smurf2 deficiency in older mice after DMM does raise concerns about its efficacy in human disease, where advanced age is often a factor. Because DMM surgery is not typically performed in older mice, and no correlation to human disease has been established, proper interpretation of these results is difficult without additional studies. Unfortunately, during the course of our investigation, we were unable to accurately define the protective mechanism behind Smurf2 deficiency.

Chondrogenic Potential of Smurf2-deficient and WT iMACs

Since we observed less cartilage degradation in the Smurf2-deficient mice compared to WT, we focused our attention to characterize Smurf2-deficient chondrocytes. We resorted to using immature articular chondrocytes in order to obtain enough primary cells for testing but testing chondrocytes isolated from skeletally mature mice may ultimately be more revealing. Even though we detected some differences in chondrogenic gene expression between WT and MT, we could not appreciate significant functional difference at the cellular level. Proliferation, monolayer dedifferentiation, and proteoglycan production in 2D and 3D culture were comparable between WT and MT iMACs.

Since Smurf2 appears to be involved in pathological and not physiological states, characterizing Smurf2-deficient primary cells *in vitro* is a challenge due to the inability to fully recapitulate the OA pathological state. While we focused on IL-1 β stimulation as a surrogate for OA pathology, it is possible that other catabolic stimuli and/or temporal control of the proinflammatory cytokine may be more effective for revealing functional differences between WT and MT chondrocytes. Although we were unable to attribute the protective role of Smurf2-deficiency to articular chondrocytes, we cannot rule out the possibility that they may still play an indirect role in mediating disease progression *in vivo*.

Age and Gender Modulate Joint Response to OA induction by DMM in Mice

Due to the earlier finding of a difference in cartilage protection between young and old Smurf2-deficient mice after DMM, Chapter III investigated in detail how aging affects different

joint structures in response to DMM-induced OA. Our findings show that cartilage degradation, subchondral bone sclerosis, and osteophyte development are accelerated with age in the male mice. The effect of age is less apparent in females because the female sex by itself confers resistance to DMM-induced OA. Nevertheless, more severe OA eventually develops in females at very advanced age (21 months).

The DMM mouse model of OA remains a popular tool for understanding OA pathology and identifying potential disease modifying targets. Our findings bring attention to the need of choosing the appropriate gender and age for the DMM model. By performing DMM in both young and older transgenic mice, the threshold for identifying effective and powerful disease modifying targets can be raised and potentially eliminate false positive results. In other words, therapeutic targets that grant protection to OA in aged mice can most likely overcome some age-induced impairment and be more effective than targets that only confer protection in young mice, which has been current practice. One might argue that DMM in aged mice results an irreversible progression of OA, in which no disease modifying agent could exist, but such a hypothesis can only be verified through repeated studies and validation of the ideal age range at which to perform DMM.

Hydrogel Stiffness derived from Covalent Incorporation of Anionic Residues Modulates Chondrocyte Matrix Production

In Chapter IV, we showed that incorporation of small anionic or zwitterionic residues in a bioinert hydrogel increased its compressive modulus in a dose-dependent manner. The increase in stiffness of the hydrogel, at higher content, however, caused a reduction in cellular metabolism and reduced collagen production. These results indicate that improving mechanical properties of hydrogel scaffolds through chemical modification will also affect chondrogenesis of encapsulated cells. Although previous studies have shown that stiff 2D and 3D matrices, produced from highly crosslinking polymers, impair chondrogenesis, our study shows that stiffness derived from increased osmotic pressure will also produce a similar effect. Finally, whether it is the scaffold material stiffness, the proteoglycan-rich pericellular matrix or the osmotic pressure that predominates in modulating the chondrogenesis of encapsulated cells requires further investigation.

2. Future Directions

Is Smurf2 a target for DMOAD?

Based on our investigation performed in this dissertation, the question as to whether Smurf2 is a viable target for DMOAD remains unanswered. The cellular player responsible for OA protection still needs to be identified. Using intraarticular injections of Smurf2 siRNA or lentivirus containing Smurf2 shRNA is a way of determining whether localized reduction of Smurf2 in WT mice can confer the same OA protection as Smurf2-deficient mice. In addition, a combination of Smurf1 and Smurf2 siRNA could also address concerns about the inefficiency of Smurf2 alone to modulate OA pathogenesis. If localized suppression of Smurf2 is effective at modifying OA progression, it would exclude involvement of other systemic factors and favor the involvement of tissues located within the joint. At that point, inducible knockout of Smurf2 from specific joint structures may be most effective at identifying the key cellular players.

Another fundamental question that needs to be addressed is how Smurf2 expression or activity is altered during OA development. Based on the low expression of Smurf2 under physiological conditions, it appears that OA should at minimum cause an upregulation of Smurf2 in order to induce non-physiological ubiquitination activity. Even though our attempts to monitor changes in Smurf2 expression *in vivo* were unsuccessful, immunohistochemical staining of DMM joints at different stages of OA development could reveal where and how Smurf2 expression was changing. While not a direct correlate, an increase in the ubiquitination/proteosomal activity have been implicated in DMM-induced OA. Radwan et al.¹⁹⁹ showed that subcutaneous injection of a proteosomal inhibitor, MG132, in mice protected against DMM-induced OA. Nevertheless, whether Smurf2's major functions in skeletal tissues is along the ubiquitin-proteosome pathway needs further clarification.

Do Different Modalities of Inducing Stiffness Affect Chondrocyte Mechano-sensing?

Our work incorporating charged anionic or zwitterionic residues demonstrates an alternative way of inducing stiffness in hydrogels without altering covalent crosslinking density or swelling behavior. Although these different methods for increasing scaffold stiffness resulted in similar chondrocyte behavior, it is worthwhile to investigate whether the mechanotransduction pathways involved are also the same. Recent reports have described the Yes-associated protein (YAP) and transcriptional coactivator with PDZ-binding motif (TAZ) as the main nuclear regulators of mechanical stimulus exerted by ECM stiffness and cell shape³⁶⁹. The link between YAP localization to the nucleus was also demonstrated in rat chondrocytes subjected to a highly

crosslinked stiff matrix³⁷⁰. Therefore, we can potentially assess whether hydrogels containing anionic residues can also induce YAP localization to the nucleus.

To determine whether the suppression of matrix synthesis caused by the stiffer hydrogel is reversible, we would need to incorporate anionic residues into a degradable system. Hydrogels with tunable degradation rates, like the one developed in our lab³⁷¹, could potentially be used to assess the reversibility of osmotic pressure-induced suppression of matrix synthesis. The reversibility of such a phenotype would open up the possibilities of a scaffold-mediated matrix synthesis while still providing an initial construct for mechanical support.

Additional Studies Involving Chemically Modified Synthetic Hydrogels

Chemical modification of a synthetic hydrogel is an underappreciated strategy for cartilage tissue engineering. The emphasis on a biomimetic scaffold entices many researchers to rely on incorporating native biomacromolecules into their tissue engineered constructs. However, such strategies are poorly controlled and do not facilitate clear understanding of cell-material interactions. While the use of purely synthetic scaffolds is a reductionist approach and can lead to oversimplification of the complexity of native tissue, it allows for finer tuning of modifications and a more direct interpretation of causality. Our use of anionic and zwitterionic chemical residues was aimed at understanding how these chemical moieties affected both the physical property of the scaffold and the behavior of encapsulated chondrocytes. In our system, we found that mechanical stiffness seemed to exert a dominant negative effect on encapsulated chondrocytes. To determine whether the anionic or zwitterionic moieties themselves have a direct impact on chondrocyte function, the stiffness of the material will have to be normalized. However, this will eventually lead to introducing more crosslinking density in the weaker hydrogels or reducing the anionic content in the stiffer gels, both of which can conflict with the goal of the study. Another study design that examines the specificity of chemical moieties is to compare a variety of anionic functional groups or with different charged densities.

Even though our study focused on differentiated chondrocytes, it may be worthwhile to assess how chondrogenic differentiation of stem cells might be affected within these constructs. There is plenty of evidence to suggest that chondrogenic differentiation of stem cells is affected by matrix stiffness^{372,373}, while the potential of small chemical moieties to direct stem cell fate in the absence any other growth factors has also been reported³⁴⁶. To decouple these competing factors, one strategy would be to reduce the chemical crosslinking density in order to counter the increased stiffness from incorporation of anionic or zwitterionic residues.

Finally, utilizing other parameters such as dynamic compression or hypoxia to stimulate chondrogenesis may reveal additional synergistic effects not otherwise seen in our investigation. Due to differences in compressive modulus among the hydrogel formulations, dynamic compression should be tested in both force-controlled and strain-controlled modes.

3. Concluding Remarks

The rising burden of OA has placed a lot of pressure on researchers to come up with an effective DMOAD. Over the years, investments in basic science research have revealed a tremendous amount about mechanisms governing OA pathophysiology and potential therapeutic targets. Despite a slower transition, increasing efforts have also been focused on identifying the source of OA pain in order to design better drugs for symptomatic management and to improve patients' quality of life. Clinical research has also advanced in the analysis of structural changes in the joint using MRI and will pave the way for phenotype OA subgroups based on imaging and other known risk factors. The work described in the dissertation provides a fraction of the knowledge needed to advance new OA therapies, but they are rooted in identifying a new therapeutic target, establishing better correlation between animal OA model and human disease, and improving scaffold-assisted delivery of cells and therapeutics for cartilage repair. Ultimately, the success of new OA therapies will rely on the comprehensive efforts from basic scientists, clinicians, and physician scientists to implement translation research that is directed at clinical needs but grounded in our mechanistic understanding of OA pathology.

References

1. CDC. Prevalence and most common causes of disability among adults—United States, 2005. *MMWR Morb Mortal Wkly Rep.* 2009;58:421–6.
2. Hunter DJ, Schofield D, Callander E. The individual and socioeconomic impact of osteoarthritis. *Nat Rev Rheumatol.* 2014 Jul;10(7):437-41.
3. Le TK, Montejano LB, Cao Z, Zhao Y, Ang D. Healthcare costs associated with osteoarthritis in US patients. *Pain Pract.* 2012 Nov; 12(8):633-40.
4. Kurtz SM, Lau E, Ong K, Zhao K, Kelly M, Bozic KJ. Future young patient demand for primary and revision joint replacement: national projections from 2010 to 2030. *Clin Orthop Relat Res.* 2009 Oct;467(10):2606-12.
5. Ackerman IN, Kemp JL, Crossley KM, Culvenor AG, Hinman RS. Hip and Knee Osteoarthritis Affects Younger People, Too. *J Orthop Sports Phys Ther.* 2017 Feb;47(2):67-79.
6. Helmick CG, Felson DT, Lawrence RC, Gabriel S, Hirsch R, Kwoh CK, Liang MH, Kremers HM, Mayes MD, Merkel PA, Pillemer SR, Reveille JD, Stone JH; National Arthritis Data Workgroup. Estimates of the prevalence of arthritis and other rheumatic conditions in the United States. Part I. *Arthritis Rheum.* 2008 Jan;58(1):15-25.
7. Smolen JS, Landewé R, Breedveld FC, Buch M, Burmester G, Dougados M, Emery P, Gaujoux-Viala C, Gossec L, Nam J, Ramiro S, Winthrop K, de Wit M, Aletaha D, Betteridge N, Bijlsma JW, Boers M, Buttgerit F, Combe B, Cutolo M, Damjanov N, Hazes JM, Kouloumas M, Kvien TK, Mariette X, Pavelka K, van Riel PL, Rubbert-Roth A, Scholte-Voshaar M, Scott DL, Sokka-Isler T, Wong JB, van der Heijde D. EULAR recommendations for the management of rheumatoid arthritis with synthetic and biological disease-modifying antirheumatic drugs: 2013 update. *Ann Rheum Dis.* 2014 Mar;73(3):492-509.
8. Smolen JS, Aletaha D, McInnes IB. Rheumatoid arthritis. *Lancet.* 2016 Oct 22;388(10055):2023-2038.
9. Bliddal H, Leeds AR, Christensen R. Osteoarthritis, obesity and weight loss: evidence, hypotheses and horizons - a scoping review. *Obes Rev.* 2014 Jul;15(7):578-86.
10. Bachmeier CJ, March LM, Cross MJ, Lapsley HM, Tribe KL, Courtenay BG, Brooks PM; Arthritis Cost and Outcome Project Group. A comparison of outcomes in osteoarthritis patients undergoing total hip and knee replacement surgery. *Osteoarthritis Cartilage.* 2001 Feb;9(2):137-46.
11. George LK, Ruiz D Jr, Sloan FA. The effects of total knee arthroplasty on physical functioning in the older population. *Arthritis Rheum.* 2008 Oct;58(10):3166-71.
12. Wainwright C, Theis JC, Garneti N, Melloh M. Age at hip or knee joint replacement surgery predicts likelihood of revision surgery. *J Bone Joint Surg Br.* 2011 Oct;93(10):1411-5.
13. Meehan JP, Danielsen B, Kim SH, Jamali AA, White RH. Younger age is associated with a higher risk of early periprosthetic joint infection and aseptic mechanical failure after total knee arthroplasty. *J Bone Joint Surg Am.* 2014 Apr 2;96(7):529-35.
14. Chen D, Shen J, Zhao W, Wang T, Han L, Hamilton JL, Im HJ. Osteoarthritis: toward a comprehensive understanding of pathological mechanism. *Bone Res.* 2017 Jan 17;5:16044.

15. Wick MC, Kastlunger M, Weiss RJ. Clinical imaging assessments of knee osteoarthritis in the elderly: a mini-review. *Gerontology*. 2014;60(5):386-94.
16. Guermazi A, Niu J, Hayashi D, Roemer FW, Englund M, Neogi T, Aliabadi P, McLennan CE, Felson DT. Prevalence of abnormalities in knees detected by MRI in adults without knee osteoarthritis: population based observational study (Framingham Osteoarthritis Study). *BMJ*. 2012 Aug 29;345:e5339.
17. Oo WM, Linklater JM, Hunter DJ. Imaging in knee osteoarthritis. *Curr Opin Rheumatol*. 2017 Jan;29(1):86-95.
18. Peterfy CG, Guermazi A, Zaim S, Tirman PF, Miaux Y, White D, Kothari M, Lu Y, Fye K, Zhao S, Genant HK. Whole-Organ Magnetic Resonance Imaging Score (WORMS) of the knee in osteoarthritis. *Osteoarthritis Cartilage*. 2004 Mar;12(3):177-90.
19. Hunter DJ, Lo GH, Gale D, Grainger AJ, Guermazi A, Conaghan PG. The reliability of a new scoring system for knee osteoarthritis MRI and the validity of bone marrow lesion assessment: BLOKS (Boston Leeds Osteoarthritis Knee Score). *Ann Rheum Dis*. 2008 Feb;67(2):206-11.
20. Hunter DJ, Guermazi A, Lo GH, Grainger AJ, Conaghan PG, Boudreau RM, Roemer FW. Evolution of semi-quantitative whole joint assessment of knee OA: MOAKS (MRI Osteoarthritis Knee Score). *Osteoarthritis Cartilage*. 2011 Aug;19(8):990-1002.
21. Hunter DJ, Zhang W, Conaghan PG, Hirko K, Menashe L, Reichmann WM, Losina E. Responsiveness and reliability of MRI in knee osteoarthritis: a meta-analysis of published evidence. *Osteoarthritis Cartilage*. 2011 May;19(5):589-605.
22. Raynauld JP, Martel-Pelletier J, Haraoui B, Choquette D, Dorais M, Wildi LM, Abram F, Pelletier JP; Canadian Licofelone Study Group. Risk factors predictive of joint replacement in a 2-year multicentre clinical trial in knee osteoarthritis using MRI: results from over 6 years of observation. *Ann Rheum Dis*. 2011;70:1382-8
23. Haviv B, Bronak S, Thein R. The complexity of pain around the knee in patients with osteoarthritis. *Isr Med Assoc J*. 2013 Apr;15(4):178-81.
24. US Department of Health and Human Services, Food and Drug Administration, Center for Drug Evaluation and Research (CDER), Center for Biologics Evaluation and Research (CBER), Center for Devices and Radiological Health (CDRH): Draft Guidance for industry. Clinical development programs for drugs, devices, and biological products intended for the treatment of osteoarthritis. July 1999.
<https://www.fda.gov/downloads/Drugs/GuidanceComplianceRegulatoryInformation/Guidances/ucm071577.pdf>
25. Bedson J, Croft PR. The discordance between clinical and radiographic knee osteoarthritis: a systematic search and summary of the literature. *BMC Musculoskelet Disord*. 2008 Sep 2;9:116.
26. Mobasheri A. The future of osteoarthritis therapeutics: targeted pharmacological therapy. *Curr Rheumatol Rep*. 2013 Oct;15(10):364.
27. Thorstensson CA, Andersson ML, Jonsson H, Saxne T, Petersson IF. Natural course of knee osteoarthritis in middle-aged subjects with knee pain: 12-year follow-up using clinical and radiographic criteria. *Ann Rheum Dis*. 2009 Dec;68(12):1890-3.

28. Leyland KM, Hart DJ, Javaid MK, Judge A, Kiran A, Soni A, Goulston LM, Cooper C, Spector TD, Arden NK. The natural history of radiographic knee osteoarthritis: a fourteen-year population-based cohort study. *Arthritis Rheum.* 2012 Jul;64(7):2243-51.
29. Bruyere O, Richy F, Reginster JY. Three year joint space narrowing predicts long term incidence of knee surgery in patients with osteoarthritis: an eight year prospective follow up study. *Ann Rheum Dis.* 2005 Dec;64(12):1727-30.
30. Kinds MB, Marijnissen AC, Vincken KL, Viergever MA, Drossaers-Bakker KW, Bijlsma JW, Bierma-Zeinstra SM, Welsing PM, Lafeber FP. Evaluation of separate quantitative radiographic features adds to the prediction of incident radiographic osteoarthritis in individuals with recent onset of knee pain: 5-year follow-up in the CHECK cohort. *Osteoarthritis Cartilage.* 2012 Jun;20(6):548-56.
31. Kraus VB, Burnett B, Coindreau J, Cottrell S, Eyre D, Gendreau M, Gardiner J, Garner P, Hardin J, Henrotin Y, Heinegård D, Ko A, Lohmander LS, Matthews G, Menetski J, Moskowitz R, Persiani S, Poole AR, Rousseau JC, Todman M; OARSI FDA Osteoarthritis Biomarkers Working Group. Application of biomarkers in the development of drugs intended for the treatment of osteoarthritis. *Osteoarthritis Cartilage.* 2011 May;19(5):515-42.
32. Mullan RH, Matthews C, Bresnihan B, FitzGerald O, King L, Poole AR, Fearon U, Veale DJ. Early changes in serum type II collagen biomarkers predict radiographic progression at one year in inflammatory arthritis patients after biologic therapy. *Arthritis Rheum.* 2007 Sep;56(9):2919-28.
33. Garner P, Aronstein WS, Cohen SB, Conaghan PG, Cline GA, Christiansen C, Beary JF, Meyer JM, Bingham CO 3rd. Relationships between biochemical markers of bone and cartilage degradation with radiological progression in patients with knee osteoarthritis receiving risedronate: the Knee Osteoarthritis Structural Arthritis randomized clinical trial. *Osteoarthritis Cartilage.* 2008 Jun;16(6):660-6.
34. Lotz M, Martel-Pelletier J, Christiansen C, Brandi ML, Bruyère O, Chapurlat R, Collette J, Cooper C, Giacobelli G, Kanis JA, Karsdal MA, Kraus V, Lems WF, Meulenbelt I, Pelletier JP, Raynauld JP, Reiter-Niesert S, Rizzoli R, Sandell LJ, Van Spil WE, Reginster JY. Value of biomarkers in osteoarthritis: current status and perspectives. *Ann Rheum Dis.* 2013;72(11):1756–1763.
35. Mow VC, Ratcliffe A, Poole AR. Cartilage and diarthrodial joints as paradigms for hierarchical materials and structures. *Biomaterials.* 1992;13(2):67-97.
36. Brody LT. Knee osteoarthritis: Clinical connections to articular cartilage structure and function. *Phys Ther Sport.* 2015 Nov;16(4):301-16.
37. Mente P and Lewis J. Elastic modulus of calcified cartilage is an order of magnitude less than that of subchondral bone. *J Orthop Res.* 1994 Sep; 12(5): 637–647
38. Oegema TR Jr, Carpenter RJ, Hofmeister F, Thompson RC Jr. The interaction of the zone of calcified cartilage and subchondral bone in osteoarthritis. *Microsc Res Tech.* 1997 May 15;37(4):324-32.
39. Verzijl N, DeGroot J, Thorpe SR, Bank RA, Shaw JN, Lyons TJ, Bijlsma JW, Lafeber FP, Baynes JW, TeKoppele JM. Effect of collagen turnover on the accumulation of advanced glycation end products. *J Biol Chem.* 2000 Dec 15;275(50):39027-31.
40. Loeser RF. Age-related changes in the musculoskeletal system and the development of osteoarthritis. *Clin Geriatr Med.* 2010 Aug;26(3): 371–386

41. Goldring MB, Otero M. Inflammation in Osteoarthritis. *Curr Opin Rheumatol*. 2011 Sep; 23(5): 471–478.
42. von der Mark K, Kirsch T, Nerlich A, Kuss A, Weseloh G, Glückert K, Stöss H. Type X collagen synthesis in human osteoarthritic cartilage. Indication of chondrocyte hypertrophy. *Arthritis Rheum*. 1992 Jul;35(7):806-11.
43. Dean DD, Martel-Pelletier J, Pelletier JP, Howell DS, Woessner, Jr JF. Evidence for metalloproteinase and metalloproteinase inhibitor imbalance in human osteoarthritic cartilage. *J Clin Invest*. 1989 Aug; 84(2): 678–685.
44. Lohmander LS, Hoerrner LA, Lark MW. Metalloproteinases, tissue inhibitor, and proteoglycan fragments in knee synovial fluid in human osteoarthritis. *Arthritis Rheum*. 1993 Feb;36(2):181-9.
45. Moldovan F, Pelletier JP, Hambor J, Cloutier JM, Martel-Pelletier J. Collagenase-3 (matrix metalloproteinase 13) is preferentially localized in the deep layer of human arthritic cartilage in situ: in vitro mimicking effect by transforming growth factor beta. *Arthritis Rheum*. 1997 Sep;40(9):1653-61.
46. Lark MW, Bayne EK, Flanagan J, Harper CF, Hoerrner LA, Hutchinson NI, Singer II, Donatelli SA, Weidner JR, Williams HR, Mumford RA, Lohmander LS. Aggrecan degradation in human cartilage. Evidence for both matrix metalloproteinase and aggrecanase activity in normal, osteoarthritic, and rheumatoid joints. *J Clin Invest*. 1997 Jul 1;100(1):93-106.
47. Song RH, Tortorella MD, Malfait AM, Alston JT, Yang Z, Arner EC, Griggs DW. Aggrecan degradation in human articular cartilage explants is mediated by both ADAMTS-4 and ADAMTS-5. *Arthritis Rheum*. 2007 Feb;56(2):575-85.
48. Goldring MB, Goldring SR. Osteoarthritis. *J Cell Physiol*. 2007 Dec;213(3):626-34.
49. Tchetina EV, Squires G, Poole AR. Increased type II collagen degradation and very early focal cartilage degeneration is associated with upregulation of chondrocyte differentiation related genes in early human articular cartilage lesions. *J Rheumatol*. 2005 May;32(5):876-86.
50. Wang X, Manner PA, Horner A, Shum L, Tuan RS, Nuckolls GH. Regulation of MMP-13 expression by RUNX2 and FGF2 in osteoarthritic cartilage. *Osteoarthritis Cartilage*. 2004 Dec;12(12):963-73.
51. Yang S, Kim J, Ryu JH, Oh H, Chun CH, Kim BJ, Min BH, Chun JS. Hypoxia-inducible factor-2alpha is a catabolic regulator of osteoarthritic cartilage destruction. *Nat Med*. 2010 Jun;16(6):687-93.
52. Wei F, Zhou J, Wei X, Zhang J, Fleming BC, Terek R, Pei M, Chen Q, Liu T, Wei L. Activation of Indian hedgehog promotes chondrocyte hypertrophy and upregulation of MMP-13 in human osteoarthritic cartilage. *Osteoarthritis Cartilage*. 2012 Jul;20(7):755-63.
53. Zhu M, Tang D, Wu Q, Hao S, Chen M, Xie C, Rosier RN, O'Keefe RJ, Zuscik M, Chen D. Activation of beta-catenin signaling in articular chondrocytes leads to osteoarthritis-like phenotype in adult beta-catenin conditional activation mice. *J Bone Miner Res*. 2009 Jan;24(1):12-21.
54. Wang J, Gardner BM, Lu Q, Rodova M, Woodbury BG, Yost JG, Roby KF, Pinson DM, Tawfik O, Anderson HC. Transcription factor Nfat1 deficiency causes osteoarthritis through dysfunction of adult articular chondrocytes. *J Pathol*. 2009 Oct;219(2):163-72.

55. Leboy P, Grasso-Knight G, D'Angelo M, Volk SW, Lian JV, Drissi H, Stein GS, Adams SL. Smad-Runx interactions during chondrocyte maturation. *J Bone Joint Surg Am.* 2001;83-A Suppl 1(Pt 1):S15-22.
56. Dong YF, Soung do Y, Schwarz EM, O'Keefe RJ, Drissi H. Wnt induction of chondrocyte hypertrophy through the Runx2 transcription factor. *J Cell Physiol.* 2006 Jul;208(1):77-86.
57. Kishimoto H, Akagi M, Zushi S, Teramura T, Onodera Y, Sawamura T, Hamanishi C. Induction of hypertrophic chondrocyte-like phenotypes by oxidized LDL in cultured bovine articular chondrocytes through increase in oxidative stress. *Osteoarthritis Cartilage.* 2010 Oct;18(10):1284-90.
58. Collins JA, Wood ST, Nelson KJ, Rowe MA, Carlson CS, Chubinskaya S, Poole LB, Furdul CM, Loeser RF. Oxidative Stress Promotes Peroxiredoxin Hyperoxidation and Attenuates Pro-survival Signaling in Aging Chondrocytes. *J Biol Chem.* 2016 Mar 25;291(13):6641-54.
59. Merz D, Liu R, Johnson K, Terkeltaub R. IL-8/CXCL8 and growth-related oncogene alpha/CXCL1 induce chondrocyte hypertrophic differentiation. *J Immunol.* 2003 Oct 15;171(8):4406-15.
60. Cecil DL, Johnson K, Rediske J, Lotz M, Schmidt AM, Terkeltaub R. Inflammation-induced chondrocyte hypertrophy is driven by receptor for advanced glycation end products. *J Immunol.* 2005 Dec 15;175(12):8296-302.
61. Roman-Blas JA, Jimenez SA. NF-kappaB as a potential therapeutic target in osteoarthritis and rheumatoid arthritis. *Osteoarthritis Cartilage.* 2006 Sep;14(9):839-48.
62. Olivetto E, Borzi RM, Vitellozzi R, Pagani S, Facchini A, Battistelli M, Penzo M, Li X, Flamigni F, Li J, Falcieri E, Facchini A, Marcu KB. Differential requirements for IKKalpha and IKKbeta in the differentiation of primary human osteoarthritic chondrocytes. *Arthritis Rheum.* 2008 Jan;58(1):227-39.
63. Marcu KB, Otero M, Olivetto E, Borzi RM, Goldring MB. NF-kappaB signaling: multiple angles to target OA. *Curr Drug Targets.* 2010 May;11(5):599-613.
64. van der Kraan PM, Blaney Davidson EN, van den Berg WB. A role for age-related changes in TGFbeta signaling in aberrant chondrocyte differentiation and osteoarthritis. *Arthritis Res Ther.* 2010;12(1):201.
65. Blaney Davidson EN, Remst DF, Vitters EL, van Beuningen HM, Blom AB, Goumans MJ, van den Berg WB, van der Kraan PM. Increase in ALK1/ALK5 ratio as a cause for elevated MMP-13 expression in osteoarthritis in humans and mice. *J Immunol.* 2009 Jun 15;182(12):7937-45.
66. Roughley PJ, White RJ. Age-related changes in the structure of the proteoglycan subunits from human articular cartilage. *J Biol Chem.* 1980 Jan 10;255(1):217-24.
67. Verzijl N, DeGroot J, Ben ZC, Brau-Benjamin O, Maroudas A, Bank RA, Mizrahi J, Schalkwijk CG, Thorpe SR, Baynes JW, Bijlsma JW, Lafeber FP, TeKoppele JM. Crosslinking by advanced glycation end products increases the stiffness of the collagen network in human articular cartilage: a possible mechanism through which age is a risk factor for osteoarthritis. *Arthritis Rheum.* 2002 Jan;46(1):114-23.
68. Martin JA, Ellerbroek SM, Buckwalter JA. Age-related decline in chondrocyte response to insulin-like growth factor-I: the role of growth factor binding proteins. *J Orthop Res.* 1997 Jul;15(4):491-8.

69. Scharstuhl A, van Beuningen HM, Vitters EL, van der Kraan PM, van den Berg WB: Loss of transforming growth factor counteraction on IL-1-mediated effects in cartilage of old mice. *Ann Rheum Dis*. 2002 Dec; 61(12):1095-1098.
70. Blaney Davidson EN, Scharstuhl A, Vitters EL, van der Kraan PM, van den Berg WB. Reduced transforming growth factor-beta signaling in cartilage of old mice: role in impaired repair capacity. *Arthritis Res Ther*. 2005;7(6):R1338-47.
71. Martin JA, Buckwalter JA. Telomere erosion and senescence in human articular cartilage chondrocytes. *J Gerontol A Biol Sci Med Sci*. 2001 Apr;56(4):B172-9.
72. Price JS, Waters JG, Darrah C, Pennington C, Edwards DR, Donell ST, Clark IM. The role of chondrocyte senescence in osteoarthritis. *Aging Cell*. 2002 Oct;1(1):57-65.
73. Shimada H, Sakakima H, Tsuchimochi K, Matsuda F, Komiya S, Goldring MB, Ijiri K. Senescence of chondrocytes in aging articular cartilage: GADD45 β mediates p21 expression in association with C/EBP β in senescence-accelerated mice. *Pathol Res Pract*. 2011 Apr 15;207(4):225-31.
74. Mobasher A, Matta C, Zákány R, Musumeci G. Chondrosenescence: definition, hallmarks and potential role in the pathogenesis of osteoarthritis. *Maturitas*. 2015 Mar;80(3):237-44.
75. Musumeci G, Loreto C, Carnazza ML, Martinez G. Characterization of apoptosis in articular cartilage derived from the knee joints of patients with osteoarthritis. *Knee Surg Sports Traumatol Arthrosc*. 2011 Feb;19(2):307-13.
76. Kühn K, D'Lima DD, Hashimoto S, Lotz M. Cell death in cartilage. *Osteoarthritis Cartilage*. 2004 Jan;12(1):1-16.
77. Li YS, Zhang FJ, Zeng C, Luo W, Xiao WF, Gao SG, Lei GH. Autophagy in osteoarthritis. *Joint Bone Spine*. 2016 Mar;83(2):143-8.
78. Caramés B, Taniguchi N, Otsuki S, Blanco FJ, Lotz M. Autophagy is a protective mechanism in normal cartilage, and its aging-related loss is linked with cell death and osteoarthritis. *Arthritis Rheum*. 2010 Mar;62(3):791-801.
79. Barbero A, Grogan S, Schäfer D, Heberer M, Mainil-Varlet P, Martin I. Age related changes in human articular chondrocyte yield, proliferation and post-expansion chondrogenic capacity. *Osteoarthritis Cartilage*. 2004 Jun;12(6):476-84.
80. Almonte-Becerril M, Navarro-Garcia F, Gonzalez-Robles A, Vega-Lopez MA, Lavalley C, Kouri JB. Cell death of chondrocytes is a combination between apoptosis and autophagy during the pathogenesis of Osteoarthritis within an experimental model. *Apoptosis*. 2010 May;15(5):631-8.
81. Buckland-Wright C. Subchondral bone changes in hand and knee osteoarthritis detected by radiography. *Osteoarthritis Cartilage*. 2004;12 Suppl A:S10-9.
82. Felson DT, Gale DR, Elon Gale M, Niu J, Hunter DJ, Goggins J, Lavalley MP. Osteophytes and progression of knee osteoarthritis. *Rheumatology (Oxford)*. 2005 Jan;44(1):100-4.
83. Li G, Yin J, Gao J, Cheng TS, Pavlos NJ, Zhang C, Zheng MH. Subchondral bone in osteoarthritis: insight into risk factors and microstructural changes. *Arthritis Res Ther*. 2013;15(6):223.
84. Pan J, Zhou X, Li W, Novotny JE, Doty SB, Wang L. In situ measurement of transport between subchondral bone and articular cartilage. *J Orthop Res*. 2009 Oct;27(10):1347-52.

85. Lane LB, Villacin A, Bullough PG. The vascularity and remodelling of subchondrial bone and calcified cartilage in adult human femoral and humeral heads. An age- and stress-related phenomenon. *J Bone Joint Surg Br.* 1977 Aug;59(3):272-8.
86. Burr DB, Radin EL. Microfractures and microcracks in subchondral bone: are they relevant to osteoarthritis? *Rheum Dis Clin North Am.* 2003 Nov;29(4):675-85.
87. Taljanovic MS, Graham AR, Benjamin JB, Gmitro AF, Krupinski EA, Schwartz SA, Hunter TB, Resnick DL. Bone marrow edema pattern in advanced hip osteoarthritis: quantitative assessment with magnetic resonance imaging and correlation with clinical examination, radiographic findings, and histopathology. *Skeletal Radiol.* 2008 May;37(5):423-31.
88. Maroudas A, Bullough P, Swanson SA, Freeman MA. The permeability of articular cartilage. *J Bone Joint Surg Br.* 1968 Feb;50(1):166-77.
89. Bailey AJ, Mansell JP, Sims TJ, Banse X. Biochemical and mechanical properties of subchondral bone in osteoarthritis. *Biorheology.* 2004;41(3-4):349-58.
90. Hilal G, Martel-Pelletier J, Pelletier JP, Ranger P, Lajeunesse D. Osteoblast-like cells from human subchondral osteoarthritic bone demonstrate an altered phenotype in vitro: possible role in subchondral bone sclerosis. *Arthritis Rheum.* 1998 May;41(5):891-9.
91. Hilal G, Martel-Pelletier J, Pelletier JP, Duval N, Lajeunesse D. Abnormal regulation of urokinase plasminogen activator by insulin-like growth factor 1 in human osteoarthritic subchondral osteoblasts. *Arthritis Rheum.* 1999;42:2112–2122.
92. Hilal G, Massicotte F, Martel-Pelletier J, Fernandes JC, Pelletier JP, Lajeunesse D. Endogenous prostaglandin E2 and insulin-like growth factor 1 can modulate the levels of parathyroid hormone receptor in human osteoarthritic osteoblasts. *J Bone Miner Res.* 2001 Apr;16(4):713-21.
93. Westacott CI, Webb GR, Warnock MG, Sims JV, Elson CJ. Alteration of cartilage metabolism by cells from osteoarthritic bone. *Arthritis Rheum.* 1997 Jul;40(7):1282-91.
94. Prasadam I, van Gennip S, Friis T, Shi W, Crawford R, Xiao Y. ERK-1/2 and p38 in the regulation of hypertrophic changes of normal articular cartilage chondrocytes induced by osteoarthritic subchondral osteoblasts. *Arthritis Rheum.* 2010 May;62(5):1349-60.
95. Imhof H, Sulzbacher I, Grampp S, Czerny C, Youssefzadeh S, Kainberger F. Subchondral bone and cartilage disease: a rediscovered functional unit. *Invest Radiol.* 2000 Oct;35(10):581-8.
96. Lories RJ, Luyten FP. The bone-cartilage unit in osteoarthritis. *Nat Rev Rheumatol.* 2011 Jan;7(1):43-9.
97. Yuan XL, Meng HY, Wang YC, Peng J, Guo QY, Wang AY, Lu SB. Bone-cartilage interface crosstalk in osteoarthritis: potential pathways and future therapeutic strategies. *Osteoarthritis Cartilage.* 2014 Aug;22(8):1077-89.
98. Pottenger LA, Phillips FM, Draganich LF. The effect of marginal osteophytes on reduction of varus-valgus instability in osteoarthritic knees. *Arthritis Rheum.* 1990 Jun;33(6):853-8.
99. Hsia AW, Anderson MJ, Heffner MA, Lagmay EP, Zavodovskaya R, Christiansen BA. Osteophyte formation after ACL rupture in mice is associated with joint restabilization and loss of range of motion. *J Orthop Res.* 2016 Mar 31.

100. van der Kraan PM, van den Berg WB. Osteophytes: relevance and biology. *Osteoarthritis Cartilage*. 2007 Mar;15(3):237-44.
101. Gilbertson EM. Development of periarticular osteophytes in experimentally induced osteoarthritis in the dog. A study using microradiographic, microangiographic, and fluorescent bone-labelling techniques. *Ann Rheum Dis*. 1975 Feb;34(1):12-25.
102. Hayes CW, Jamadar DA, Welch GW, Jannausch ML, Lachance LL, Capul DC, Sowers MR. Osteoarthritis of the knee: comparison of MR imaging findings with radiographic severity measurements and pain in middle-aged women. *Radiology*. 2005 Dec;237(3):998-1007.
103. Sowers M, Karvonen-Gutierrez CA, Jacobson JA, Jiang Y, Yosef M. Associations of anatomical measures from MRI with radiographically defined knee osteoarthritis score, pain, and physical functioning. *J Bone Joint Surg Am*. 2011 Feb 2;93(3):241-51.
104. Liu L, Kaneko H, Sadatsuki R, Hada S, Yusup A, Kinoshita M, Futami I, Shimura Y, Kurosawa H, Saita Y, Takazawa Y, Ikeda H, Kaneko K, Ishijima M. MRI-detected osteophyte is a predictor for receiving total knee arthroplasty in patients with end-stage knee osteoarthritis. *Osteoarthritis Cartilage*. 2014;22:S470-S471.
105. Gelse K, Söder S, Eger W, Diemtar T, Aigner T. Osteophyte development--molecular characterization of differentiation stages. *Osteoarthritis Cartilage*. 2003 Feb;11(2):141-8.
106. Little CB, Barai A, Burkhardt D, Smith SM, Fosang AJ, Werb Z, Shah M, Thompson EW. Matrix metalloproteinase 13-deficient mice are resistant to osteoarthritic cartilage erosion but not chondrocyte hypertrophy or osteophyte development. *Arthritis Rheum*. 2009 Dec;60(12):3723-33.
107. Junker S, Krumbholz G, Frommer KW, Rehart S, Steinmeyer J, Rickert M, Schett G, Müller-Ladner U, Neumann E. Differentiation of osteophyte types in osteoarthritis - proposal of a histological classification. *Joint Bone Spine*. 2016 Jan;83(1):63-7.
108. Rhee DK, Marcelino J, Baker M, Gong Y, Smits P, Lefebvre V, Jay GD, Stewart M, Wang H, Warman ML, Carpten JD. The secreted glycoprotein lubricin protects cartilage surfaces and inhibits synovial cell overgrowth. *J Clin Invest*. 2005 Mar;115(3):622-31.
109. Bonnevie ED, Galesso D, Secchieri C, Cohen I, Bonassar LJ. Elastoviscous Transitions of Articular Cartilage Reveal a Mechanism of Synergy between Lubricin and Hyaluronic Acid. *PLoS One*. 2015 Nov 24;10(11):e0143415.
110. Igarashi M, Kaga I, Takamori Y, Sakamoto K, Miyazawa K, Nagaoka I. Effects of glucosamine derivatives and uronic acids on the production of glycosaminoglycans by human synovial cells and chondrocytes. *Int J Mol Med*. 2011 Jun;27(6):821-7.
111. Hoff P, Buttgereit F, Burmester GR, Jakstadt M, Gaber T, Andreas K, Matziolis G, Perka C, Röhner E. Osteoarthritis synovial fluid activates pro-inflammatory cytokines in primary human chondrocytes. *Int Orthop*. 2013 Jan;37(1):145-51.
112. Benito MJ, Veale DJ, FitzGerald O, van den Berg WB, Bresnihan B. Synovial tissue inflammation in early and late osteoarthritis. *Ann Rheum Dis*. 2005 Sep;64(9):1263-7.
113. Baker K, Grainger A, Niu J, Clancy M, Guermazi A, Crema M, Hughes L, Buckwalter J, Wooley A, Nevitt M, Felson DT. Relation of synovitis to knee pain using contrast-enhanced MRIs. *Ann Rheum Dis*. 2010 Oct;69(10):1779-83.

114. Wenham CY, Conaghan PG. The Role of Synovitis in Osteoarthritis. *Ther Adv Musculoskelet Dis*. 2010 Dec; 2(6): 349–359.
115. Roemer FW, Guermazi A, Felson DT, Niu J, Nevitt MC, Crema MD, Lynch JA, Lewis CE, Torner J, Zhang Y. Presence of MRI-detected joint effusion and synovitis increases the risk of cartilage loss in knees without osteoarthritis at 30-month follow-up: the MOST study. *Ann Rheum Dis*. 2011 Oct;70(10):1804-9.
116. Scanzello CR, Goldring SR. The role of synovitis in osteoarthritis pathogenesis. *Bone*. 2012 Aug;51(2):249-57.
117. Henrotin YE, De Groote DD, Labasse AH, Gaspar SE, Zheng SX, Geenen VG, Reginster JY. Effects of exogenous IL-1 beta, TNF alpha, IL-6, IL-8 and LIF on cytokine production by human articular chondrocytes. *Osteoarthritis Cartilage*. 1996 Sep;4(3):163-73.
118. Wojdasiewicz P, Poniatowski ŁA, Szukiewicz D. The role of inflammatory and anti-inflammatory cytokines in the pathogenesis of osteoarthritis. *Mediators Inflamm*. 2014;2014:561459.
119. Goldring MB, Birkhead J, Sandell LJ, Kimura T, Krane SM. Interleukin 1 suppresses expression of cartilage-specific types II and IX collagens and increases types I and III collagens in human chondrocytes. *J Clin Invest*. 1988 Dec;82(6):2026-37.
120. Stöve J, Huch K, Günther KP, Scharf HP. Interleukin-1beta induces different gene expression of stromelysin, aggrecan and tumor-necrosis-factor-stimulated gene 6 in human osteoarthritic chondrocytes in vitro. *Pathobiology*. 2000 May-Jun;68(3):144-9.
121. Mengshol JA, Vincenti MP, Coon CI, Barchowsky A, Brinckerhoff CE. Interleukin-1 induction of collagenase 3 (matrix metalloproteinase 13) gene expression in chondrocytes requires p38, c-Jun N-terminal kinase, and nuclear factor kappaB: differential regulation of collagenase 1 and collagenase 3. *Arthritis Rheum*. 2000 Apr;43(4):801-11.
122. Martel-Pelletier J, McCollum R, DiBattista J, Faure MP, Chin JA, Fournier S, Sarfati M, Pelletier JP. The interleukin-1 receptor in normal and osteoarthritic human articular chondrocytes. Identification as the type I receptor and analysis of binding kinetics and biologic function. *Arthritis Rheum*. 1992 May;35(5):530-40.
123. Sadouk MB, Pelletier JP, Tardif G, Kiansa K, Cloutier JM, Martel-Pelletier J. Human synovial fibroblasts coexpress IL-1 receptor type I and type II mRNA. The increased level of the IL-1 receptor in osteoarthritic cells is related to an increased level of the type I receptor. *Lab Invest*. 1995 Sep;73(3):347-55.
124. Guerne PA, Carson DA, Lotz M. IL-6 production by human articular chondrocytes. Modulation of its synthesis by cytokines, growth factors, and hormones in vitro. *J Immunol*. 1990 Jan 15;144(2):499-505.
125. Lotz M, Terkeltaub R, Villiger PM. Cartilage and joint inflammation. Regulation of IL-8 expression by human articular chondrocytes. *J Immunol*. 1992 Jan 15;148(2):466-73.
126. Baugé C, Attia J, Leclercq S, Pujol JP, Galéra P, Boumédiène K. Interleukin-1beta up-regulation of Smad7 via NF-kappaB activation in human chondrocytes. *Arthritis Rheum*. 2008 Jan;58(1):221-6.

127. Séguin CA, Bernier SM. TNFalpha suppresses link protein and type II collagen expression in chondrocytes: Role of MEK1/2 and NF-kappaB signaling pathways. *J Cell Physiol.* 2003 Dec;197(3):356-69.
128. Saklatvala J. Tumour necrosis factor alpha stimulates resorption and inhibits synthesis of proteoglycan in cartilage. *Nature.* 1986 Aug 7-13;322(6079):547-9.
129. López-Armada MJ, Caramés B, Martín MA, Cillero-Pastor B, Lires-Dean M, Fuentes-Boquete I, Arenas J, Blanco FJ. Mitochondrial activity is modulated by TNFalpha and IL-1beta in normal human chondrocyte cells. *Osteoarthritis Cartilage.* 2006 Oct;14(10):1011-22.
130. Lo YY, Cruz TF. Involvement of reactive oxygen species in cytokine and growth factor induction of c-fos expression in chondrocytes. *J Biol Chem.* 1995 May 19;270(20):11727-30.
131. Davies CM, Guilak F, Weinberg JB, Fermor B. Reactive nitrogen and oxygen species in interleukin-1-mediated DNA damage associated with osteoarthritis. *Osteoarthritis Cartilage.* 2008 May;16(5):624-30.
132. Henderson B, Pettipher ER. Arthritogenic actions of recombinant IL-1 and tumour necrosis factor alpha in the rabbit: evidence for synergistic interactions between cytokines in vivo. *Clin Exp Immunol.* 1989 Feb;75(2):306-10.
133. Joos H, Wildner A, Hogrefe C, Reichel H, Brenner RE. Interleukin-1 beta and tumor necrosis factor alpha inhibit migration activity of chondrogenic progenitor cells from non-fibrillated osteoarthritic cartilage. *Arthritis Res Ther.* 2013;15(5):R119.
134. Bender S, Haubeck HD, Van de Leur E, Dufhues G, Schiel X, Lauwerijns J, Greiling H, Heinrich PC. Interleukin-1 beta induces synthesis and secretion of interleukin-6 in human chondrocytes. *FEBS Lett.* 1990 Apr 24;263(2):321-4.
135. Rasheed Z, Akhtar N, Haqqi TM. Advanced glycation end products induce the expression of interleukin-6 and interleukin-8 by receptor for advanced glycation end product-mediated activation of mitogen-activated protein kinases and nuclear factor-kB in human osteoarthritis chondrocytes. *Rheumatology (Oxford).* 2011 May;50(5):838-51.
136. Nietfeld JJ, Wilbrink B, Helle M, van Roy JL, den Otter W, Swaak AJ, Huber-Bruning O. Interleukin-1-induced interleukin-6 is required for the inhibition of proteoglycan synthesis by interleukin-1 in human articular cartilage. *Arthritis Rheum.* 1990 Nov;33(11):1695-701.
137. Matsukawa A, Yoshimura T, Maeda T, Ohkawara S, Takagi K, Yoshinaga M. Neutrophil accumulation and activation by homologous IL-8 in rabbits. IL-8 induces destruction of cartilage and production of IL-1 and IL-1 receptor antagonist in vivo. *J Immunol.* 1995 May 15;154(10):5418-25.
138. Yoshimura T, Matsushima K, Tanaka S, Robinson EA, Appella E, Oppenheim JJ, Leonard EJ. Purification of a human monocyte-derived neutrophil chemotactic factor that has peptide sequence similarity to other host defense cytokines. *Proc Natl Acad Sci U S A.* 1987 Dec;84(24):9233-7.
139. de Hooge AS, van de Loo FA, Bennink MB, Arntz OJ, de Hooge P, van den Berg WB. Male IL-6 gene knock out mice developed more advanced osteoarthritis upon aging. *Osteoarthritis Cartilage.* 2005 Jan;13(1):66-73.

140. Kwan Tat S, Padrines M, Théoleyre S, Heymann D, Fortun Y. IL-6, RANKL, TNF-alpha/IL-1: interrelations in bone resorption pathophysiology. *Cytokine Growth Factor Rev.* 2004 Feb; 15(1):49-60.
141. Sakao K, Takahashi KA, Arai Y, Saito M, Honjo K, Hiraoka N, Asada H, Shin-Ya M, Imanishi J, Mazda O, Kubo T. Osteoblasts derived from osteophytes produce interleukin-6, interleukin-8, and matrix metalloproteinase-13 in osteoarthritis. *J Bone Miner Metab.* 2009;27(4):412-23.
142. Caron JP, Fernandes JC, Martel-Pelletier J, Tardif G, Mineau F, Geng C, Pelletier JP. Chondroprotective effect of intraarticular injections of interleukin-1 receptor antagonist in experimental osteoarthritis. Suppression of collagenase-1 expression. *Arthritis Rheum.* 1996 Sep;39(9):1535-44.
143. Fernandes J, Tardif G, Martel-Pelletier J, Lascau-Coman V, Dupuis M, Moldovan F, Sheppard M, Krishnan BR, Pelletier JP. In vivo transfer of interleukin-1 receptor antagonist gene in osteoarthritic rabbit knee joints: prevention of osteoarthritis progression. *Am J Pathol.* 1999 Apr;154(4):1159-69.
144. Chevalier X, Goupille P, Beaulieu AD, Burch FX, Bensen WG, Conrozier T, Loeuille D, Kivitz AJ, Silver D, Appleton BE. Intraarticular injection of anakinra in osteoarthritis of the knee: a multicenter, randomized, double-blind, placebo-controlled study. *Arthritis Rheum.* 2009 Mar 15;61(3):344-52.
145. Cohen SB, Proudman S, Kivitz AJ, Burch FX, Donohue JP, Burstein D, Sun YN, Banfield C, Vincent MS, Ni L, Zack DJ. A randomized, double-blind study of AMG 108 (a fully human monoclonal antibody to IL-1R1) in patients with osteoarthritis of the knee. *Arthritis Res Ther.* 2011 Jul 29;13(4):R125.
146. Spector TD. Bisphosphonates: potential therapeutic agents for disease modification in osteoarthritis. *Aging Clin Exp Res.* 2003 Oct;15(5):413-8.
147. Hayami T, Pickarski M, Wesolowski GA, McLane J, Bone A, Destefano J, Rodan GA, Duong LT. The role of subchondral bone remodeling in osteoarthritis: reduction of cartilage degeneration and prevention of osteophyte formation by alendronate in the rat anterior cruciate ligament transection model. *Arthritis Rheum.* 2004 Apr;50(4):1193-206.
148. Ding M, Danielsen CC, Hvid I. The effects of bone remodeling inhibition by alendronate on three-dimensional microarchitecture of subchondral bone tissues in guinea pig primary osteoarthrosis. *Calcif Tissue Int.* 2008 Jan;82(1):77-86.
149. Thomsen JS, Straarup TS, Danielsen CC, Oxlund H, Brüel A. No effect of risedronate on articular cartilage damage in the Dunkin Hartley guinea pig model of osteoarthritis. *Scand J Rheumatol.* 2013;42(5):408-16.
150. Spector TD, Conaghan PG, Buckland-Wright JC, Garner P, Cline GA, Beary JF, Valent DJ, Meyer JM. Effect of risedronate on joint structure and symptoms of knee osteoarthritis: results of the BRISK randomized, controlled trial [ISRCTN01928173]. *Arthritis Res Ther.* 2005;7(3):R625-33.
151. Bingham CO 3rd, Buckland-Wright JC, Garner P, Cohen SB, Dougados M, Adami S, Clauw DJ, Spector TD, Pelletier JP, Raynauld JP, Strand V, Simon LS, Meyer JM, Cline GA, Beary JF. Risedronate decreases biochemical markers of cartilage degradation but does not decrease symptoms or slow radiographic progression in patients with medial compartment osteoarthritis of the knee: results of the two-year multinational knee osteoarthritis structural arthritis study. *Arthritis Rheum.* 2006 Nov;54(11):3494-507.

152. Garnero P, Aronstein WS, Cohen SB, Conaghan PG, Cline GA, Christiansen C, Beary JF, Meyer JM, Bingham CO 3rd. Relationships between biochemical markers of bone and cartilage degradation with radiological progression in patients with knee osteoarthritis receiving risedronate: the Knee Osteoarthritis Structural Arthritis randomized clinical trial. *Osteoarthritis Cartilage*. 2008 Jun;16(6):660-6.
153. Bruyère O, Reginster JY, Bellamy N, Chapurlat R, Richette P, Cooper C; SEKOIA investigators. Clinically meaningful effect of strontium ranelate on symptoms in knee osteoarthritis: a responder analysis. *Rheumatology (Oxford)*. 2014 Aug;53(8):1457-64.
154. Wang X, Hunter D, Xu J, Ding C. Metabolic triggered inflammation in osteoarthritis. *Osteoarthritis Cartilage*. 2015 Jan;23(1):22-30.
155. Clockaerts S, Van Osch GJ, Bastiaansen-Jenniskens YM, Verhaar JA, Van Glabbeek F, Van Meurs JB, Kerkhof HJ, Hofman A, Stricker BH, Bierma-Zeinstra SM. Statin use is associated with reduced incidence and progression of knee osteoarthritis in the Rotterdam study. *Ann Rheum Dis*. 2012 May;71(5):642-7.
156. Mansi IA, Mortensen EM, Pugh MJ, Wegner M, Frei CR. Incidence of musculoskeletal and neoplastic diseases in patients on statin therapy: results of a retrospective cohort analysis. *Am J Med Sci*. 2013 May;345(5):343-8.
157. Wang Y, Tonkin A, Jones G, Hill C, Ding C, Wluka AE, Forbes A, Cicuttini FM. Does statin use have a disease modifying effect in symptomatic knee osteoarthritis? Study protocol for a randomised controlled trial. *Trials*. 2015 Dec 23;16:584.
158. Brandt KD, Mazucca SA, Katz BP, Lane KA, Buckwalter KA, Yocum DE, Wolfe F, Schnitzer TJ, Moreland LW, Manzi S, Bradley JD, Sharma L, Oddis CV, Hugenberg ST, Heck LW. Effects of doxycycline on progression of osteoarthritis: results of a randomized, placebo-controlled, double-blind trial. *Arthritis Rheum*. 2005 Jul;52(7):2015-25.
159. Snijders GF, van den Ende CH, van Riel PL, van den Hoogen FH, den Broeder AA; NOAC study group. The effects of doxycycline on reducing symptoms in knee osteoarthritis: results from a triple-blinded randomised controlled trial. *Ann Rheum Dis*. 2011 Jul;70(7):1191-6.
160. Jin X, Jones G, Cicuttini F, Wluka A, Zhu Z, Han W, Antony B, Wang X, Winzenberg T, Blizzard L, Ding C. Effect of Vitamin D Supplementation on Tibial Cartilage Volume and Knee Pain Among Patients With Symptomatic Knee Osteoarthritis: A Randomized Clinical Trial. *JAMA*. 2016 Mar 8;315(10):1005-13.
161. Karsdal MA, Byrjalsen I, Alexandersen P, Bihlet A, Andersen JR, Riis BJ, Bay-Jensen AC2, Christiansen C; CSMC021C2301/2 investigators. Treatment of symptomatic knee osteoarthritis with oral salmon calcitonin: results from two phase 3 trials. *Osteoarthritis Cartilage*. 2015 Apr;23(4):532-43.
162. Boguski MS. Comparative genomics: the mouse that roared. *Nature*. 2002 Dec 5;420(6915):515-6.
163. Staines KA, Poulet B, Wentworth DN, Pitsillides AA. The STR/ort mouse model of spontaneous osteoarthritis - an update. *Osteoarthritis Cartilage*. 2016 Dec 11. pii: S1063-4584(16)30478-2.
164. McCoy AM. Animal Models of Osteoarthritis: Comparisons and Key Considerations. *Vet Pathol*. 2015 Sep;52(5):803-18.

165. Sokoloff L, Crittenden LB, Yamamoto RS, Jay GE Jr. The genetics of degenerative joint disease in mice. *Arthritis Rheum.* 1962 Dec;5:531-46.
166. Uchida K, Urabe K, Naruse K, Ogawa Z, Mabuchi K, Itoman M. Hyperlipidemia and hyperinsulinemia in the spontaneous osteoarthritis mouse model, STR/Ort. *Exp Anim.* 2009 Apr;58(2):181-7.
167. Mason RM, Chambers MG, Flannelly J, Gaffen JD, Dudhia J, Bayliss MT. The STR/ort mouse and its use as a model of osteoarthritis. *Osteoarthritis Cartilage.* 2001 Feb;9(2):85-91.
168. Hu K, Xu L, Cao L, Flahiff CM, Brussiau J, Ho K, Setton LA, Youn I, Guilak F, Olsen BR, Li Y. Pathogenesis of osteoarthritis-like changes in the joints of mice deficient in type IX collagen. *Arthritis Rheum.* 2006 Sep;54(9):2891-900.
169. Vasheghani F, Monemdjou R, Fahmi H, Zhang Y, Perez G, Blati M, St-Arnaud R, Pelletier JP, Beier F, Martel-Pelletier J, Kapoor M. Adult cartilage-specific peroxisome proliferator-activated receptor gamma knockout mice exhibit the spontaneous osteoarthritis phenotype. *Am J Pathol.* 2013 Apr;182(4):1099-106.
170. Weng T, Xie Y, Yi L, Huang J, Luo F, Du X, Chen L, Liu C, Chen D, Chen L. Loss of Vhl in cartilage accelerated the progression of age-associated and surgically induced murine osteoarthritis. *Osteoarthritis Cartilage.* 2014 Aug;22(8):1197-205.
171. Beuhold LA, Killar L, Zhao W, Sung ML, Warner L, Kulik J, Turner J, Wu W, Billingham C, Meijers T, Poole AR, Babij P, DeGennaro LJ. Postnatal expression in hyaline cartilage of constitutively active human collagenase-3 (MMP-13) induces osteoarthritis in mice. *J Clin Invest.* 2001;107:35-44.
172. Chen R, Mian M, Fu M, Zhao JY, Yang L, Li Y, Xu L. Attenuation of the progression of articular cartilage degeneration by inhibition of TGF- β 1 signaling in a mouse model of osteoarthritis. *Am J Pathol.* 2015 Nov;185(11):2875-85.
173. Weng T, Yi L, Huang J, Luo F, Wen X, Du X, Chen Q, Deng C, Chen D, Chen L. Genetic inhibition of fibroblast growth factor receptor 1 in knee cartilage attenuates the degeneration of articular cartilage in adult mice. *Arthritis Rheum.* 2012 Dec;64(12):3982-92.
174. Glasson SS, Askew R, Sheppard B, Carito B, Blanchet T, Ma HL, Flannery CR, Peluso D, Kanki K, Yang Z, Majumdar MK, Morris EA. Deletion of active ADAMTS5 prevents cartilage degradation in a murine model of osteoarthritis. *Nature.* 2005 Mar 31;434(7033):644-8.
175. Majumdar MK, Askew R, Schelling S, Stedman N, Blanchet T, Hopkins B, Morris EA, Glasson SS. Double-knockout of ADAMTS-4 and ADAMTS-5 in mice results in physiologically normal animals and prevents the progression of osteoarthritis. *Arthritis Rheum.* 2007;56:3670-3674.
176. Kalbhen DA. Chemical model of osteoarthritis--a pharmacological evaluation. *J Rheumatol.* 1987 May;14 Spec No:130-1.
177. Guzman RE, Evans MG, Bove S, Morenko B, Kilgore K. Mono-iodoacetate-induced histologic changes in subchondral bone and articular cartilage of rat femorotibial joints: an animal model of osteoarthritis. *Toxicol Pathol.* 2003 Nov-Dec;31(6):619-24.
178. Ogbonna AC, Clark AK, Malcangio M. Development of monosodium acetate-induced osteoarthritis and inflammatory pain in ageing mice. *Age (Dordr).* 2015 Jun;37(3):9792.

179. Combe R, Bramwell S, Field MJ. The monosodium iodoacetate model of osteoarthritis: a model of chronic nociceptive pain in rats? *Neurosci Lett*. 2004 Nov 11;370(2-3):236-40.
180. Morais SV, Czczeko NG, Malafaia O, Ribas JM Filho, Garcia JB, Miguel MT, Zini C, Massignan AG. Osteoarthritis model induced by intra-articular monosodium iodoacetate in rats knee. *Acta Cir Bras*. 2016 Nov;31(11):765-773.
181. van Osch GJ, van der Kraan PM, van den Berg WB. Site-specific cartilage changes in murine degenerative knee joint disease induced by iodoacetate and collagenase. *J Orthop Res*. 1994 Mar;12(2):168-75.
182. van Osch GJ, Blankevoort L, van der Kraan PM, Janssen B, Hekman E, Huiskes R, van den Berg WB. Laxity characteristics of normal and pathological murine knee joints in vitro. *J Orthop Res*. 1995 Sep;13(5):783-91.
183. van Dalen SC, Blom AB, Slöetjes AW, Helsen MM, Roth J, Vogl T, van de Loo FA, Koenders MI, van der Kraan PM, van den Berg WB, van den Bosch MH, van Lent PL. Interleukin-1 is not involved in synovial inflammation and cartilage destruction in collagenase-induced osteoarthritis. *Osteoarthritis Cartilage*. 2017 Mar;25(3):385-396.
184. Furman BD, Strand J, Hembree WC, Ward BD, Guilak F, Olson SA. Joint degeneration following closed intraarticular fracture in the mouse knee: a model of posttraumatic arthritis. *J Orthop Res*. 2007 May;25(5):578-92.
185. Poulet B, Hamilton RW, Shefelbine S, Pitsillides AA. Characterizing a novel and adjustable noninvasive murine joint loading model. *Arthritis Rheum*. 2011 Jan;63(1):137-47.
186. Christiansen BA, Anderson MJ, Lee CA, Williams JC, Yik JH, Haudenschild DR. Musculoskeletal changes following non-invasive knee injury using a novel mouse model of post-traumatic osteoarthritis. *Osteoarthritis Cartilage*. 2012 Jul;20(7):773-82.
187. Christiansen BA, Guilak F, Lockwood KA, Olson SA, Pitsillides AA, Sandell LJ, Silva MJ, van der Meulen MC, Haudenschild DR. Non-invasive mouse models of post-traumatic osteoarthritis. *Osteoarthritis Cartilage*. 2015 Oct;23(10):1627-38.
188. Pond MJ, Nuki G. Experimentally-induced osteoarthritis in the dog. *Ann Rheum Dis*. 1973 Jul;32(4):387-8.
189. Moskowitz RW, Davis W, Sammarco J, Martens M, Baker J, Mayor M, Burnstein AH, Frankel VH. Experimentally-induced degenerative joint lesions following partial medial meniscectomy in the rabbit. *Arthritis Rheum*. 1973 May-Jun;16(3):397-405.
190. Janusz MJ, Bendele AM, Brown KK, Taiwo YO, Hsieh L, Heitmeyer SA. Induction of osteoarthritis in the rat by surgical tear of the meniscus: Inhibition of joint damage by a matrix metalloproteinase inhibitor. *Osteoarthritis Cartilage*. 2002 Oct;10(10):785-91.
191. Bendele A, McComb J, Gould T, McAbee T, Sennello G, Chlipala E, Guy M. Animal models of arthritis: relevance to human disease. *Toxicol Pathol*. 1999 Jan-Feb;27(1):134-42.
192. Visco DM, Orevillo CJ, Kammerman J, Kincaid SA, Widmer WR, Christen AJ. Progressive chronic osteoarthritis in a surgically induced model in mice. *Trans Orthop Res Soc*. 1996;21:241
193. Clements KM, Price JS, Chambers MG, Visco DM, Poole AR, Mason RM. Gene deletion of either interleukin-1beta, interleukin-1beta-converting enzyme, inducible nitric oxide synthase, or

- stromelysin 1 accelerates the development of knee osteoarthritis in mice after surgical transection of the medial collateral ligament and partial medial meniscectomy. *Arthritis Rheum.* 2003 Dec;48(12):3452-63.
194. Kamekura S, Hoshi K, Shimoaka T, Chung U, Chikuda H, Yamada T, Uchida M, Ogata N, Seichi A, Nakamura K, Kawaguchi H. Osteoarthritis development in novel experimental mouse models induced by knee joint instability. *Osteoarthritis Cartilage.* 2005 Jul;13(7):632-41.
 195. Glasson SS, Blanchet TJ, Morris EA. The surgical destabilization of the medial meniscus (DMM) model of osteoarthritis in the 129/SvEv mouse. *Osteoarthritis Cartilage* 2007;15(9):1061–9.
 196. Culley KL, Dragomir CL, Chang J, Wondimu EB, Coico J, Plumb DA, Otero M, Goldring MB. Mouse models of osteoarthritis: surgical model of posttraumatic osteoarthritis induced by destabilization of the medial meniscus. *Methods Mol Biol.* 2015;1226:143-73.
 197. Takayama K, Kawakami Y, Kobayashi M, Greco N, Cummins JH, Matsushita T, Kuroda R, Kurosaka M, Fu FH, Huard J. Local intra-articular injection of rapamycin delays articular cartilage degeneration in a murine model of osteoarthritis. *Arthritis Res Ther.* 2014 Nov 17;16(6):482.
 198. Li W, Cai L, Zhang Y, Cui L, Shen G. Intra-articular resveratrol injection prevents osteoarthritis progression in a mouse model by activating SIRT1 and thereby silencing HIF-2 α . *J Orthop Res.* 2015 Jul;33(7):1061-70.
 199. Radwan M, Wilkinson DJ, Hui W, Destrument AP, Charlton SH, Barter MJ, Gibson B, Coulombe J, Gray DA, Rowan AD, Young DA. Protection against murine osteoarthritis by inhibition of the 26S proteasome and lysine-48 linked ubiquitination. *Ann Rheum Dis.* 2015 Aug;74(8):1580-7.
 200. Johnson K, Zhu S, Tremblay MS, Payette JN, Wang J, Bouchez LC, Meeusen S, Althage A, Cho CY, Wu X, Schultz PG. A stem cell-based approach to cartilage repair. *Science.* 2012 May 11;336(6082):717-21.
 201. Brown TD, Johnston RC, Saltzman CL, Marsh JL, Buckwalter JA. Posttraumatic osteoarthritis: a first estimate of incidence, prevalence, and burden of disease. *J Orthop Trauma.* 2006 Nov-Dec;20(10):739-44.
 202. Nukavarapu SP, Dorcenus DL. Osteochondral tissue engineering: current strategies and challenges. *Biotechnol Adv.* 2013 Sep-Oct;31(5):706-21.
 203. Falah M, Nierenberg G, Soudry M, Hayden M, Volpin G. Treatment of articular cartilage lesions of the knee. *Int Orthop.* 2010 Jun;34(5):621-30.
 204. Richter DL, Schenck RC Jr, Wascher DC, Treme G. Knee Articular Cartilage Repair and Restoration Techniques: A Review of the Literature. *Sports Health.* 2016 Mar-Apr;8(2):153-60.
 205. Davies-Tuck ML, Wluka AE, Wang Y, Teichtahl AJ, Jones G, Ding C, Cicuttini FM. The natural history of cartilage defects in people with knee osteoarthritis. *Osteoarthritis Cartilage.* 2008 Mar;16(3):337-42.
 206. Tuan RS, Chen AF, Klatt BA. Cartilage regeneration. *J Am Acad Orthop Surg.* 2013 May;21(5):303-11.
 207. Langer R, Vacanti JP. Tissue engineering. *Science.* 1993 May 14;260(5110):920-6.

208. Caldwell KL, Wang J. Cell-based articular cartilage repair: the link between development and regeneration. *Osteoarthritis Cartilage*. 2015 Mar;23(3):351-62.
209. Bernhard JC, Vunjak-Novakovic G. Should we use cells, biomaterials, or tissue engineering for cartilage regeneration? *Stem Cell Res Ther*. 2016 Apr 18;7(1):56.
210. Freed LE, Marquis JC, Nohria A, Emmanuel J, Mikos AG, Langer R. Neocartilage formation in vitro and in vivo using cells cultured on synthetic biodegradable polymers. *J Biomed Mater Res*. 1993 Jan;27(1):11-23.
211. Brittberg M, Lindahl A, Nilsson A, Ohlsson C, Isaksson O, Peterson L. Treatment of deep cartilage defects in the knee with autologous chondrocyte transplantation. *N Engl J Med*. 1994 Oct 6;331(14):889-95.
212. Pelttari K, Wixmerten A, Martin I. Do we really need cartilage tissue engineering? *Swiss Med Wkly*. 2009 Oct 17;139(41-42):602-9.
213. Wang M, Yuan Z, Ma N, Hao C, Guo W, Zou G, Zhang Y, Chen M, Gao S, Peng J, Wang A, Wang Y, Sui X, Xu W, Lu S, Liu S, Guo Q. Advances and Prospects in Stem Cells for Cartilage Regeneration. *Stem Cells Int*. 2017;2017:4130607.
214. Cigan AD, Durney KM, Nims RJ, Vunjak-Novakovic G, Hung CT, Ateshian GA. Nutrient Channels Aid the Growth of Articular Surface-Sized Engineered Cartilage Constructs. *Tissue Eng Part A*. 2016 Sep;22(17-18):1063-74.
215. Klein TJ, Malda J, Sah RL, Hutmacher DW. Tissue engineering of articular cartilage with biomimetic zones. *Tissue Eng Part B Rev*. 2009 Jun;15(2):143-57.
216. Khan IM, Gilbert SJ, Singhrao SK, Duance VC, Archer CW. Cartilage integration: evaluation of the reasons for failure of integration during cartilage repair. A review. *Eur Cell Mater*. 2008 Sep 3;16:26-39.
217. Levine DW, Mondano L, Halpin M. FDA regulatory pathways for knee cartilage repair products. *Sports Med Arthrosc*. 2008 Dec;16(4):202-7.
218. Williams DF. The biomaterials conundrum in tissue engineering. *Tissue Eng Part A*. 2014 Apr;20(7-8):1129-31.
219. Zeng L, Chen X, Zhang Q, Yu F, Li Y, Yao Y. Redifferentiation of dedifferentiated chondrocytes in a novel three-dimensional microcavitary hydrogel. *J Biomed Mater Res A*. 2015 May;103(5):1693-702.
220. Nehrer S, Breinan HA, Ramappa A, Hsu HP, Minas T, Shortkroff S, Sledge CB, Yannas IV, Spector M. Chondrocyte-seeded collagen matrices implanted in a chondral defect in a canine model. *Biomaterials*. 1998 Dec;19(24):2313-28.
221. Zhang L, Yuan T, Guo L, Zhang X. An in vitro study of collagen hydrogel to induce the chondrogenic differentiation of mesenchymal stem cells. *J Biomed Mater Res A*. 2012 Oct;100(10):2717-25.
222. Burdick JA, Prestwich GD. Hyaluronic acid hydrogels for biomedical applications. *Adv Mater*. 2011 Mar 25;23(12):H41-56.

223. Wang DA, Varghese S, Sharma B, Strehin I, Fermanian S, Gorham J, Fairbrother DH, Cascio B, Elisseeff JH. Multifunctional chondroitin sulphate for cartilage tissue-biomaterial integration. *Nat Mater*. 2007 May;6(5):385-92.
224. Levett PA, Melchels FP, Schrobback K, Hutmacher DW, Malda J, Klein TJ. A biomimetic extracellular matrix for cartilage tissue engineering centered on photocurable gelatin, hyaluronic acid and chondroitin sulfate. *Acta Biomater*. 2014 Jan;10(1):214-23.
225. Hu X, Li D, Zhou F, Gao C. Biological hydrogel synthesized from hyaluronic acid, gelatin and chondroitin sulfate by click chemistry. *Acta Biomater*. 2011 Apr;7(4):1618-26.
226. Seo SJ, Mahapatra C, Singh RK, Knowles JC, Kim HW. Strategies for osteochondral repair: Focus on scaffolds. *J Tissue Eng*. 2014 Jul 8;5:2041731414541850.
227. Holland TA, Tabata Y, Mikos AG. Dual growth factor delivery from degradable oligo(poly(ethylene glycol) fumarate) hydrogel scaffolds for cartilage tissue engineering. *J Control Release*. 2005 Jan 3;101(1-3):111-25.
228. Coburn JM, Gibson M, Monagle S, Patterson Z, Elisseeff JH. Bioinspired nanofibers support chondrogenesis for articular cartilage repair. *Proc Natl Acad Sci U S A*. 2012 Jun 19;109(25):10012-7.
229. Matricali GA, Dereymaeker GP, Luyten FP. Donor site morbidity after articular cartilage repair procedures: a review. *Acta Orthop Belg*. 2010 Oct;76(5):669-74.
230. Ma B, Leijten JC, Wu L, Kip M, van Blitterswijk CA, Post JN, Karperien M. Gene expression profiling of dedifferentiated human articular chondrocytes in monolayer culture. *Osteoarthritis Cartilage*. 2013 Apr;21(4):599-603.
231. Friedenstein AJ, Piatetzky-Shapiro II, Petrakova KV. Osteogenesis in transplants of bone marrow cells. *J Embryol Exp Morphol*. 1966 Dec;16(3):381-90.
232. Pittenger MF, Mackay AM, Beck SC, Jaiswal RK, Douglas R, Mosca JD, Moorman MA, Simonetti DW, Craig S, Marshak DR. Multilineage potential of adult human mesenchymal stem cells. *Science*. 1999 Apr 2;284(5411):143-7.
233. Wakitani S, Goto T, Pineda SJ, Young RG, Mansour JM, Caplan AI, Goldberg VM. Mesenchymal cell-based repair of large, full-thickness defects of articular cartilage. *J Bone Joint Surg Am*. 1994 Apr;76(4):579-92.
234. Abrahamsson CK, Yang F, Park H, Brunger JM, Valonen PK, Langer R, Welter JF, Caplan AI, Guilak F, Freed LE. Chondrogenesis and mineralization during in vitro culture of human mesenchymal stem cells on three-dimensional woven scaffolds. *Tissue Eng Part A*. 2010 Dec;16(12):3709-18.
235. Park JS, Yang HJ, Woo DG, Yang HN, Na K, Park KH. Chondrogenic differentiation of mesenchymal stem cells embedded in a scaffold by long-term release of TGF-beta 3 complexed with chondroitin sulfate. *J Biomed Mater Res A*. 2010 Feb;92(2):806-16.
236. Bouffi C, Thomas O, Bony C, Giteau A, Venier-Julienne MC, Jorgensen C, Montero-Menei C, Noël D. The role of pharmacologically active microcarriers releasing TGF-beta3 in cartilage formation in vivo by mesenchymal stem cells. *Biomaterials*. 2010 Sep;31(25):6485-93.

237. Dahlin RL, Ni M, Meretoja VV, Kasper FK, Mikos AG. TGF- β 3-induced chondrogenesis in co-cultures of chondrocytes and mesenchymal stem cells on biodegradable scaffolds. *Biomaterials*. 2014 Jan;35(1):123-32.
238. Bai X, Li G, Zhao C, Duan H, Qu F. BMP7 induces the differentiation of bone marrow-derived mesenchymal cells into chondrocytes. *Med Biol Eng Comput*. 2011 Jun;49(6):687-92.
239. Le Blanc K, Tammik L, Sundberg B, Haynesworth SE, Ringdén O. Mesenchymal stem cells inhibit and stimulate mixed lymphocyte cultures and mitogenic responses independently of the major histocompatibility complex. *Scand J Immunol*. 2003 Jan;57(1):11-20.
240. Pers YM, Ruiz M, Noël D, Jorgensen C. Mesenchymal stem cells for the management of inflammation in osteoarthritis: state of the art and perspectives. *Osteoarthritis Cartilage*. 2015 Nov;23(11):2027-35.
241. Yoon D, Kim H, Lee E, Park MH, Chung S, Jeon H, Ahn CH, Lee K. Study on chemotaxis and chemokinesis of bone marrow-derived mesenchymal stem cells in hydrogel-based 3D microfluidic devices. *Biomater Res*. 2016 Aug 2;20:25.
242. Nejadnik H, Hui JH, Feng Choong EP, Tai BC, Lee EH. Autologous bone marrow-derived mesenchymal stem cells versus autologous chondrocyte implantation: an observational cohort study. *Am J Sports Med*. 2010 Jun;38(6):1110-6.
243. Zhong L, Huang X, Karperien M, Post JN. The Regulatory Role of Signaling Crosstalk in Hypertrophy of MSCs and Human Articular Chondrocytes. *Int J Mol Sci*. 2015 Aug 14;16(8):19225-47.
244. Lv FJ, Tuan RS, Cheung KM, Leung VY. Concise review: the surface markers and identity of human mesenchymal stem cells. *Stem Cells*. 2014 Jun;32(6):1408-19.
245. Bühring HJ, Battula VL, Tremel S, Schewe B, Kanz L, Vogel W. Novel markers for the prospective isolation of human MSC. *Ann N Y Acad Sci*. 2007 Jun;1106:262-71.
246. Kopesky PW, Vanderploeg EJ, Kisiday JD, Frisbie DD, Sandy JD, Grodzinsky AJ. Controlled delivery of transforming growth factor β 1 by self-assembling peptide hydrogels induces chondrogenesis of bone marrow stromal cells and modulates Smad2/3 signaling. *Tissue Eng Part A*. 2011 Jan;17(1-2):83-92.
247. Akkiraju H, Bonor J, Nohe A. CK2.1, a novel peptide, induces articular cartilage formation in vivo. *J Orthop Res*. 2016 Jun 17.
248. Moghadam MN, Kolesov V, Vogel A, Klok HA, Pioletti DP. Controlled release from a mechanically-stimulated thermosensitive self-heating composite hydrogel. *Biomaterials*. 2014 Jan;35(1):450-5.
249. Maturavongsadit P, Luckanagul JA, Metavarayuth K, Zhao X, Chen L, Lin Y, Wang Q. Promotion of In Vitro Chondrogenesis of Mesenchymal Stem Cells Using In Situ Hyaluronic Hydrogel Functionalized with Rod-Like Viral Nanoparticles. *Biomacromolecules*. 2016 Jun 13;17(6):1930-8.
250. Shi D, Xu X, Ye Y, Song K, Cheng Y, Di J, Hu Q, Li J, Ju H, Jiang Q, Gu Z. Photo-Cross-Linked Scaffold with Kartogenin-Encapsulated Nanoparticles for Cartilage Regeneration. *ACS Nano*. 2016 Jan 26;10(1):1292-9.

251. Madry H, Rey-Rico A, Venkatesan JK, Johnstone B, Cucchiari M. Transforming growth factor Beta-releasing scaffolds for cartilage tissue engineering. *Tissue Eng Part B Rev.* 2014 Apr;20(2):106-25.
252. Hicks DL, Sage AB, Shelton E, Schumacher BL, Sah RL, Watson D. Effect of bone morphogenetic proteins 2 and 7 on septal chondrocytes in alginate. *Otolaryngol Head Neck Surg.* 2007 Mar;136(3):373-9.
253. Gooch KJ, Blunk T, Courter DL, Sieminski AL, Bursac PM, Vunjak-Novakovic G, Freed LE. IGF-I and mechanical environment interact to modulate engineered cartilage development. *Biochem Biophys Res Commun.* 2001 Sep 7;286(5):909-15.
254. Veilleux N, Spector M. Effects of FGF-2 and IGF-1 on adult canine articular chondrocytes in type II collagen-glycosaminoglycan scaffolds in vitro. *Osteoarthritis Cartilage.* 2005 Apr;13(4):278-86.
255. Jeschke B, Meyer J, Jonczyk A, Kessler H, Adamietz P, Meenen NM, Kantlehner M, Goepfert C, Nies B. RGD-peptides for tissue engineering of articular cartilage. *Biomaterials.* 2002 Aug;23(16):3455-63.
256. Adams MA. The mechanical environment of chondrocytes in articular cartilage. *Biorheology.* 2006;43(3-4):537-45.
257. De Croos JN, Dhaliwal SS, Grynpas MD, Pilliar RM, Kandel RA. Cyclic compressive mechanical stimulation induces sequential catabolic and anabolic gene changes in chondrocytes resulting in increased extracellular matrix accumulation. *Matrix Biol.* 2006 Aug;25(6):323-31.
258. Hu JC, Athanasiou KA. The effects of intermittent hydrostatic pressure on self-assembled articular cartilage constructs. *Tissue Eng.* 2006 May;12(5):1337-44.
259. Elder BD, Athanasiou KA. Hydrostatic pressure in articular cartilage tissue engineering: from chondrocytes to tissue regeneration. *Tissue Eng Part B Rev.* 2009 Mar;15(1):43-53.
260. Mauck RL, Nicoll SB, Seyhan SL, Ateshian GA, Hung CT. Synergistic action of growth factors and dynamic loading for articular cartilage tissue engineering. *Tissue Eng.* 2003 Aug;9(4):597-611.
261. Schuh E, Hofmann S, Stok KS, Notbohm H, Müller R, Rotter N. The influence of matrix elasticity on chondrocyte behavior in 3D. *J Tissue Eng Regen Med.* 2012 Nov;6(10):e31-42.
262. Callahan LA, Ganiou AM, Childers EP, Weiner SD, Becker ML. Primary human chondrocyte extracellular matrix formation and phenotype maintenance using RGD-derivatized PEGDM hydrogels possessing a continuous Young's modulus gradient. *Acta Biomater.* 2013 Apr;9(4):6095-104.
263. Allen JL, Cooke ME, Alliston T. ECM stiffness primes the TGF β pathway to promote chondrocyte differentiation. *Mol Biol Cell.* 2012 Sep;23(18):3731-42.
264. Fermor B, Christensen SE, Youn I, Cernanec JM, Davies CM, Weinberg JB. Oxygen, nitric oxide and articular cartilage. *Eur Cell Mater.* 2007 Apr 11;13:56-65.
265. Ströbel S, Loparic M, Wendt D, Schenk AD, Candrian C, Lindberg RL, Moldovan F, Barbero A, Martin I. Anabolic and catabolic responses of human articular chondrocytes to varying oxygen percentages. *Arthritis Res Ther.* 2010;12(2):R34.

266. Duval E, Leclercq S, Elissalde JM, Demoor M, Galéra P, Boumédiène K. Hypoxia-inducible factor 1alpha inhibits the fibroblast-like markers type I and type III collagen during hypoxia-induced chondrocyte redifferentiation: hypoxia not only induces type II collagen and aggrecan, but it also inhibits type I and type III collagen in the hypoxia-inducible factor 1alpha-dependent redifferentiation of chondrocytes. *Arthritis Rheum*. 2009 Oct;60(10):3038-48.
267. Robins JC, Akeno N, Mukherjee A, Dalal RR, Aronow BJ, Koopman P, Clemens TL. Hypoxia induces chondrocyte-specific gene expression in mesenchymal cells in association with transcriptional activation of Sox9. *Bone*. 2005 Sep;37(3):313-22.
268. Chen G, Deng C, Li Y-P. TGF- β and BMP Signaling in Osteoblast Differentiation and Bone Formation. *Int J Biol Sci* 2012;8(2):272–288.
269. Redini F, Galera P, Mauviel A, Loyau G, Pujol JP. Transforming growth factor beta stimulates collagen and glycosaminoglycan biosynthesis in cultured rabbit articular chondrocytes. *FEBS Lett* 1988;234(1):172–6.
270. Yang X, Chen L, Xu X, Li C, Huang C, Deng CX. TGF-beta/Smad3 signals repress chondrocyte hypertrophic differentiation and are required for maintaining articular cartilage. *J Cell Biol* 2001;153(1):35–46
271. Rahman MS, Akhtar N, Jamil HM, Banik RS, Asaduzzaman SM. TGF- β /BMP signaling and other molecular events: regulation of osteoblastogenesis and bone formation. *Bone Res* 2015;3:15005.
272. Bauge C, Girard N, Lhuissier E, Bazille C, Boumediene K. Regulation and Role of TGF- β Signaling Pathway in Aging and Osteoarthritis Joints. *Aging Disease* 2014;5(6):394–405.
273. Verdier MP, Seité S, Guntzer K, Pujol JP, Boumédiène K. Immunohistochemical analysis of transforming growth factor beta isoforms and their receptors in human cartilage from normal and osteoarthritic femoral heads. *Rheumatol Int* 2005;25(2):118–24.
274. Blaney Davidson EN, Vitters EL, van der Kraan PM, van den Berg WB. Expression of transforming growth factor-beta (TGFbeta) and the TGFbeta signalling molecule SMAD-2P in spontaneous and instability-induced osteoarthritis: role in cartilage degradation, chondrogenesis and osteophyte formation. *Ann Rheum Dis* 2006;65(11):1414–21.
275. Serra R, Johnson M, Filvaroff EH, LaBorde J, Sheehan DM, Derynck R, Moses HL. Expression of a truncated, kinase-defective TGF-beta type II receptor in mouse skeletal tissue promotes terminal chondrocyte differentiation and osteoarthritis. *J Cell Biol* 1997;139(2):541–52.
276. Li TF, Gao L, Sheu TJ, Sampson ER, Flick LM, Kontinen YT, Chen D, Schwarz EM, Zuscik MJ, Jonason JH, O'Keefe RJ. Aberrant hypertrophy in Smad3-deficient chondrocytes is rescued by restoring transforming growth factor beta-activated kinase 1/activating transcription factor 2 signaling: a potential clinical implication for osteoarthritis. *Arthritis Rheum* 2010;62(8):2359–69.
277. Hershko A and Ciechanover A. The ubiquitin system. *Ann Rev Biochem* 1998;67:425–79.
278. Tang LY, Yamashita M, Coussens NP, Tang Y, Wang X, Li C, Deng CX, Cheng SY, Zhang YE. Ablation of Smurf2 reveals an inhibition in TGF- β signalling through multiple mono-ubiquitination of Smad3. *EMBO J*. 2011;30(23):4777–89.
279. Jin L, Pahuja KB, Wickliffe KE, Gorur A, Baumgartel C, Schekman R, Rape M. Ubiquitin-dependent regulation of COPII coat size and function. *Nature* 2012 Feb 22;482(7386):495–500.

280. Inoue Y and Imamura T. Regulation of TGF- β family signaling by E3 ubiquitin ligases. *Cancer science* 2008; 99(11): 2107–12.
281. Bizet AA, Tran-Khanh N, Saksena A, Liu K, Buschmann MD, Philip A. CD109-mediated degradation of TGF- β receptors and inhibition of TGF- β responses involve regulation of SMAD7 and Smurf2 localization and function. *J Cell Biochem* 2012 Jan;113(1):238–46.
282. Xing L, Zhang M, Chen D. Smurf control in bone cells. *J Cell Biochem* 2010;110(3):554–563.
283. Yamashita M, Ying SX, Zhang GM, Li C, Cheng SY, Deng CX, Zhang YE. Ubiquitin ligase Smurf1 controls osteoblast activity and bone homeostasis by targeting MEKK2 for degradation. *Cell* 2005;121(1):101–13.
284. Wu Q, Kim KO, Sampson ER, Chen D, Awad H, O'Brien T, Puzas JE, Drissi H, Schwarz EM, O'Keefe RJ, Zuscik MJ, Rosier RN. Induction of an osteoarthritis-like phenotype and degradation of phosphorylated Smad3 by Smurf2 in transgenic mice. *Arthritis Rheum* 2008;58(10):3132–44.
285. Ramkumar C, Kong Y, Cui H, Hao S, Jones SN, Gerstein RM, Zhang H. Smurf2 regulates the senescence response and suppresses tumorigenesis in mice. *Cancer Res* 2012;72(11):2714–9.
286. Blank M, Tang Y, Yamashita M, Burkett SS, Cheng SY, Zhang YE. A tumor suppressor function of Smurf2 associated with controlling chromatin landscape and genome stability through RNF20. *Nat Med* 2012;18(2):227–34.
287. Suire C, Brouard N, Hirschi K, Simmons PJ. Isolation of the stromal-vascular fraction of mouse bone marrow markedly enhances the yield of clonogenic stromal progenitors. *Blood* 2012;119(11):e86–95.
288. Gosset M, Berenbaum F, Thirion S, Jacques C. Primary culture and phenotyping of murine chondrocytes. *Nat Protoc* 2008;3(8):1253–60.
289. Glasson SS, Chambers MG, Van Den Berg WB, Little CB. The OARSI histopathology initiative—recommendations for histological assessments of osteoarthritis in the mouse. *Osteoarthritis Cartilage* 2010;18 Suppl 3:S17–23.
290. Seeman E. Age- and menopause-related bone loss compromise cortical and trabecular microstructure. *J Gerontol A Biol Sci Med Sci* 2013;68(10):1218–25.
291. McNulty MA, Loeser RF, Davey C, Callahan MF, Ferguson CM, Carlson CS. Histopathology of Naturally Occurring and Surgically Induced Osteoarthritis in Mice. *Osteoarthritis Cartilage* 2012;20(8):949–956.
292. Stok KS, Pelled G, Zilberman Y, Kallai I, Goldhahn J, Gazit D, Müller R. Revealing the interplay of bone and cartilage in osteoarthritis through multimodal imaging of murine joints. *Bone* 2009;45(3):414–22.
293. Halloran BP, Ferguson VL, Simske SJ, Burghardt A, Venton LL, Majumdar S. Changes in bone structure and mass with advancing age in the male C57BL/6J mouse. *J Bone Miner Res* 2002;17(6):1044–50.
294. Glatt V, Canalis E, Stadmeier L, Bouxsein ML. Age-Related Changes in Trabecular Architecture Differ in Female and Male C57BL/6J Mice. *J Bone Miner Res* 2007;22(8):1197–1207.

295. Yamamoto K, Shishido T, Masaoka T, Imakiire A. Morphological studies on the ageing and osteoarthritis of the articular cartilage in C57 black mice. *J Orthop Surg* 2005;13(1):8–18.
296. Burr DB, Gallant MA. Bone remodelling in osteoarthritis. *Nat Rev Rheumatol* 2012;8:665–673.
297. Tetlow LC, Adlam DJ, Wooley DE. Matrix metalloproteinase and proinflammatory cytokine production by chondrocytes of human osteoarthritic cartilage. *Arthritis Rheum* 2001;44(3):585–94.
298. Rowan AD and Young DA. Collagenase gene regulation by pro-inflammatory cytokines in cartilage. *Frontiers in Bioscience*. 2007;12:536–50.
299. Lin X, Liang M, Feng XH. Smurf2 is a ubiquitin E3 ligase mediating proteasome-dependent degradation of Smad2 in transforming growth factor-beta signaling. *J Biol Chem* 2000;275(47):36818–22.
300. Kavsak P, Rasmussen R, Causing C, Bonni S, Zhu H, Thomsen GH, Wrana JL. Smad7 Binds to Smurf2 to Form an E3 Ubiquitin Ligase that Targets the TGF- β Receptor for Degradation. *Mol Cell* 2000;6:1365–1375.
301. Blaney Davidson EN, van der Kraan PM, van den Berg WB. TGF-beta and osteoarthritis. *Osteoarthritis Cartilage* 2007;15(6):597–604.
302. Wu Q, Wang M, Zuscik MJ, Chen D, O'Keefe RJ, Rosier RN. Regulation of embryonic endochondral ossification by Smurf2. *J Orthop Res* 2008;26(5):704–12.
303. Keller B, Yang T, Chen Y, Munivez E, Bertin T, Zabel B, Lee B. Interaction of TGF β and BMP signaling pathways during chondrogenesis. *PLoS One* 2011;6(1)e16421:1–9.
304. Bailey AJ, Mansell JP. Do subchondral bone changes exacerbate or precede articular cartilage destruction in osteoarthritis of the elderly? *Gerontology*. 1997;43(5):296-304.
305. Felson DT, Neogi T. Osteoarthritis: is it a disease of cartilage or of bone? *Arthritis Rheum*. 2004 Feb;50(2):341-4.
306. Sanchez C, Deberg MA, Piccardi N, Msika P, Reginster JY, Henrotin YE. Osteoblasts from the sclerotic subchondral bone downregulate aggrecan but upregulate metalloproteinases expression by chondrocytes. This effect is mimicked by interleukin-6, -1beta and oncostatin M pre-treated non-sclerotic osteoblasts. *Osteoarthritis Cartilage*. 2005 Nov;13(11):979-87.
307. Sharma AR, Jagga S, Lee SS, Nam JS. Interplay between cartilage and subchondral bone contributing to pathogenesis of osteoarthritis. *Int J Mol Sci*. 2013 Sep 30;14(10):19805-30.
308. van Osch GJ, van der Kraan PM, Vitters EL, Blankevoort L, van den Berg WB. Induction of osteoarthritis by intra-articular injection of collagenase in mice. Strain and sex related differences. *Osteoarthritis Cartilage*. 1993 Jul; 1(3):171-7.
309. Xu W, Xie Y, Wang Q, Wang X, Luo F, Zhou S, Wang Z, Huang J, Tan Q, Jin M, Qi H, Tang J, Chen L, Du X, Zhao C, Liang G, Chen L. A novel fibroblast growth factor receptor 1 inhibitor protects against cartilage degradation in a murine model of osteoarthritis. *Sci Rep*. 2016 Apr 4; 6():24042.
310. Zhao YP, Liu B, Tian QY, Wei JL, Richbourgh B, Liu CJ. Progranulin protects against osteoarthritis through interacting with TNF- α and β -Catenin signalling. *Ann Rheum Dis*. 2015 Dec; 74(12):2244-53

311. Uchimura T, Foote AT, Smith EL, Matzkin EG, Zeng L. Insulin-Like Growth Factor II (IGF-II) Inhibits IL-1 β -Induced Cartilage Matrix Loss and Promotes Cartilage Integrity in Experimental Osteoarthritis. *J Cell Biochem*. 2015 Dec; 116(12):2858-69
312. Oh H, Chun CH, Chun JS. Dkk-1 expression in chondrocytes inhibits experimental osteoarthritic cartilage destruction in mice. *Arthritis Rheum*. 2012 Aug; 64(8):2568-78
313. Xu L, Servais J, Polur I, Kim D, Lee PL, Chung K, Li Y. Attenuation of osteoarthritis progression by reduction of discoidin domain receptor 2 in mice. *Arthritis Rheum*. 2010 Sep; 62(9):2736-44.
314. Botter SM, Glasson SS, Hopkins B, Clockaerts S, Weinans H, van Leeuwen JP, van Osch GJ. ADAMTS5^{-/-} mice have less subchondral bone changes after induction of osteoarthritis through surgical instability: implications for a link between cartilage and subchondral bone changes. *Osteoarthritis Cartilage*. 2009 May; 17(5):636-45
315. Huang H, Veien ES, Zhang H, Ayers DC, Song J. Skeletal Characterization of Smurf2-Deficient Mice and In Vitro Analysis of Smurf2-Deficient Chondrocytes. *PLoS One*. 2016 Jan 27; 11(1):e0148088.
316. Ma HL, Blanchet TJ, Peluso D, Hopkins B, Morris EA, Glasson SS. Osteoarthritis severity is sex dependent in a surgical mouse model. *Osteoarthritis Cartilage*. 2007 Jun; 15(6):695-700.
317. Radin EL, Rose RM. Role of subchondral bone in the initiation and progression of cartilage damage. *Clin Orthop Relat Res*. 1986 Dec; (213):34-40.
318. Moskowitz RW. Bone remodeling in osteoarthritis: subchondral and osteophytic responses. *Osteoarthritis Cartilage*. 1999 May; 7(3):323-4.
319. Maas O, Joseph GB, Sommer G, Wild D, Kretzschmar M. Association between cartilage degeneration and subchondral bone remodeling in patients with knee osteoarthritis comparing MRI and (99m)Tc-DPD-SPECT/CT. *Osteoarthritis Cartilage*. 2015 Oct; 23(10):1713-20.
320. Loeser RF, Olex AL, McNulty MA, Carlson CS, Callahan MF, Ferguson CM, Chou J, Leng X, Fetrow JS. Microarray analysis reveals age-related differences in gene expression during the development of osteoarthritis in mice. *Arthritis Rheum*. 2012 Mar; 64(3):705-17.
321. Suri S, Walsh DA. Osteochondral alterations in osteoarthritis. *Bone*. 2012 Aug; 51(2):204-11.
322. Kim BJ, Kim DW, Kim SH, Cho JH, Lee HJ, Park DY, Park SR, Choi BH, Min BH. Establishment of a reliable and reproducible murine osteoarthritis model. *Osteoarthritis Cartilage*. 2013 Dec; 21(12):2013-20
323. van Osch GJ, van der Kraan PM, van Valburg AA, van den Berg WB. The relation between cartilage damage and osteophyte size in a murine model for osteoarthritis in the knee. *Rheumatol Int*. 1996; 16(3):115-9.
324. Nagaosa Y, Lanyon P, Doherty M. Characterisation of size and direction of osteophyte in knee osteoarthritis: a radiographic study. *Ann Rheum Dis*. 2002 Apr; 61(4):319-24.
325. Dieppe P, Cushnaghan J, Young P, Kirwan J. Prediction of the progression of joint space narrowing in osteoarthritis of the knee by bone scintigraphy. *Ann Rheum Dis*. 1993 Aug; 52(8):557-63.

326. Bettica P, Cline G, Hart DJ, Meyer J, Spector TD. Evidence for increased bone resorption in patients with progressive knee osteoarthritis: longitudinal results from the Chingford study. *Arthritis Rheum.* 2002 Dec; 46(12):3178-84.
327. Huebner JL, Bay-Jensen AC, Huffman KM, He Y, Leeming DJ, McDaniel GE, Karsdal MA, Kraus VB. Alpha C-telopeptide of type I collagen is associated with subchondral bone turnover and predicts progression of joint space narrowing and osteophytes in osteoarthritis. *Arthritis Rheumatol.* 2014 Sep; 66(9):2440-9.
328. Harman SM, Talbert GB. The effect of maternal age on ovulation, corpora lutea of pregnancy, and implantation failure in mice. *J Reprod Fertil.* 1970 Oct; 23(1):33-9.
329. Shin SY, Pozzi A, Boyd SK, Clark AL. Integrin $\alpha 1\beta 1$ protects against signs of post-traumatic osteoarthritis in the female murine knee partially via regulation of epidermal growth factor receptor signalling. *Osteoarthritis Cartilage.* 2016 Oct; 24(10):1795-806.
330. Kraus VB, Feng S, Wang S, White S, Ainslie M, Graverand MP, Brett A, Eckstein F, Hunter DJ, Lane NE, Taljanovic MS, Schnitzer T, Charles HC. Subchondral bone trabecular integrity predicts and changes concurrently with radiographic and magnetic resonance imaging-determined knee osteoarthritis progression. *Arthritis Rheum.* 2013 Jul; 65(7):1812-21.
331. Palmer AW, Guldberg RE, Levenston ME. Analysis of cartilage matrix fixed charge density and three-dimensional morphology via contrast-enhanced microcomputed tomography. *Proc Natl Acad Sci U S A.* 2006 Dec 19; 103(51):19255-60.
332. Loeser RF. Aging processes and the development of osteoarthritis. *Curr Opin Rheumatol.* 2013 Jan; 25(1):108-13.
333. Roos EM. Joint injury causes knee osteoarthritis in young adults. *Curr Opin Rheumatol.* 2005 Mar; 17(2):195-200.
334. Brophy RH, Gray BL, Nunley RM, Barrack RL, Clohisy JC. Total knee arthroplasty after previous knee surgery: expected interval and the effect on patient age. *J Bone Joint Surg Am.* 2014 May 21; 96(10):801-5.
335. Ebert JR, Robertson WB, Woodhouse J, Fallon M, Zheng MH, Ackland T, Wood DJ. Clinical and magnetic resonance imaging-based outcomes to 5 years after matrix-induced autologous chondrocyte implantation to address articular cartilage defects in the knee. *Am J Sports Med.* 2011 Apr; 39(4):753-63.
336. Saris D, Price A, Widuchowski W, Bertrand-Marchand M, Caron J, Drogset JO, Emans P, Podskubka A, Tsuchida A, Kili S, Levine D, Brittberg M; SUMMIT study group. Matrix-Applied Characterized Autologous Cultured Chondrocytes Versus Microfracture: Two-Year Follow-up of a Prospective Randomized Trial. *Am J Sports Med.* 2014 Jun; 42(6):1384-94.
337. U.S. Food & Drug Administration. FDA approves first autologous cellularized scaffold for the repair of cartilage defects of the knee [Press Release]. 2016. Retrieved from <http://www.fda.gov/NewsEvents/Newsroom/PressAnnouncements/ucm533153.htm>
338. Hubbell JA. Materials as morphogenetic guides in tissue engineering. *Curr Opin Biotechnol.* 2003 Oct; 14(5):551-8.
339. Kim IL, Mauck RL, Burdick JA. Hydrogel design for cartilage tissue engineering: a case study with hyaluronic acid. *Biomaterials.* 2011 Dec; 32(34):8771-82.

340. Varghese S, Hwang NS, Canver AC, Theprungsirikul P, Lin DW, Elisseeff J. Chondroitin sulfate based niches for chondrogenic differentiation of mesenchymal stem cells. *Matrix Biol.* 2008 Jan;27(1):12-21.
341. Steinmetz NJ, Bryant SJ. Chondroitin sulfate and dynamic loading alter chondrogenesis of human MSCs in PEG hydrogels. *Biotechnol Bioeng.* 2012 Oct;109(10):2671-82.
342. Khanlari A, Detamore MS, Gehrke SH. Increasing Cross-Linking Efficiency of Methacrylated Chondroitin Sulfate Hydrogels by Copolymerization with Oligo(Ethylene Glycol) Diacrylates. *Macromolecules.* 2013 Dec;46(24):9609-17.
343. Hegewald AA, Ringe J, Bartel J, Krüger I, Notter M, Barnewitz D, Kaps C, Sittinger M. Hyaluronic acid and autologous synovial fluid induce chondrogenic differentiation of equine mesenchymal stem cells: a preliminary study. *Tissue Cell.* 2004 Dec;36(6):431-8.
344. Hildebrand A, Romarís M, Rasmussen LM, Heinegård D, Twardzik DR, Border WA, Ruoslahti E. Interaction of the small interstitial proteoglycans biglycan, decorin and fibromodulin with transforming growth factor beta. *Biochem J.* 1994 Sep 1;302 (Pt 2):527-34.
345. Ruoslahti E, Yamaguchi Y. Proteoglycans as modulators of growth factor activities. *Cell.* 1991 Mar 8;64(5):867-9.
346. Benoit DS, Schwartz MP, Durney AR, Anseth KS. Small functional groups for controlled differentiation of hydrogel-encapsulated human mesenchymal stem cells. *Nat Mater.* 2008 Oct;7(10):816-23.
347. Nuttelman CR, Benoit DS, Tripodi MC, Anseth KS. The effect of ethylene glycol methacrylate phosphate in PEG hydrogels on mineralization and viability of encapsulated hMSCs. *Biomaterials.* 2006 Mar;27(8):1377-86.
348. Liu P, Song J. Sulfobetaine as a zwitterionic mediator for 3D hydroxyapatite mineralization. *Biomaterials.* 2013 Mar;34(10):2442-54.
349. Liu P, Emmons E, Song J. A comparative study of zwitterionic ligands-mediated mineralization and the potential of mineralized zwitterionic matrices for bone tissue engineering. *J Mater Chem B Mater Biol Med.* 2014 Nov 21;2(43):7524-7533.
350. Liu P, Skelly JD, Song J. Three-dimensionally presented anti-fouling zwitterionic motifs sequester and enable high-efficiency delivery of therapeutic proteins. *Acta Biomater.* 2014 Oct;10(10):4296-303.
351. Kiani C, Chen L, Wu YJ, Yee AJ, Yang BB. Structure and function of aggrecan. *Cell Res.* 2002 Mar;12(1):19-32.
352. Maroudas AI. Balance between swelling pressure and collagen tension in normal and degenerate cartilage. *Nature.* 1976 Apr 29;260(5554):808-9.
353. Lu XL, Wan LQ, Guo XE, Mow VC. A linearized formulation of triphasic mixture theory for articular cartilage, and its application to indentation analysis. *J Biomech.* 2010 Mar 3;43(4):673-9.
354. Nguyen QT, Hwang Y, Chen AC, Varghese S, Sah RL. Cartilage-like mechanical properties of poly (ethylene glycol)-diacrylate hydrogels. *Biomaterials.* 2012 Oct;33(28):6682-90.

355. Lee S, Tong X, Yang F. The effects of varying poly(ethylene glycol) hydrogel crosslinking density and the crosslinking mechanism on protein accumulation in three-dimensional hydrogels. *Acta Biomater.* 2014 Oct;10(10):4167-74.
356. Nicodemus GD, Skaalure SC, Bryant SJ. Gel structure has an impact on pericellular and extracellular matrix deposition, which subsequently alters metabolic activities in chondrocyte-laden PEG hydrogels. *Acta Biomater.* 2011 Feb;7(2):492-504.
357. Cruise GM, Scharp DS, Hubbell JA. Characterization of permeability and network structure of interfacially photopolymerized poly(ethylene glycol) diacrylate hydrogels. *Biomaterials.* 1998 Jul;19(14):1287-94.
358. Liu X, Tong Z, Hu O. Swelling Equilibria of Hydrogels with Sulfonate Groups in Water and in Aqueous Salt Solutions. *Macromolecules.* 1995 May;28(11): 3813-17.
359. Liang J, Karakoçak BB, Struckhoff JJ, Ravi N. Synthesis and Characterization of Injectable Sulfonate-Containing Hydrogels. *Biomacromolecules.* 2016 Dec 12;17(12):4064-4074.
360. Smilkov H, Kamenova I, Kamenska E, Betchev Ch, Georgiev G. Biocompatible zwitterionic copolymer networks with controllable swelling and mechanical characteristics of their hydrogels. *J Mater Sci Mater Med.* 2008 Jun;19(6):2389-95.
361. Bryant SJ, Chowdhury TT, Lee DA, Bader DL, Anseth KS. Crosslinking density influences chondrocyte metabolism in dynamically loaded photocrosslinked poly(ethylene glycol) hydrogels. *Ann Biomed Eng.* 2004 Mar;32(3):407-17.
362. Bryant SJ, Anseth KS. Hydrogel properties influence ECM production by chondrocytes photoencapsulated in poly(ethylene glycol) hydrogels. *J Biomed Mater Res.* 2002 Jan;59(1):63-72.
363. Villanueva I, Hauschulz DS, Mejc D, Bryant SJ. Static and dynamic compressive strains influence nitric oxide production and chondrocyte bioactivity when encapsulated in PEG hydrogels of different crosslinking densities. *Osteoarthritis Cartilage.* 2008 Aug;16(8):909-18.
364. Schuh E, Kramer J, Rohwedel J, Notbohm H, Müller R, Gutschmann T, Rotter N. Effect of matrix elasticity on the maintenance of the chondrogenic phenotype. *Tissue Eng Part A.* 2010 Apr;16(4):1281-90.
365. Zhang T, Gong T, Xie J, Lin S, Liu Y, Zhou T, Lin Y. Softening Substrates Promote Chondrocytes Phenotype via RhoA/ROCK Pathway. *ACS Appl Mater Interfaces.* 2016 Sep 7;8(35):22884-91.
366. Farnsworth NL, Mead BE, Antunez LR, Palmer AE, Bryant SJ. Ionic osmolytes and intracellular calcium regulate tissue production in chondrocytes cultured in a 3D charged hydrogel. *Matrix Biol.* 2014 Nov;40:17-26.
367. Chandran PL, Horkay F. Aggrecan, an unusual polyelectrolyte: review of solution behavior and physiological implications. *Acta Biomater.* 2012 Jan;8(1):3-12.
368. Xu Z, Greenblatt MB, Yan G, Feng H, Sun J, Lotinun S, Brady N, Baron R, Glimcher LH, Zou W. SMURF2 regulates bone homeostasis by disrupting SMAD3 interaction with vitamin D receptor in osteoblasts. *Nat Commun.* 2017 Feb 20;8:14570.
369. Dupont S, Morsut L, Aragona M, Enzo E, Giulitti S, Cordenonsi M, Zanconato F, Le Digabel J, Forcato M, Bicciato S, Elvassore N, Piccolo S. Role of YAP/TAZ in mechanotransduction. *Nature.* 2011 Jun 8;474(7350):179-83.

370. Zhong W, Li Y, Li L, Zhang W, Wang S, Zheng X. YAP-mediated regulation of the chondrogenic phenotype in response to matrix elasticity. *J Mol Histol.* 2013 Oct;44(5):587-95.
371. Xu J, Feng E, Song S. Bioorthogonally cross-linked hydrogel network with precisely controlled disintegration time over a broad range. *J. Am. Chem. Soc.* 2014 Mar;136(11):4105-8
372. Arora A, Kothari A, Katti DS. Pericellular plasma clot negates the influence of scaffold stiffness on chondrogenic differentiation. *Acta Biomater.* 2016 Dec;46:68-78.
373. Wu Y, Yang Z, Law JB, He AY, Abbas AA, Denslin V, Kamarul T, Hui JH, Lee EH. The Combined Effect of Substrate Stiffness and Surface Topography on Chondrogenic Differentiation of Mesenchymal Stem Cells. *Tissue Eng Part A.* 2017 Jan;23(1-2):43-54.